

A STUDY OF THE BINDING OF GOLD TO PLASMA PROTEINS

By

DHIMIA THAMIR AL-ANI

Thesis submitted for the

Degree of

Master of Philosophy

Department of Physics

The University of Aston in Birmingham

July 1979

TO MY MOTHER

ABSTRACT

A STUDY OF THE BINDING OF GOLD

TO PLASMA PROTEINS

A thesis submitted for the degree of M.Phil.

in the University of Aston in Birmingham

July 1979

by

Dhamia Thahir AL-ANI

Summary

The treatment of rheumatoid arthritis with gold salts such as sodium aurothiomalate (Myocrisin) is clinically well established. Because of their potential toxicity, however, it is desirable to understand as much as possible of the mechanism of action of the drugs and their transport in the blood.

This thesis describes the characteristics of neutron activation analysis as a very sensitive method of analysis for studying the distribution of gold in blood during chrysotherapy.

Electrophoresis was used to fractionate blood samples from twelve patients into the protein fractions and measurements were made to estimate the gold content of whole blood, plasma and serum and the gold bound to the prealbumin, albumin and  $\alpha_1$ ,  $\alpha_2$ ,  $\beta$ , and  $\gamma$ -globulins, and to the blood cells.

The results are summarised in tables. The tables show the concentration of ratios of the gold content of each plasma to serum, whole blood to plasma, and of blood cells to plasma, and that of total protein fractions to the serum, also shows the concentration ratios of gold content in each protein fraction to that of the total of the protein fractions.

The results show there is little, if any, binding of gold to the fibrinogen, the majority of protein-bound gold is associated with the albumin fraction but that significant amounts are also bound to the other proteins. There is a small amount of gold bound to the blood cells except for three patients who show high gold levels. The ratio of the gold content of cathode and anode ends of the electrophoresis strip to that of the total protein fractions were measured to check if there was any gold loss, and it was found there is a small amount of such loss.

Key words.

Gold  
Rheumatoid Arthritis  
Blood  
Activation Analysis

## ACKNOWLEDGEMENTS

I acknowledge with thanks Dr. P. E. Francois for his guidance right from the start in carrying out this investigation and for his many valuable suggestions.

I would also like to thank Professor S. E. Hunt and Dr. D. Crumpton for their help and support. My thanks are due to the Fazakerley Hospital staff who helped by preparing the blood samples and with the electrophoresis. Also to the Research Reactor staff in London University and at Risley who provided the irradiation facilities for the blood samples.

Throughout the experimental work I have received expert technical assistance from Mr. J. Phull for which I am grateful.

For the financial support I would like to thank the Iraqi Atomic Energy Organization.

I would like to express my thanks to Lynda Page for typing this thesis.

Also I would like to thank my family at home for all kinds of support and encouragement.

Finally, I am grateful to my husband, my sons Omar and Odiea for their understanding of my absence during the difficult period of my studies.

## TABLE OF CONTENTS

Page No.

Abstract

Acknowledgements

Table of contents

List of Figures

### CHAPTER 1 INTRODUCTION

1.1	Rheumatoid Arthritis.	1
1.2	The Treatment of Rheumatoid Arthritis.	2
1.3	In Vivo Binding Distribution Studies of Gold to Blood Components.	3
1.4	Methods of Analysis.	9
1.4.1	Atomic Absorption Spectroscopy.	9
1.4.2	X-ray Fluorescence.	10
1.4.3	Activation Analysis	10

### CHAPTER 2 ACTIVATION ANALYSIS

2.1	Neutron Reactions.	13
2.2	Neutron Sources.	14
2.2.1	Radioactive Neutron Source.	14
2.2.2	Accelerators as Sources of Neutron.	16
2.2.3	Nuclear Reactors as Neutron Source.	18
2.3	Activation Analysis.	20
2.4	Historical.	21
2.5	Methods of Activation.	22
2.5.1	Photon Radioactivation Analysis.	22
2.5.2	Charged Particle Radioactivation Analysis.	23
2.5.3	Fast Neutron Radioactivation Analysis.	24
2.5.4	Thermal Neutron Radioactivation Analysis.	25
2.6	Theory of Activation Analysis.	26

	Page No.	
2.7	Comparator Method.	29
2.8	Activation Sensitivity.	29
2.9	Interferences.	32
<u>CHAPTER 3</u> <u>GAMMA-RAY DETECTORS</u>		
3.1	Gamma Interaction with Matter.	37
	3.1.1 Photoelectric Effect.	40
	3.1.2 Compton Effect.	41
	3.1.3 Pair Production	42
3.2	Detection Methods.	43
3.3	Types of Detectors.	44
3.4	Scintillation Counting.	45
3.5	The Scintillation Phenomenon.	46
3.6	Classification of Scintillators.	47
3.7	Scintillation Efficiency.	48
3.8	Advantages of NaI (Tl) detector.	50
3.9	Disadvantages of NaI (Tl) detector.	50
3.10	Choice of the Detector.	51
3.11	Gamma-ray Spectrum.	52
<u>CHAPTER 4</u> <u>EXPERIMENTAL AND RESULTS</u>		
4.1	Preparation of Irradiating Material.	55
4.2	Irradiation Technique.	57
4.3	Calibration of the Counting System.	57
4.4	Methods of Determining Induced Activities.	59
4.5	Counting Procedure.	62
	4.5.1 Qualitative Analysis of the Gamma-ray Spectrum	62
	4.5.2 Contaminations in Some Samples.	64
	4.5.3 Quantitative Results.	64

CHAPTER 5 DISCUSSION AND CONCLUSION

5.1	Gold Content of Fibrinogen.	70
5.2	Gold Content of the Cellular Fraction.	70
5.3	Gold Content of the Albumin Fraction.	72
5.4	Gold Content of $\alpha_1$ , $\alpha_2$ , $\beta$ , $\gamma$ -globulins.	73
5.5	The Correlation between Serum Gold level and the Clinical Response.	73
5.6	Zinc in the Prealbumin Fraction from Patients number 20, 21 and 22.	74
5.7	Bromine in Patient number one.	75
5.8	Gold Content of Cathode and Anode Ends.	75
5.9	Conclusion.	76

APPENDIX COMPUTER PROGRAMME

68	Algol Programme of the Calculation of Quantitative Analysis.	78
----	--	----

## LIST OF FIGURES

### Figure No.

- 2.1 Distribution of neutron energies in a reactor (ref. 45).
- 2.2 Variation of the cross-section for thermal neutrons with mass number.
- 2.3 The growth and decay curve of the activation method.
- 3.1 Relative values of the three attenuation coefficients in aluminium (ref. 65).
- 3.2 Response of a sodium iodide crystal to the 661 KeV gamma-ray of  $^{137}\text{Cs}$ .
- 4.1 Some of the protein fractions and a spot of whole blood.
- 4.2 The samples sealed in polythene bags ready for irradiation.
- 4.3 The sodium iodide crystal and the photomultiplier tube.
- 4.4 The counting system.
- 4.5 A calibration curve using  $^{22}\text{Na}$ ,  $^{137}\text{Cs}$ ,  $^{60}\text{Co}$  sources. The gold 0.412 MeV gamma-ray corresponds to channel number 26.
- 4.6 A calibration curve using  $^{22}\text{Na}$ ,  $^{137}\text{Cs}$ ,  $^{60}\text{Co}$  sources. The gold 0.412 MeV gamma-ray corresponds to channel number 21.
- 4.7 Pulse height spectrum of  $^{137}\text{Cs}$ .
- 4.8 Pulse height spectrum of an irradiated gold foil.
- 4.9 Efficiency calibration curve using an irradiated gold foil.  
X - represent the results of the present work.  
O - represent the results of reference 63.
- 4.10 Method of Covell, N is the total counts contained in the peak channel,  $a_0$  and n channels on either side.
- 4.11 Pulse height spectrum of the background.
- 4.12 Pulse height spectrum of gold activity in a standard showing a very small residual sodium activity.

Figure No.

- 4.13 Pulse height spectrum of the whole blood specimen from patient number five showing the gold activity in channel number 26.
- 4.14 Pulse height spectrum of the serum specimen from patient number five showing the gold activity in channel number 26.
- 4.15 Pulse height spectrum of the plasma specimen from patient number five showing the gold activity in channel number 26.
- 4.16 Pulse height spectrum of the albumin region from patient number five showing the gold activity in channel number 26.
- 4.17 Pulse height spectrum of the prealbumin region from patient number five showing the gold activity in channel number 26.
- 4.18 Pulse height spectrum of the  $\alpha_1$ -globulin region from patient number five showing the gold activity in channel number 26.
- 4.19 Pulse height spectrum of the  $\alpha_2$ -globulin region from patient number five showing the gold activity in channel number 26.
- 4.20 Pulse height spectrum of the  $\beta$ -globulin region from patient number five showing the gold activity in channel number 26.
- 4.21 Pulse height spectrum of the  $\gamma$ -globulin region from patient number five showing the gold activity in channel number 26.
- 4.22 Pulse height spectrum of the blood cells from patient number five showing the gold activity in channel number 26.
- 4.23 Pulse height spectrum of a cathode-end specimen.
- 4.24 Pulse height spectrum of an anode-end specimen.
- 4.25 Pulse height spectrum of the gold activity in a plasma specimen from patient number 21.
- 4.26 Pulse height spectrum of the gold activity in a second plasma specimen from patient number 21.

Figure No.

- 4.27 Pulse height spectrum of the gold activity in the prealbumin plus the cathode-end showing a high activity at channel number 54 corresponding to 1.1 MeV.
- 4.28 Pulse height spectrum of the gold activity in a specimen from patient number one showing another activity corresponding to 0.58 MeV and 0.77 MeV at channel number 33 and 41 respectively.

CHAPTER 1  
INTRODUCTION

1.1 Rheumatoid Arthritis

Rheumatoid Arthritis may be described as one of the most crippling of all diseases. It can effect any one from the young to the adult, aged individual, but it is most common between the ages of 20-50 years. It is also apparent that three times as many women as men suffer from the disease.<sup>1.</sup>

Rheumatoid Arthritis may be described as a chronic inflammatory disease mainly affecting and deforming the joints, it also causes swelling and pain, a limitation of movement and stiffness.<sup>2.</sup> History shows that it was William Ausgrave of Exeter (1657-1721) who first drew attention to the occurrence of poly arthritis as a sequel to gonorrhoea and so introduced the concept of infective arthritis. Sauvages (1763) described a secondary type of arthritis which formed swellings about the size of a nut on the fingers. Garred (1859) proposed the name rheumatoid arthritis. This was to replace the many aliases under which it was then spoken of, such as rheumatic gout, rheumatism and chronic rheumatic arthritis and that name became widely adopted.

Strangeways (1907) under the auspices of the Cambridge Committee for the study of special diseases, increased the knowledge of the pathology of rheumatoid arthritis. This research reviewed the possibility that the change might be due to infection. The so-called "Rheumatoid Factors" in the blood of sufferers were described by Rose in 1948.<sup>3.</sup>

## 1.2 The Treatment of Rheumatoid Arthritis

The treatments for rheumatoid arthritis pain include the physical side (exercises, water baths, etc.) and the use of drugs according to the stage of the disease; depending on the different stages, different drugs are used.

Aspirin is usually used in the first stage of the treatment to which Paracetomal can be added. Anti-inflammatory agents, such as Phenylbataz (Batarolidin) and iodocid are useful in some cases.<sup>4</sup> Forestier's report in 1929<sup>5</sup> showed that patients treated with gold salts showed a marked benefit. The use of the gold therapy was based on the knowledge that gold salts could inhibit growth of tubercle bacilli in vitro and that benefit was reported in tuberculous patients treated with gold salts. Because of some clinical similarities between rheumatoid arthritis and tuberculosis it seemed reasonable that gold salts might help rheumatoid patients. Also it is suggested that gold has a general anti-inflammatory effect because it inhibits fibrinolysin, the enzyme producing inflammation. Gold is still widely used in the treatment of rheumatoid arthritis.

Sodium aurothiomalate (Myocrisin) which contains fifty per cent gold by the weight is the compound most frequently used. It is usual to give weekly intramuscular injections beginning with 10 mg and to increase this by 10 mg every second week up to 40 or 50 mg per injection and continue until a total of 0.5 to 1 gram has been given. The formula and physical state, etc. are shown in Table 1<sup>6</sup>.

Fraser (1945)<sup>7</sup>. reported on one hundred and three cases of rheumatoid arthritis which were observed over a period of one year. Fifty seven received injections of Myocrisin and forty six an inactive control substance. Some clinical improvement was observed in eighty two per cent of the patients on Myocrisin and in forty five per cent of the patients on the control, but the degree of improvement was more marked in the former group. Toxic reactions occurred in seventy five per cent of the patients who received Myocrisin as skin, mouth, kidney, alimentary tract and general lesions in various percentages. Mostly the skin developed a minor reaction, but the majority of these cases were mild. It is of interest to note that thirty seven per cent of the patients who were given the control substance had 'toxic reactions' mostly of the skin with a few of kidney and mouth.

### 1.3 In Vivo Binding Distribution Studies of Gold to Blood Components

Blood is the transport medium of the body, and normal blood contains trace amounts of various elements. The concentration of these elements may reach abnormal levels in the blood due to internal reasons such as excretion by the tissues in the body or external reasons due to the use of drugs in the treatment of diseases. As gold salts are widely used in the treatment of rheumatoid arthritis and as the gold has a potential toxicity and the mechanism of its therapeutic action is still not understood, it is desirable to study the distribution of the gold among the cellular components of the blood and its association with plasma proteins. Several such studies have been made but the results of these measurements have often been conflicting.

Table 1

Gold sodium thiomalate (Myocrisin)

Formula	Solubility in water	Physical state	Gold content %
$\begin{array}{c} \text{COONa} \\   \\ \text{H}-\text{C}-\text{S}-\text{Au} \\   \\ \text{H}-\text{C}-\text{H} \\   \\ \text{COO Na} \end{array}$	+	Aqueous solution	50

For instance, most workers have found the majority of gold associated with plasma proteins to be bound to the albumin, but J.S. Lawrence (1961)<sup>8</sup>. in his studies with radioactive gold, <sup>198</sup>Au, in blood from ten rheumatoid arthritis patients found that the gold was completely bound to the proteins, especially fibrinogen. While E.G. McQueen and P.W. Dybes, in 1969,<sup>9</sup>. in their studies on the transport of gold in the body, using the blood of rabbits which were treated with intramuscular sodium aurothiomalate, found that there was no fibrinogen binding and the gold was virtually confined to the albumin. Nicholas D.H. Balaz's, et. al. (1972),<sup>10</sup>. work on the determination of gold in body fluids showed there was no gold bound to fibrinogen. Manfred Harth in 1973<sup>11</sup>. studied two groups of rheumatoid arthritis patients during treatment with sodium aurothiomalate (Myocrisin) and found that little or no gold was bound to fibrinogen. Also, A. Ooharra, et. al. (1974)<sup>12</sup>. studied the distribution of gold in vivo using blood samples from mature rabbits after having administered radioactive gold and estimated that no gold was bound to the fibrinogen, and the gold was bound to the serum albumin.

There is disagreement also about the binding of gold to blood cells. J.S. Lawrence (1961)<sup>8</sup>. showed in the result of his study on samples of blood from any patients that the red cell content of gold was, on average, about one-quarter of the plasma level on the first day after administration, which seemed a high binding, and afterwards it fell, but less rapidly than the plasma level, so that by the end of the second week it approached, and in some instances exceeded, the latter. Also, Patricia M. Smith, et. al. (1973)<sup>13</sup>. found that gold was localised in red blood cells as well as in the serum of some patients with rheumatoid arthritis. H. Kamel and Brown, in 1976,<sup>14</sup>. agreed about the

presence of gold in the blood cells but only at a concentration of four per cent of the serum level. While H. Coke (1963)<sup>15</sup>. in his studies on gold salts, found there was no gold in the blood cells. R.H. Freyberg (1966)<sup>16</sup>. also found no gold bound to the blood cells. The same result was obtained by Nicholas D.H. Balazs, et. al.<sup>10</sup>. who detected no gold in red cells.

Uncertainties also exist about the correlation between serum and plasma gold levels and the clinical response. F.E. Krusius, in 1970<sup>17</sup>. in their studies on blood samples from twenty five patients during the treatment of rheumatoid arthritis, showed that there is a relationship between plasma gold level and the therapeutic efficacy and toxicity. They showed that at lower plasma levels there was poor therapeutic response and at high plasma levels toxic reactions appeared. A. Lorber, et. al. (1973)<sup>18</sup>. found that the serum gold level correlated to the clinical response. While J.D. Jessop, et. al. (1973)<sup>19</sup>. showed only that a toxic reaction occurred with patients of high serum gold level. Also in 1974<sup>20</sup>. Paul Young, et. al. in work on serum gold level determinations found that a correlation existed between serum gold level and the clinical response. The same result was obtained from work done on blood specimens taken from rheumatoid arthritis patients by I. Bahous and W. Muller (1976)<sup>21</sup>. who found that a positive correlation existed between serum gold level and the effect of chrysolterapy, patients with low serum gold level showed relapses more often than others who had higher levels, and as the gold levels increased side effects were more frequent.

On the other hand, R.H. Freyberg, et. al. (1941)<sup>22</sup>. showed that toxic reactions were much more frequent in patients receiving larger weekly injections of gold but therapeutic results were independent of the gold amounts given. J.S. Lawrence (1961)<sup>8</sup>. found there was no obvious relationship between the plasma gold level and the activity of the disease. S.S.S.Ørensen (1970)<sup>23</sup>. in his pharmacodynamic studies on patients being treated with gold showed there was no correlation between serum gold level and the clinical response or side effects. R.C. Gerber, et. al. in 1972,<sup>24</sup>. showed there was no correlation between serum gold level and the clinical improvement. Also J.D. Jessop, et. al. (1973)<sup>19</sup>. and Norman L. Gottlie, et. al. (1974)<sup>25</sup>. and D. Schorn, et. al. (1975)<sup>26</sup>. and Micha Abeles, et. al. (1977)<sup>27</sup> all agreed that there was no correlation between serum gold levels and the activity of the disease process.

There has been interest also in estimating the gold bound to the protein fractions such as albumin, prealbumin  $\alpha_1$ ,  $\alpha_2$ ,  $\beta$ ,  $\gamma$  - globulins R. Eberl and H. Altman (1970)<sup>28</sup>. in their studies of the bound forms of the gold in the blood serum following intravenous or intramuscular administrations of various gold salts found the majority of the gold was bound to the albumin, but some gold was also bound to the other serum protein fractions. S.S.S.Ørensen (1970)<sup>23</sup>. in his studies showed that the larger part of the gold was bound to the albumin fraction and only an insignificant amount was freely diffusible. A. Lorber, et. al. (1972)<sup>29</sup>. found that albumin contains most of the gold in circulation and at high serum gold levels there was increased and significant binding to the other protein fractions. Also, A.E.

Finkelstein, et. al. in 1976,<sup>30.</sup> studied two groups of four patients taking oral gold compounds as capsules in the treatment of rheumatoid arthritis, they found the gold distributed to the serum protein fractions, most to the albumin and the rest to the globulins. In 1977<sup>31.</sup> H. Kamel, et. al. found that the gold bound to the albumin and the other protein fractions as well. Roberta J. Ward, et. al. (1977)<sup>32.</sup> in their work to determine gold in the plasma and plasma protein fractions showed that the gold was mostly bound to the albumin but still significant amounts were associated with the other protein fractions. Micha Abeles, et. al. (1977)<sup>27.</sup> in their studies on gold metabolism found that all circulating gold is in the protein fractions of plasma, ninety five per cent of which was bound to the albumin fraction and the remaining five per cent with the high molecular weight fractions.

However, N. Simon (1954)<sup>33.</sup> studied gold distribution in the plasma and plasma protein fractions from a patient who had received an intrapleural injection of radioactive colloidal gold, <sup>198</sup>Au, and found by using a Gerger-Muller detector that the radioactive gold was bound to the  $\alpha$  and  $\beta$  globulin fractions only, no gold being bound to  $\gamma$ - globulin or albumin. M. Schattenkirchner and Z. Grobanski (1977)<sup>34.</sup> studied a group of patients undergoing treatment for rheumatoid arthritis and they have found that most of the gold was bound to albumin fraction but not to the other protein fractions except for a little gold associated with  $\alpha_1$  - globulin.

Summarising, by going through the work done by previous research workers, it was noticed that they nearly all agreed on the point that the majority of the gold was bound to the albumin fraction, but

they disagreed upon:

1. The possibility of the gold being bound to,
  - i - The fibrinogen.
  - ii - The blood cells.
2. The correlation of serum gold level and clinical improvement.
3. The extent of binding to the globulins.

From this previous work it seemed that the amount of the gold present in the plasma of patients is of the order of  $\mu$  g/ml.

This thesis describes work done on blood samples from a further group of patients in an attempt to clear up some of these disagreements. The patients were all being treated with Myocrisin by Mr. J.H.R. Redding, at Fazackerly Hospital, Liverpool. In our experimental work we studied the gold content in  $10 \mu$  L of blood samples. These, therefore, would be expected to contain about  $10^{-8}$  g of gold. To observe the presence of one per cent of this on a particular protein fraction would require the detection of about  $10^{-10}$  g of gold.

#### 1.4 Methods of Analysis

To study trace elements in any subject from medical or other fields, there is a need for a method of analysis. There are several methods of analysis available, but the matter of choosing the most suitable method to serve the aim of the analysis with least errors and high sensitivity is the most important step. The well known methods are:

- 1.4.1 Atomic Absorption Spectroscopy - this is an analytical

process in which there is conversion to the atomic state and the study of the absorption of radiant energy by those atoms. This enables one to do trace element analysis, but still this method involves some errors as a result of the dissolving and diluting processes. 35. 36.

1.4.2 X-ray Fluorescence - which is based on the principle that when a material is bombarded with charged particles or photons of high energy, inner shell electrons are ejected from different orbitals of the atom and the vacancies left are filled with electrons coming from the outer shells, and as a result of this replacement x-rays are emitted. Measurement of the x-ray characteristic energies and the intensities serve as the qualitative and quantitative analysis wanted, but the methods of target preparation involved, such as the digestion of the sample, are still a major problem which causes loss of some of the element of interest, or in the case of observations of a very low concentration this method can be unsuitable. 37.

1.4.3 Activation Analysis - is based on the principle that when material is irradiated by nuclear particles produced in a nuclear reactor, particle accelerator or other suitable source, some of the atoms present in the material will interact with the bombarding particles and be converted to different isotopes of the same element or isotopes of different elements depending on the nature of the bombarding particles. In many cases the isotopes produced are radioactive. If each different induced radioactivity can be distinguished or separated from all other radioactivities produced, then the amount

of each radioactivity is a measure of the quantity of the parent isotope present in the material. This process will be described in more detail in Chapter 2. Activation analysis particularly using slow neutrons in a reactor is one of the most sensitive analytical methods known and this is why it has wide applications in various fields as there are many important problems concerning "trace elements" which are present in concentrations low enough to be outside the border of most conventional chemical methods.<sup>38. 39. 40.</sup>

The advantages of activation analysis for the determination of impurities at p.p.m. and p.p.b. levels are:

1. High sensitivity.
2. The rapidity of analysis.
3. The insensitivity to the chemical form of element.
4. The method is essentially non-destructive.
5. The equipment requirements may be relatively inexpensive.
6. The measurement is unaffected by contamination during the measurement as far as this happens after the irradiation process.
7. Independence of distribution with the sample.

For investigations of the distribution of the gold, especially in low molecular weight protein fractions in which the gold content is low, a very sensitive method like neutron activation analysis is needed. Neutron activation analysis has been found to be very sensitive as appeared in the result obtained by Roberta J. Ward, et.al. (1977)<sup>32.</sup> who compared the two methods of analysis neutron activation and atomic absorption spectroscopy. In order to study the gold distribution in blood we have made measurements using neutron activation

analysis on blood samples from a group of twelve patients, all of whom have received chrysotherapy for rheumatoid arthritis. The plasma protein fractions were separated by electrophoresis, and since the gold is classified in the periodic table under the heavy elements and has a high cross-section for thermal neutrons, the reaction  $^{197}\text{Au}(n, \gamma)$   $^{198}\text{Au}$  was used. The blood samples were irradiated in neutron flux of about  $10^{12}$  n/cm<sup>2</sup>.sec for seven hours and left to stand for five days before counting took place.

This reaction has a cross-section of ninety eight barns.  $^{198}\text{Au}$  has a half-life of 2.7 days and decays emitting a gamma-ray of 0.412 MeV, so the reaction was followed by measurement of the radioactivity by using a NaI (Tl) well type scintillation crystal, the signals from the photomultiplier attached to the crystal were fed to a 252 channel multichannel analyser. By using gamma-ray spectroscopy the gold levels bound to plasma, serum, whole blood, plasma protein fractions and blood cells were determined.

CHAPTER 2

ACTIVATION ANALYSIS AND NEUTRON SOURCES

2.1 Neutron Reactions

The interaction of neutrons passing through matter is different from that of either charged particles or photons. The neutron carries no charge, so there is no coulomb repulsion to prevent its interaction with nuclei and so it is able to cross the nuclear boundary with very low velocity.

The main interactions of neutrons with nuclei are:

- a - Elastic scattering  $x(n,n)x$  - in which the nucleus is unchanged in either isotopic composition or internal energy after interaction with the neutron. The kinetic energy of the system is conserved and the energy level of the target nucleus is the same before and after the collision.
- b - Inelastic scattering  $x(n,n')x$  - in which the nucleus after re-emission of the neutron is left in an excited state and that happens when the neutron energy is great enough to raise the nucleus above its first level. The excited nucleus may decay to the ground state by the emission of one or more gamma-rays and the energy of the emitted neutron is given as the difference between its incident energy and the energy of the excited level plus the kinetic energy of the nucleus.
- c - Radioactive capture  $x(n,\gamma)Y$  - for neutrons below the inelastic scatter threshold the only reactions which occur with appreciable cross-section are elastic scattering and radioactive absorption. The radioactive capture process is possible at all neutron energies but is most probable at low energies (less than 1 KeV). When a neutron is cap-

tured by the nucleus the resulting compound nucleus is formed in a highly excited state, because the capture neutron brings in to the system both the kinetic energy and its binding energy ( $\sim 8$  MeV). Since the compound nucleus lies above its ground state it decays either by the re-emission of a neutron or by emitting one or more gamma photons. However, the excitation energy of the compound nucleus is shared between its nucleons, and the emission of one of these nucleons is not possible until the nucleon gains an energy greater than its binding energy in the nucleus. Therefore, when the excitation energy is shared among a large number of nucleons, the average time for emitting a nucleon is much more than the average time required for gamma emission, so the compound nucleus may decay by emitting gamma-rays. Neutron capture may also lead to the emission of charged particles as in  $x(n,p)Y$ ,  $x(n,\alpha)Y$  reactions. At higher neutron energies two or more neutrons may be emitted after it strikes the nucleus, like  $(n,2n)$ ,  $(n,3n)$  reactions.<sup>41. 42.</sup>

## 2.2. Neutron Sources

Because of the neutron's short life time, free neutrons do not occur in nature and must be artificially produced. There are many sources available giving neutrons with different fluxes and energies.<sup>43. 44.</sup>

### 2.2.1 Radioactive Neutron Source

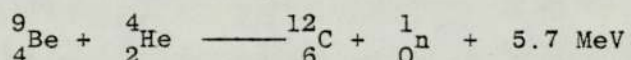
This kind of source is made up of a target material mixed or alloyed with a naturally decaying radioactive component which supplies the bombarding radiation for the production of neutrons by a nuclear reaction.

There are several types of radioactive neutron sources, differentiated both by the nature of the target material and of the radioactive nuclide producing the bombarding radiation. Radioactive sources are usually of relatively small volume which is one of their main advantages.

1. ( $\alpha$ ,n) sources.

i - Polonium - Beryllium.

The Po-Be neutron source has historical interest because the reaction was used in the discovery of the neutron. The ( $\alpha$ , n) reaction by which alpha particles release neutrons from beryllium can be represented by



The neutron yield is about  $10^6$  neutron per second per curie (nps/Ci) of polonium, with an energy range from 6.7 MeV-10.9 MeV. This source emits gamma rays of very low intensity.

ii - Radium - Beryllium.

The Ra-Be ( $\alpha$ , n) source is a common way to generate neutrons because of its easy preparation and the long half-life of radium which is about 1620 years, its disadvantage is the emission of high energy gamma radiation. The neutrons produced have average energy about 5 MeV.

iii - Plutonium - Beryllium.

A cylindrical source of 2cm in diameter and 3cm height yields about  $10^6$  neutrons per second per curie of plutonium. As the half-life of

plutonium is about  $2.3 \times 10^4$  years and the gamma-rays emitted in the radioactive decay of  $^{239}\text{Pu}$  are weak and of low energy, together with the low cost of plutonium these make this source more useful.

iv - Americium - Beryllium.

Americium has a half-life of about 470 years. Although this isotope decays by emitting alpha particles of about 5.4 MeV, these particles are followed by gamma-rays of 40 to 60 KeV in the majority of the disintegrations. The number of neutrons produced per second per curie is about  $2.1 \times 10^6$  nps/Ci of Americium which is useful for rapid activation analysis of many elements in milligram quantities.

2. Radioactive ( $\gamma$ , n) sources.

There are only two nuclides which have thresholds for the ( $\gamma$ , n) reaction within the range of energies of gamma-rays emitted by radioactive nuclei in their decay processes. They are  $^2\text{H}$  and  $^9\text{Be}$  and these can be used as target materials. Radioactive photoneutron sources offer the possibility of obtaining monoenergetic neutrons. If a radioactive nucleus emits only one gamma-ray with energy above the threshold for the ( $\gamma$ , n) reaction in either beryllium or deuterium the neutrons emitted should all be of the same energy, the neutron yield per second per curie is about  $10^4$ .

2.2.2 Accelerators as sources of Neutron

It is obvious that accelerators which can impart energies to beams of charged particles in excess of the threshold energy for release of neutrons in a target material are adaptable as sources of neutrons. As the control of the energy of the charged particles in the beams of accelerators has improved along with methods of measuring

the energy of the beam, it has become possible to generate neutrons with well defined energies. The main reactions most frequently used to produce neutrons are:

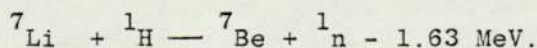
1. Neutrons from  $(\alpha, n)$  and  $(\alpha, 2n)$  reactions.

Many accelerators of nuclear charged particles can be used to accelerate alpha particles to energies higher than those which can be obtained from radioactive sources. For a combination of reasons the  $(\alpha, n)$  reaction has not been found to be very useful as a source of neutrons in accelerators, the chief reason seems to be that the production of alpha particle beams is difficult and neutron yields are low, for example, even with 30 MeV alpha particles the neutron yield is only about  $2 \times 10^9$  n/sec -  $\mu$  A - sr for beryllium.

2. Neutrons from  $(p, n)$  reaction.

The  $(p, n)$  reaction has been much more popular than the  $(\alpha, n)$  reaction as a source of neutrons in accelerators. The lower threshold energies and greater yields of neutrons have contributed to this popularity, for example, thick target yields in excess of  $10^9$  n/sec -  $\mu$  A have been obtained with a 3 MeV Van de Graff accelerator. Up to the present time the  ${}^7\text{Li} (p, n) {}^7\text{Be}$  reaction has been most widely used as a source of neutrons with energies in the kilovolt region.

The equation for the reaction is:

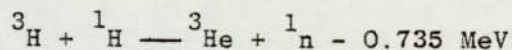


3. Neutrons from Hydrogen isotopes reactions.

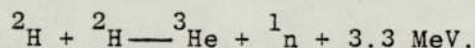
Now tritium has become more readily available, it is frequently

used to produce neutrons. One reaction in which tritium may be used to generate neutrons is the  ${}^3\text{H}(p, n){}^3\text{He}$  reaction.

The reaction equation may be written

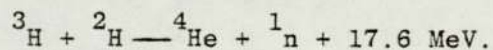


Another reaction is  ${}^2\text{H}(d, n){}^3\text{He}$  which has been widely used in the production of monoenergetic neutrons, one of the convenient characteristics of the  ${}^2\text{H}(d, n){}^3\text{He}$  reaction is a high yield of neutrons at deuteron energies below 1 MeV. The reaction equation is:



The competing reaction  ${}^2\text{H}(d, p){}^3\text{H}$  always occurs along with the (d, n) reaction when deuterons are bombarded by deuterons. The fact that protons are emitted in numbers nearly equal to those for the neutrons is advantageous in helping to estimate the neutron production by measurement of the protons.

The  ${}^3\text{H}(d, n){}^4\text{He}$  reaction is outstanding among (d, n) reactions which have been used for generating mono energetic neutrons for its high positive value of Q. The equation of the reaction is:



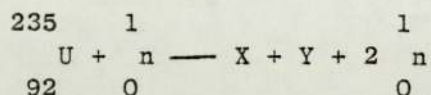
This reaction is characterised by an intense production of neutrons of high energy,  $\sim 14$  MeV, at beam energies in the 0.1 - 1.0 MeV range.

### 2.2.3 Nuclear Reactors as Neutron Source

Most nuclear reactors consist of a core that contains the reactor

fuel as well as neutron moderating and cooling materials. Uranium -  $^{235}\text{U}$  is the most commonly used fuel, although  $^{233}\text{U}$  and  $^{239}\text{Pu}$  may be also used. The major source of neutrons is the fission of nuclei of  $^{235}\text{U}$ . Each  $^{235}\text{U}$  nucleus that undergoes fission emits on the average about 2.5 neutrons.

The reaction taking place in the reactor can be represented by:



The neutrons produced from the fissions have energies ranging from 0.1 to about 20 MeV. The most probable energy is about 0.72 MeV and the mean energy is about 2.0 MeV.

A few neutrons, however, arise from the fission of  $^{238}\text{U}$  present in natural uranium and some from the interaction of gamma-rays (the  $\gamma, n$  reaction) with such materials as deuterium or beryllium that may be present. The maximum neutron flux that has been attained in nuclear reactors is about  $10^{15}$  n/cm.<sup>2</sup> sec. The high energies with which neutrons are released in the fission process accounts for the extensive neutron moderator which serves to reduce the energies of the fission neutrons to thermal energies with a minimum of loss by neutron capture or by escape from the moderator. The neutron moderator is a low atomic-mass material such as water, heavy water, or graphite. The energetic neutrons resulting from fission collide with the nuclei of the moderator and slow down. This results in a more efficient fission process since the fission cross-section of  $^{235}\text{U}$  is larger for moderated neutrons than for unmoderated neutrons. Additional moderating material is placed around the core to further slow and to reflect escaping neutrons. The core in most reactors is surrounded by a heavy thick-walled material or immersed in a deep pool of water which serves as a radiation shield.

Nuclear reactors designed for research are provided with facilities to allow samples to be irradiated for analysis and other purposes, so a variety of nuclear reactions, useful in activation analysis, can be obtained with reactor neutrons. These reactions include  $(n, \gamma)$ ,  $(n, p)$ ,  $(n, \alpha)$ ,  $(n, 2n)$  and  $(n, f)$ . The feasibility of using any reaction depends on factors such as the type of sample matrix, cross-section, neutron flux, nuclear and chemical properties of the reaction product, and possible interferences which are discussed in more detail later in this chapter.

By studying all the neutrons sources mentioned above it seemed that particle accelerators can provide ~~more~~<sup>more</sup> thermal neutron fluxes by slowing down the fast neutrons of  $(d, n)$  and  $(p, n)$  reactions. However, beam instabilities, target damage problems and the cost of utilising an accelerator solely for activation analysis are serious limitations. The radioactive sources yield very poor neutron fluxes compared with those obtained from the nuclear reactors. Nuclear reactors are good sources for intense neutron fluxes especially thermal neutrons as shown in Figure 2.1 which makes them the most suitable for thermal neutron radioactive analysis.<sup>45</sup>

### 2.3 Activation Analysis

Activation analysis is a technique which can be used for the quantitative and qualitative determination of many elements, at concentrations well below the limits of traditional analytical methods. The technique is different in principle from the other methods of chemical analysis such as spectrography, colorimetry, polarography,

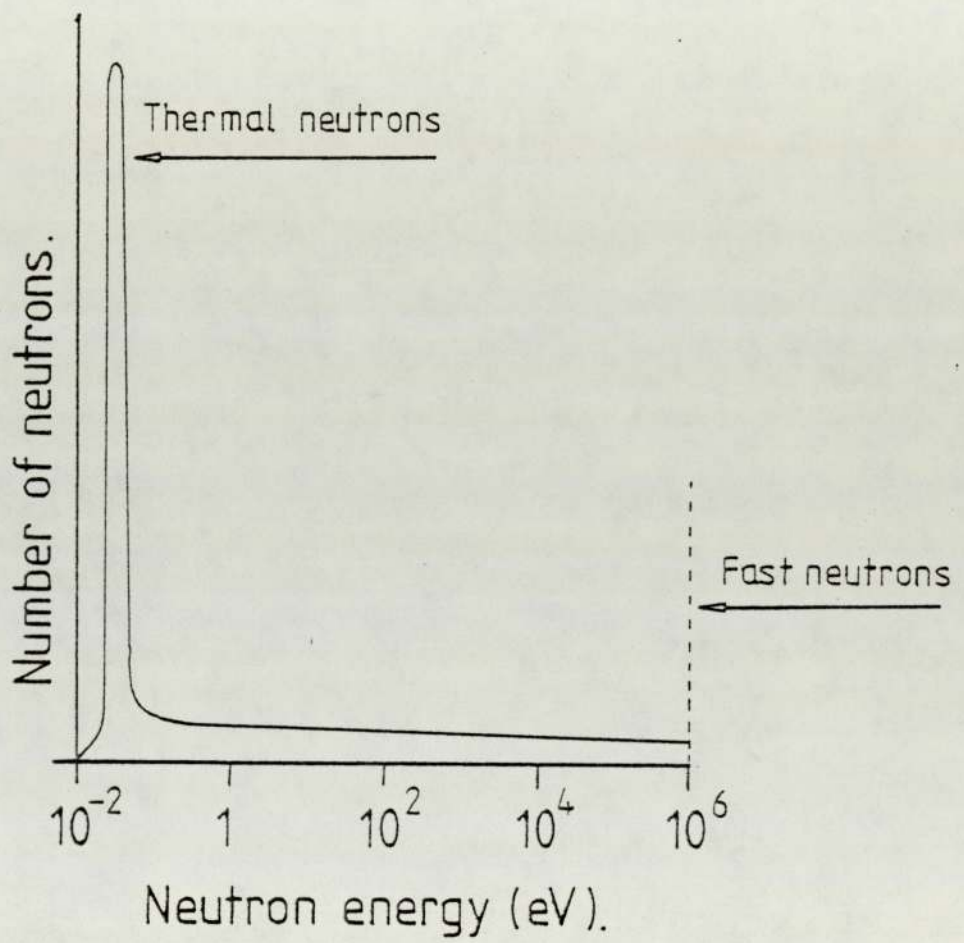


Figure 2.1 Distribution of neutron energies in a reactor (ref. 45)

etc., which depend on the properties of the electrons in the outer parts of the atom, because activation analysis depends on the nuclear properties of the atom and relies on the fact that many substances become radioactive when bombarded by neutrons, charged particles, such as protons or deuterons, or by photons.

#### 2.4 Historical

Analysis by radioactivation was first suggested by Hevesey and Levy (1936)<sup>46</sup>. when they used thermal neutrons derived from a 300 mCi Ra-Be source to detect dysprosium and europium activities in rare earth mixtures, without chemical separation procedures. This original experiment detected the Beta-particles emitted with a Geiger-Muller counter. Since then this technique has been widely used and extended by the use of other incident particles, which were first employed for the purpose of micro-analysis of traces of gallium in iron by Seaborg and Livingood in (1938)<sup>47</sup>. when a sample of iron bombarded with high energy deuterons to detect a gallium impurity at a level of six parts per million.

Activation analysis of biological material was first used by Bruce and Robertson (1947)<sup>48</sup>. to estimate protein-bound iodine by the reaction  $^{127}\text{I} (n, \gamma) ^{128}\text{I}$ . They used samples of thyroglobulin from thyroid tissue and exposed them to slow neutrons from a reactor for one hour: After removal from the reactor they recorded the activity using an end-window Geiger-Muller counter. Tobie and Dunn in (1947)<sup>49</sup>. discussed the limitations of the radioactive and the micro-chemical methods of analysis in the study of the trace elements, and they described the principles of activation analysis and its feature of extreme sensitivity

for quantitative measurements. In their experimental work they irradiated twenty two samples with slow neutrons from the Hanford pile, nineteen of them obtained from different organs of a female mouse injected with 100  $\mu$  g of stable gold in form of sodium gold thiosulfate salt, the other three samples were 20 ml of blood from a leukaemic patient with the samples fractionated into plasma, white cells and red cells, all these samples were used to study the gold distribution. Since then the technique has been considerably refined and extended by the use of other incident particles and emitted radiations in a wide variety of problems. The rapid growth of the use of activation analysis was due in part to:

1. The availability of nuclear reactors and particle accelerators. The number of irradiation facilities continues to grow.
2. The development of gamma-ray spectrometry and other counting techniques, e.g. NaI (TI) scintillation spectrometry with high efficiency, and semi-conductor detectors offering high resolution gamma-ray spectrometry.

## 2.5 Methods of Activation

In principle activation analysis may be based on any artificially induced nuclear reaction. These may be classified under three main headings. <sup>50.</sup> 45.

### 2.5.1 Photon Radioactivation Analysis

Energy may be given to a nucleus by bombardment with energetic gamma-ray quanta promoting emission of nuclear particles or trans-  
lation of nuclei into excited states.

Photon activation have been used mainly for the determination of those elements that cannot be measured satisfactorily after irradiation with reactor neutrons, such as oxygen, nitrogen, carbon, beryllium, etc. There is always a threshold energy below which no activation is observed. Photon neutron thresholds usually exceed 6 MeV but as the photon energy increases nuclear reactions such as  $(\gamma, 2n)$ ,  $(\gamma, pn)$  become more marked. Whereas thermal neutron radioactivation analysis relies on the observation of neutron-rich isotopes produced by neutron capture, the use of high energy photons generally results in neutron deficient isotopes, produced by  $(\gamma, n)$  reactions. The radioactive products of these reactions are normally pure positron emitters.

High photon fluxes with an energy of 25 MeV are available from electron linear accelerators.

Isotopic gamma sources are used in the determination of beryllium because the reaction  ${}^9\text{Be}(\gamma, n){}^8\text{Be}$  has a threshold energy of only 1.66 MeV.

#### 2.5.2 Charged Particle Radioactivation Analysis

Charged particles such as protons, deuterons, and other nuclei may be accelerated and used to bombard the sample. The activation applications of charged-particle techniques have been developed for light elements that cannot be conveniently determined by irradiation by reactor neutrons. The major advances in this type of activation have taken advantage of its sensitivity. Unlike neutron radioactivation analysis, this method enables a selected area and depth to be specified for the analysis, this can be considered an advantage for some analytical problems where the aim

of the analysis might be different to that when using neutrons. Also it can offer a non-destructive method of analysis of a light element in a high atomic number matrix because of the differences in the coulomb barriers which depend on the positive charges on the nuclei. On the other hand, a disadvantage is the limited range of the charged particles in the sample which results in considerable heat dissipation in the surface layers, which may abrade the sample.

Particle energies of 1 MeV or less can be obtained with a Cockcroft-Walton voltage multiplier or by other types of high voltage rectifiers; these machines are relatively cheap and can yield high ion currents.

Van de Graaff generators provide higher accelerating voltages, up to approximately 6MeV for a single-stage machine. Higher particle energies can be attained with multiple-stage Van de Graaff generators, cyclotrons or linear accelerators.

### 2.5.3 Fast Neutron Radioactivation Analysis

The reactions associated with fast neutron radioactivation analysis are  $(n, p)$ ,  $(n, \alpha)$ ,  $(n, 2n)$ , etc.

The cross-section of these nuclear reactions are generally lower than those of thermal neutron capture and the majority have an associated threshold energy. The threshold for the fast neutron reactions is typically between 1 and 12 MeV.

For some elements fast neutron activation is of interest if the  $(n, \gamma)$  capture cross-section is small, for example, nitrogen, oxygen, fluorine, lithium.

#### 2.5.4 Thermal Neutron Radioactivation Analysis

Thermal neutrons are defined as neutrons with energies comparable to the thermal agitation energy of the atoms and molecules of the substance through which they are passing.

At 300 K<sup>0</sup> these neutrons have energies in the range 0 to ~ 1eV, an average velocity of 2200 m sec<sup>-1</sup> and a mean energy of 0.025 eV.

The absence of a coulomb barrier for neutrons means that they readily enter target nuclei and induce nuclear reactions with cross-sections that generally exceed those of reactions with other particles.

The total reaction cross-section is given approximately by:

$$\sigma = \pi (R + \lambda)^2$$

where  $\lambda$  - is the de Broglie wavelength of the incident neutron in the centre of mass system.

R - is the sum of the radii of the two reacting particles.

Figure 2.2 shows the variation of the geometrical cross-section (target area presented to a neutron) of the nucleus with mass number which shows that most of the heavy elements have high capture cross-section for neutrons.

Thermal neutron reactions proceed almost entirely through the formation of a compound nucleus. Since the excitation energy hardly exceeds the binding energy of the captured neutron, this is emitted principally as gamma radiation, so the dominant reaction for thermal neutrons is the (n,  $\gamma$ ) reaction.

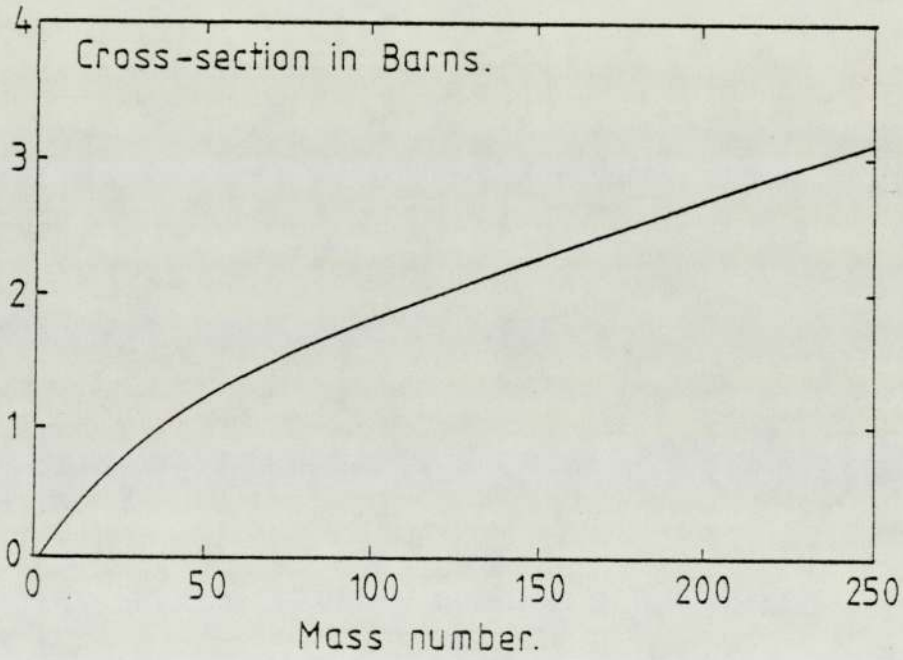


Figure 2.2 Variation of the cross-section for thermal neutrons with mass number.

There is no question that neutrons, especially thermal neutrons, have been more widely used for activation than any other type of particles. This situation has arisen from:

1. The small number of interfering nuclear reactions with thermal neutrons compared with charged particle reactions.
2. The majority of elements have relatively high thermal neutron capture cross-sections.
3. Self-shielding effects are less pronounced.
4. There are greatly relaxed size and shape restrictions, and many samples can be irradiated simultaneously.
5. Very high fluxes of neutrons up to  $10^{15}$  n /cm<sup>2</sup>.sec are available, particularly from reactors.

## 2.6 Theory of Activation Analysis

Activation analysis involves the production of radioactive nuclides from stable (or sometimes radioactive) elements present in the sample under investigation. Each of these radioactive nuclides has certain characteristic properties such as the half-life and the type and energy of the emitted radiation. These characteristics can be identified and measured by relatively simple equipment which enables qualitative and quantitative measurements to be made.

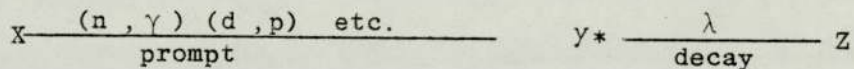
Activation analysis consists of two main steps:

- a) Activation of the sample.
- b) Study of the induced radioactivity.

A further stage, involving chemical treatment of the sample, for example, to separate or concentrate a particular element is sometimes used.

Activation analysis may be defined as an analytical method that involves a nuclear change of an isotope brought about by charged particles, neutrons or high energy gamma-rays, etc.

Consider an element that is made radioactive by irradiation in a constant homogeneous flux of energetic charged particles, photons or neutrons. Let the stable isotope X be transmuted to a radioactive product y\* which decays with its decay constant  $\lambda$  to a stable daughter product Z. The scheme of the activation and the decay can be represented as:<sup>44</sup>



The net rate of formation of y\* is given by:

$$\frac{dN_y}{dt} = \phi \sigma_x N_x - \lambda_y N_y$$

where  $N_x$  represents the number of atoms of X exposed to the flux of the bombarding particles or photons.

$\phi$  represents the flux of the bombarding particles.

$\sigma_x$  represents the cross-section of the reaction.

$N_y$  represents the number of atoms of the product y\*.

$\lambda_y N_y$  is the rate of disintegration of y\* to Z.

$\phi \sigma_x N_x$  is the rate of formation of y\*.

On integration over the irradiation period  $t_i$  the number of the radioactive atoms present is  $N_y(t_i)$

where 
$$N_y(t_i) = \frac{\phi \sigma_x N_x}{\lambda_y} (1 - e^{-\lambda_y t_i})$$

The number of disintegrations per second of the  $N_y(t_i)$  radioactive atoms is given by:

$$A_y(t_i) = N_y(t_i) \cdot \lambda_y = \phi \sigma_x N_x (1 - e^{-\lambda_y t_i})$$

This is, therefore, the activity present at the end of the irradiation time  $t_i$ .

If  $t_i$  is long compared with the half-life of the product radionuclide  $e^{-\lambda_y t_i}$  \_\_\_\_\_ 0 and the maximum activity  $A_y$  is given by:

$$A_y = \phi \sigma_x N_x$$

If the half-life of the product is long compared with  $t$ : then  $1 - e^{-\lambda_y t_i}$  \_\_\_\_\_  $\lambda_y t_i$  and the resulting activity  $A_y(r)$  is given by:

$$A_y(r) = \phi \sigma_x N_x \lambda_y t_i$$

The activity that is detected after a stand time,  $t_s$ , after the end of irradiation by a detector of efficiency  $E$  is given by:

$$A_y(d) = E \phi \sigma_x N_x (1 - e^{-\lambda_y t_i}) e^{-\lambda_y t_s}$$

The theory outlined above assumes that the irradiation flux is constant, no self shielding occurs and the number of atoms of the target isotope remains effectively constant during the irradiation time.

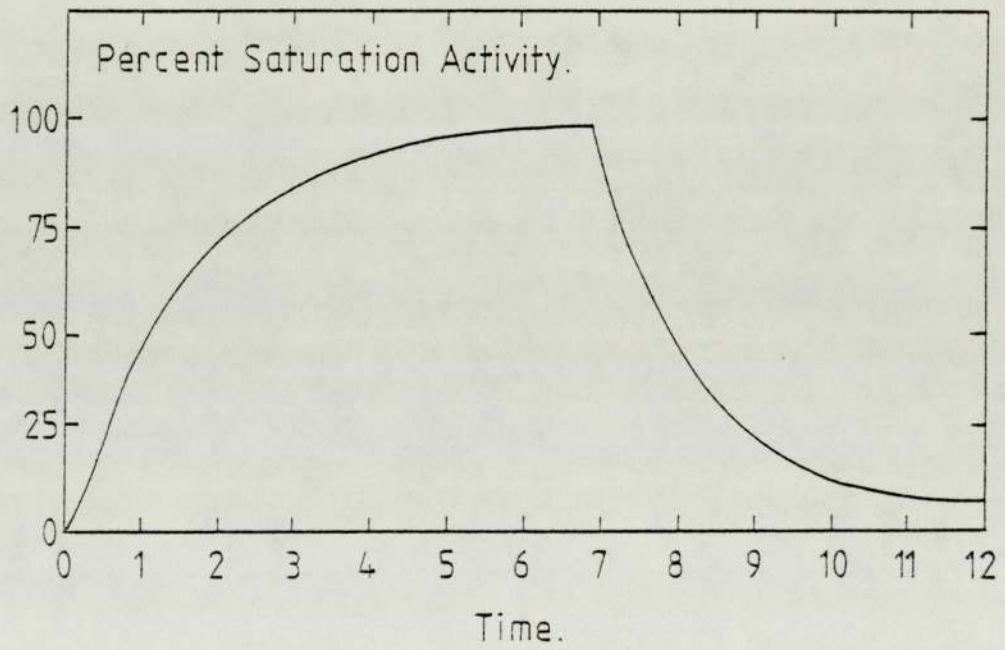


Figure 2.3 The growth and decay curve of the activation method.

## 2.7 Comparator Method

In the comparator or standard method a known weight (same size and shape) of the element is irradiated with the sample to be analysed for the same time, in the same flux.

The resultant prompt or delayed radiations from sample and standard are detected with the same suitable detector.

If the radiations emitted by the element in the sample and the standard are compared, then provided the irradiation and counting conditions are identical, the weight of the element in the sample is given by: <sup>44.</sup>

$$\text{Weight of element in sample} = \frac{(\text{Activity in sample}) \times (\text{Weight of element in standard})}{\text{Activity in standard}}$$

As this is a comparative method between standard and the sample which were irradiated in the same flux and detected in the same detector, the technique avoids the need for a precise knowledge of cross-section, flux and efficiency.

## 2.8 Activation Sensitivity

The sensitivity of activation analysis depends on the amount of the induced activity required in the sample and the efficiency with which this activity can be assayed.

The yield of induced activity in a given sample is a function of three parameters:

- 1 - The neutron flux.
- 2 - The irradiation time.
- 3 - The cross-section for activation.

The neutron flux is the number of neutrons crossing an area of  $1 \text{ cm}^2$  in one second at the position of the sample. The induced activity will be proportional to the neutron flux, if the other factors remain unchanged. The irradiation time must be chosen in relation to the half-life of the desired activity. The cross-section of the target element for neutrons or other bombarding particles, is often measured in barns where  $1 \text{ barn} = 10^{-24} \text{ cm}^2$ .

The general equation governing analysis by activation can be written:

$$\text{Grams of } x \text{ present in sample} = \frac{\text{Act } x \text{ at. wt}}{6.02 \times 10^{23} \left(1 - e^{-\frac{0.693}{t_{1/2}} t}\right)}$$

where

- Act - is the activity at the end of bombardment (disintegration /sec.)
- at. wt - is the atomic weight of isotope activated.
- $\phi$  - is the flux of neutrons ( $\text{n/cm}^2 \cdot \text{sec}$ ).
- $\sigma$  - is the cross-section ( $\text{cm}^2$ )
- t - time of bombardment.
- $t_{1/2}$  - half-life of isotope produced.

From this equation it can be seen that the activity for a given number of grams of material is directly proportional to the neutron flux. Furthermore, the number of grams of a material that gives a specified activity is inversely proportional to the flux. Thus the

higher the neutron flux, the higher the sensitivity for detection of a given isotope. W. Wayne Meinke in 1955<sup>51</sup>. worked out the sensitivity limits for various elements, using thermal neutron activation with different fluxes and he found that for gold samples irradiated in a neutron flux of about  $10^{13}$  n/cm<sup>2</sup>.sec, the sensitivity was 0.00015  $\mu$  g. The same was done by P. Yule (1955)<sup>52</sup>. and he found that the sensitivity to detect gold using neutron flux of about  $4.3 \times 10^{12}$  n/cm<sup>2</sup>.sec was 0.00007  $\mu$  g. The results above were obtained on the basis of different assumptions about the irradiation and counting conditions, such as irradiation time, etc., which accounts for the differences in their conclusions.

In order to estimate the minimum quantity of gold we could detect we made the following assumptions:

1. The reactor flux would be  $10^{12}$  n/cm<sup>2</sup>.sec. This is the flux available in a typical research reactor.
2. The samples would be irradiated for seven hours. This is largely determined by the convenience of the reactor operation.
3. A disintegration rate of 10 dis/sec is needed for easy measurement.

Under these conditions the minimum quantity of gold which can be detected is given by:

$$\begin{aligned} \text{Grams of gold} &= \frac{10 \times 197}{6.02 \times 10^{23} \times 10^{12} \times 98 \times 10^{-24} (1 - e^{-\frac{0.693 \times 7}{64.8}})} \\ &= 4.7 \times 10^{-10} \text{ grams.} \end{aligned}$$

So the quantities of gold expected on our samples should be easily detectable.

## 2.9 Interferences

A number of types of interferences, e.g. radioactive products other than that of interest, are possible in reactor neutron activation. The extent of interference in general depends on the sample matrix, its constituents, the reactions that are produced, and the nature of the neutron flux.

In addition to the activation reaction which occurs with the element being determined, the matrix material and the other impurities present are also irradiated and it is possible for the same radio element to be produced from these materials. Thus in reactor irradiations interference may occur due to reactions with slow neutrons and with fast neutrons. Interference may occur either directly - called primary interferences, or as a second - order interferences.<sup>53.</sup>

The primary interferences happen when reactions take place with nuclides originally present in the sample. While the second-order interferences are due to reactions with radioactive decay products.

Interference problems can result also from neutron-flux differences such as neutron-flux gradients arising from neutron self-shadowing by the sample matrix. Neutron self-shadowing can be considered as a neutron flux gradient in which the flux decreases towards the centre of the sample but this kind of interference would not effect our work because the sample container is a polythene cylinder of 2.5 cm diameter and 7.5 cm long which calculation shows has a negligible effect on the neutron flux.

It is important in the activation analysis method to study the sources of interference expected and to estimate their likely effect on the determinations.

As far as it concerns our work it seemed that the sample matrix must be studied. As the plasma contains many elements, such as Sodium, Potassium, Magnesium, Calcium, Chlorine, as shown in Table 2.1.<sup>54</sup> So the possibility of other activities arising from these elements after the blood samples had been irradiated were studied. Theoretical calculations were done by using the information available about the concentrations, cross-sections, and the expected irradiation conditions, for example, an irradiation time of seven hours in neutron flux about  $2.3 \times 10^{12}$  n/cm<sup>2</sup>.sec to estimate the activity immediately after the irradiation. The calculated results are shown in Table 2.2 which shows that the elements such as Magnesium, Calcium, Potassium, Chlorine and Sodium could effect the gamma-ray spectrum of the irradiated blood samples.

It must be remembered that sodium in particular may be present as a contaminant of the samples apart from its presence in the blood. Because the interfering activities have shorter lives than the gold it would be reasonable to allow the samples to stand for a few days before counting. The calculated activities after a delay of five days are also shown in Table 2.2. The gold activity is then comparable with the remaining activities and should be distinguishable by gamma-ray spectrometry.

Another interesting expected interference comes from the mercury. There are several different radioactive isotopes obtained by irradiation of mercury but one which may affect the measured gold amount arises because atomic number is one place higher than that of the gold in the periodic table, this may cause an increase in the apparent concentration of the unknown (gold) from the reaction  $^{198}\text{Hg} (n, p) ^{198}\text{Au}$ . But, because it is present in blood in only a very low concentration, <sup>55</sup> and has only a very low cross section for the reaction, it has no effect as the activity calculation in Table 2.2. shows.

Table 2.1

Elements	Mean values of concentration in the plasma (g/10 $\mu$ L)
Sodium	$3300 \times 10^{-8}$
Chlorine	$3660 \times 10^{-8}$
Potassium	$161 \times 10^{-8}$
Calcium	$95 \times 10^{-8}$
Magnesium	$22 \times 10^{-8}$
Mercury	$0.003 \times 10^{-8}$
Gold	$10^{-8}$

Table 2.2

Elements	Concentration in plasma g/10 $\mu$ L	half-life	cross-section $\times 10^{-24}$ cm <sup>2</sup>	Radio-active element product	Activity immediately after irradiation dis/sec	Activity at the fifth day after irradiation dis/sec
Sodium	$3300 \times 10^{-8}$	15.4 hr.	0.53	<sup>24</sup> Na	$123 \times 10^3$	481
Chlorine	$3660 \times 10^{-8}$	37.3min.	0.4	<sup>38</sup> Cl	$238 \times 10^3$	Zero
Potassium	$161 \times 10^{-8}$	12.5 hr.	1.2	<sup>42</sup> K	$9 \times 10^3$	11.6
Calcium	$95 \times 10^{-8}$	8.8min	1.1	<sup>49</sup> Ca	$13 \times 10^3$	Zero
Magnesium	$22 \times 10^{-8}$	2.5 hr	13.3	<sup>56</sup> Mn	$27.5 \times 10^3$	Zero
Mercury	$0.003 \times 10^{-8}$	44 min	.02	<sup>198</sup> Au	$.000001 \times 10^3$	Zero
Gold	$10^{-8}$	2.7days	98	<sup>198</sup> Au	$.2 \times 10^3$	$.05 \times 10^3$

CHAPTER 3

GAMMA RAY DETECTORS

3.1 Gamma Interaction with Matter

Gamma-rays are electromagnetic radiations of very small wavelength and are propagated at the speed of light ( $2.99793 \times 10^{10}$  cm/sec in Vacuo).

The origins of gamma-rays are:

1. Gamma-rays produced as a result of the capture of an external nuclear particle by a nucleus.
2. Gamma-rays emitted by a fragment of a nucleus due to fission of the latter.
3. Gamma-rays produced by an inelastic scattering process.
4. Gamma-rays occurring simultaneously with the emission of beta and alpha rays.

The quantity of energy attributed to a specific quantum is a function of the frequency and vice versa, the quantum energy of a wave of frequency  $\nu$  is given by:

$$E = h \nu$$

where -  $h$  is Plank's constant, the value of which is  $4.134 \times 10^{-15}$  ev/s.

The intensity of given radiation is determined by the number of quanta emitted per unit time.

The absorption of gamma-rays by matter differs fundamentally from that of charged particles. The latter dissipate their energy continuously

in a sequence of many ionization and excitation events. Gamma-rays, on the other hand, are absorbed or scattered in single events. If a narrow collimated beam of gamma-rays is incident on an absorber, it undergoes a time exponential attenuation.<sup>56</sup> The most important interactions which can occur are:

- (i) the compton effect,
- (ii) the photoelectric effect,
- (iii) the pair production.

The fraction  $f$  of the incident quanta which are absorbed, for example, undergo one of these interactions, in their passage through a material of thickness  $(d)$  cm is:

$$f = 1 - \exp(-\mu d)$$

where  $\mu$  - is the linear attenuation coefficient, in  $\text{cm}^{-1}$ , which indicates the amount of absorpotion of the rays on passing through 1 cm of the absorber.

$\mu$  is made up of the linear attenuation coefficients corresponding to each of the three types of interactions,  $\sigma$  the compton linear attenuation coefficient,  $\tau$  the photoelectric linear attenuation coefficient and  $\chi$  the pair production linear attenuation coefficient, so

$$\mu = \sigma + \tau + \chi$$

Each of these depends on the energy of the gamma-ray  $(E)$ , and the

atomic number of the absorber. At low energy  $\tau$  is the largest component, but it decreases rapidly with increasing  $E$ , though with heavy elements it may still be appreciably up to a few MeV.  $\sigma$  decreases steadily with increasing  $E$ .  $\chi$  is zero at energies below 1.02 MeV, and becomes important at high gamma energy. The mass attenuation coefficient is more fundamental than the linear attenuation coefficient because it is independent of the density and the physical state of the absorber.

It is given by<sup>56</sup>.

$$\mu/\rho = (\tau/\rho + \sigma/\rho + \chi/\rho) \text{ cm}^2/\text{g}$$

where  $\rho$  - is the density ( $\text{g}/\text{cm}^3$ )

The interactions can also be expressed as cross-sections per atom

$$\mu_a = \left( \tau_a + \sigma_a + \chi_a \right) \text{ (cm}^2/\text{atom)} \quad 56.$$

If  $N$  is Avogadro's number

$A$  is the atomic weight of the absorber,

then 
$$\frac{\mu}{\rho} = \frac{N}{A} \mu_a$$

The different interaction processes are considered in more detail in the following sections.

### 3.1.1 Photoelectric Effect

The photoelectric effect is the process in which a photon of energy  $h\nu$  ejects a bound electron from an atom. Total absorption of energy can only occur if the electron is initially bound in the atom. The electron kinetic energy is <sup>56</sup>.

$$E_e = h\nu - I_b$$

So the kinetic energy  $E_e$ , equals the difference between the energy  $h\nu$ , of the absorbed gamma quantum and the binding energy  $I_b$ , of the ejected electron. It is necessary in this process for the energy of gamma quantum to exceed the binding energy of the ejected electron. Bethe <sup>57</sup>. has derived an expression for the photoelectric absorption cross-section which may be written:

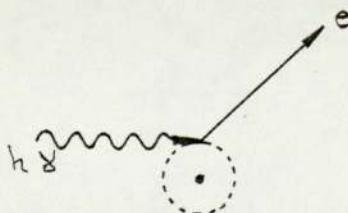
$$\tau_a = \phi_0 Z^5 \left( \frac{1}{137} \right)^4 4\sqrt{2} \frac{(m_0 c^2)^{7/2}}{h\nu} \text{ cm}^2/\text{atom}$$

where  $\phi_0$  is a convenient unit for measuring the cross-section and is equal to  $6.651 \times 10^{-25} \text{ cm}^2$

$Z$  is the atomic number of absorber

$h\nu$  is the incident photon energy in KeV.

$\tau_a$  is strongly dependent on the atomic number and on the energy of the incident photon, it is proportional to  $Z^5$  and inversely proportional to  $(h\nu)^{7/2}$  which means that the photoelectric effect is especially



important in the absorption of low energy photons by heavy elements.

In the energy region below 0.1MeV the photoelectric absorption is complicated by the presence of absorption edges, at which the photoelectric cross-section decreases sharply with E, As E becomes less than the electron binding energy, then K and L edges appear.

### 3.1.2 Compton Effect

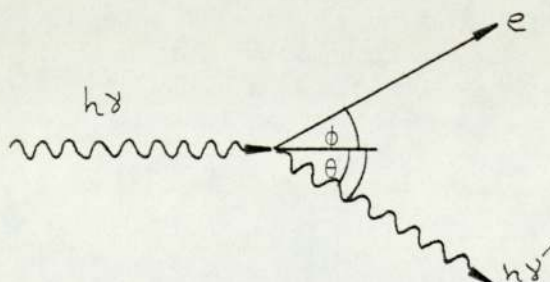
The Compton effect is an elastic collision between a photon and free electron. It usually occurs with an outer electron since the energy of the photon is then very much higher than the binding energy of the electron in the atom. In this process only part of the photon energy is transferred to the electron, the remainder is taken away by the scattered photon. The electron recoils with energy  $T_{c.e.}$  in a direction making an angle  $\phi$  with that of the incident photon. The recoil electrons have energies from zero to a maximum (Compton edge) given by <sup>56</sup>.

$$T_{c.e.} = \frac{E}{1 + \frac{1}{2\alpha}}$$

where  $E =$  energy of incident photon in MeV.

$$\alpha = \frac{E}{m_0 c^2}$$

The scattered photon has a reduced energy  $E = h\gamma'$  and is scattered through an angle  $\theta$  from the direction of the incident photon.



$$h\nu' = \frac{m_0 c^2}{1 - \cos \theta + \frac{m_0 c^2}{h\nu}}$$

The Compton cross-section per electron was derived by

Klein - Nishia (1929)<sup>58</sup>. as

$$\sigma_e = 2\pi r_0^2 \left\{ \frac{1+\alpha}{\alpha^2} \left| \frac{2(1+\alpha)}{1+2\alpha} - \frac{\text{Ln}(1+2\alpha)}{\alpha} \right| + \text{Ln} \frac{(1+2\alpha)}{2\alpha} - \frac{1+3\alpha}{(1+2\alpha)^2} \right\} \text{cm}^2/\text{electron}$$

where

$$\alpha = \frac{E}{m_0 c^2}$$

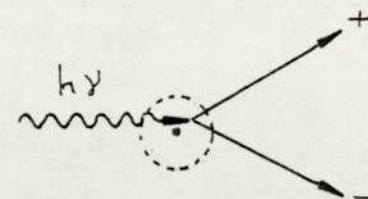
$r_0$  is the classical electron radius =  $(e^2/m_0 c^2) = 2.818 \times 10^{-13}$  cm.

The Compton scattering per electron is approximately proportional to  $E^{-1}$  at energies exceeding 0.5 MeV, and independent of Z. The Compton absorption is proportional to the first power of the electron density and is independent of the Z of the absorber. This independence results from the assumption that the orbital electrons involved are free. The assumption is acceptable because most Compton processes take place at energies which are high compared to the binding energies of the atomic electrons.

### 3.1.3 Pair Production

When the energy of the incident photon exceeds  $2 m_0 c^2 = 1.02$  MeV, the pair production interaction becomes possible. In this process, which occurs only in the field of a charged particle, normally the nucleus, the photon is completely absorbed and its energy is converted

into the rest mass energy ( $2m_0 c^2$ ) and the kinetic energy  $T_{pp}$  of an electron - positron pair. The total kinetic energy of the pair is

$$T_{pp} = E - 2m_0 c^2$$


The two particles united and two annihilation photons are emitted, each with an energy of 0.51 MeV, those gamma quanta are emitted in opposite directions.<sup>56.</sup>

The pair production cross-section obtained by Bethe<sup>59.</sup> is:

$$\sigma_{pp} = \sigma_0 Z^2 \left( \frac{28}{9} \ln 2\alpha - \frac{218}{27} \right) \text{ cm}^2$$

where  $\sigma_0$  is the absorption coefficient given by  $\frac{8\pi}{3} \left( \frac{e}{m_0 c^2} \right)^2 = 6.65 \times 10^{-25} \text{ cm}^2/\text{electron}$  and  $\alpha = \frac{h\gamma}{m_0 c^2}$

The pair production cross-section is zero for photon energies less than 1.02 MeV, for greater energies, it increases at first slowly, then more rapidly. It is also proportional to  $Z^2$ .

### 3.2 Detection Methods

When a nuclear probe interacts with an atomic nucleus the reaction may result in the emission of particles or radiations and may lead to a radioactive product.

Detection of any resulting particles or radiations can be utilised in nuclear methods of analysis. Some of the parameters needed to help in the identification of a product nuclide are:

1. Energy and nature of the emitted radiations.

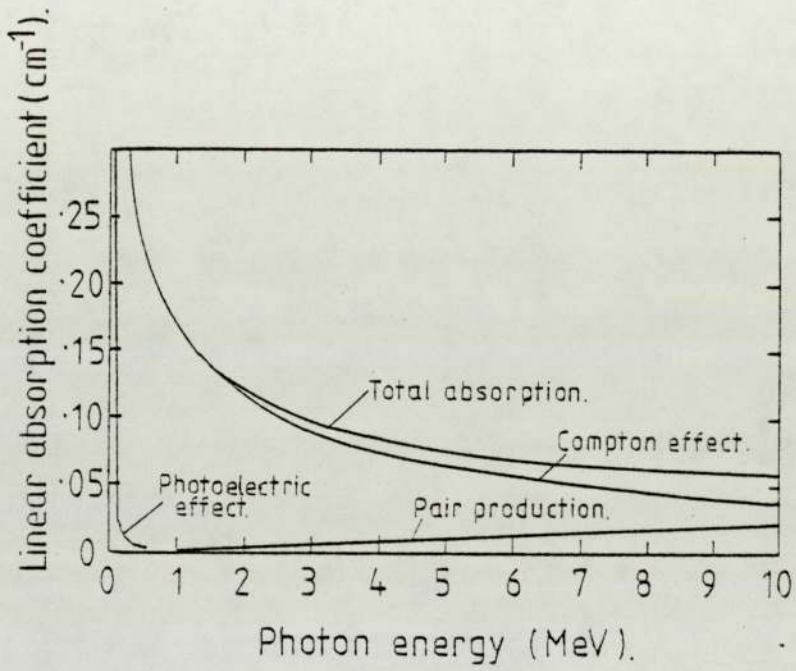


Figure 3.1 Relative values of the three attenuation coefficients in aluminium (ref. 65).

2. Presence of coincident radiation.
3. Half-life.
4. Intensity of gamma-ray or the particles emitted.

Most nuclear analytical methods depend on the measurement of the gamma-rays emitted by a nucleus returning to its ground state. The energy spectrum of the rays is invariably a line spectrum, the pattern of which is typical of the particular nuclide. The reason for this is that the nucleus can absorb and yield up energy only in specific quantities.

### 3.3. Types of Detectors

The ionization produced in the medium which a particle or ray pass through can be detected by one of several methods. The charge may be collected directly by electrical means as it is in the gas ionization counter and semiconductor counters, or it may be detected by the consequent emission of light quanta as in the scintillation counters.

The purpose of radiation detectors is to convert the ionization produced by radiation into electronic signals.

Three of the oldest types of detectors are the ionization chamber, proportional counter and Geiger Muller tube; each of these detectors employ gas filled chambers containing two electrodes between which there is an electric field. When radiation causes ionization in the gas the electrons produced are drawn rapidly to the anode while the heavy positive ions move more slowly to the cathode. The result is that

current flows through the circuit and this is used to measure the amount of the radiation causing the ionization.

Semiconductor detectors are also used for gamma-ray detection, and their operation principle is similar to that of gas-filled detector except that the detecting medium is a solid fabricated from single crystals of high purity semiconductor materials, most germanium and silicon. This kind of detector has good linearity and high resolution which is very necessary in studying complex gamma-ray spectra.

The scintillation detector is also very good and widely used in the detection of gamma-rays. In this detector, ionizing particles pass through certain substances and ionized and excited states are produced which, during their return to the normal state, emit light. This light is picked up by a photo multiplier tube and the resulting pulse of current out of the photo multiplier indicates the passage of the ionizing radiation through the scintillator. This detector will be explained in more detail in the following section.<sup>60</sup>

### 3.4 Scintillation Counting

Scintillation counters incorporate a phosphor with the ability to convert some fraction of the energy of an incident quantum into a signal. When a gamma-ray passes through the phosphor it loses energy to the electrons of the phosphor by either the photoelectric effect, Compton scattering or pair production ( $E > 1.02$  MeV) processes. The excited electrons are liberated into the phosphor lattice and are soon bound to another atom. The vacancy left is filled by another electron, causing

a quantum of light to be emitted as the electron changes from a higher bound state to a lower one.

The phosphor has the photo cathode of a photo multiplier on one side of it, so that electrons will be emitted for light quanta which strike this face.

These electrons will be multiplied by secondary emission from a series of dynodes held at increasing potentials. The resulting current pulse produces a signal at the input of the preamplifier. The signal is finally fed to a multi channel analyzer and then counted.

### 3.5 The Scintillation Phenomenon

The impurities and lattice defects which occur in the energy bands of the NaI crystal create centres in the forbidden area between the valence and conduction bands.

The main types of these centres are:

1. Luminescence centres from which the captured electrons or excitons decay to the ground state accompanied by photon emission.
2. Quenching centres in which radiation less thermal dissipation of excitation energy may occur.
3. Traps which are metastable energy levels from which electrons or excitons may later return to the conduction band by getting thermal energy from the lattice vibrations, or fall to the valence band by a radiation less transition.

The addition of  $Tl^+$  ions to a NaI crystal creates more absorption

centres. The absorption of ionising radiation results in the emission of a light photon from a luminescence centre in the following steps:

1. The production of electron-hole pairs, when electrons are lifted up to the conduction band and a hole is created in the valence band.
2. Recombination of the electrons and holes to produce an exciton, which is a bound electron-hole pair in the exciton band.
3. Capture of the exciton by luminescence centre ( $Tl^+$  activator)
4. Thermal activation by capture of photons from which the luminescence emission occurs.

This is what happens during the absorption and conversion of the absorbed energy into luminescent emission, but the scintillation counting process involves five consecutive stages:<sup>61.</sup>

- Absorption of the particle or electromagnetic energy by the scintillator.
- Conversion of the absorbed energy into luminescent emission.
- Collection of the photons on the photosensitive cathode of a photo multiplier.
- Emission of the photoelectrons from the cathode.
- The electron multiplication process.

### 3.6 Classification of Scintillators

Several solids, gases and even some liquids are used as scintillators, the work of the scintillator depends upon absorption and the resulting excitation, which in turn is responsible for the light

flashes. The phosphors available are:

- 1 - Inorganic crystals, such as, NaI activated with thallium.
- 2 - Organic crystals, liquids and vapours and also plastic phosphors which are polymerised solutions of an organic phosphor in styrene.

Scintillator crystals of inorganic substances are the most satisfactory suited for gamma-ray detection as they have high photoelectric detection efficiencies because of their high average atomic number. Among the inorganic varieties, sodium iodide activated with thallium is the most commonly employed but, compared with sodium iodide, the higher density of cesium iodide favours better absorption of the gamma-ray, on the other hand the light output from this kind of crystal is only one quarter of the output of the sodium iodide crystal. The shape and size of the crystal also tend to affect the measurements, especially where quantitative analysis is concerned.

Particularly good geometry is obtained by using a well type crystal in which a recess, or well, is cut in the crystal parallel to the axis, the source is placed inside it and so it almost completely surrounded by the scintillating crystal.

Plastic and liquid scintillators are rarely used for gamma spectrometry since they are prepared mainly from hydrocarbons so the atomic number is low and then the absorption capacity is very much less than that of the crystal scintillators, also they have very small efficiencies for the photoelectric effect process so there are no photopeaks .<sup>61</sup>

### 3.7 Scintillation Efficiency

Scintillation counting is probably the most widely used technique in

the determination of absolute gamma-ray disintegration rates, primarily because of the reproducibility of the detector efficiency for monoenergetic sources. Well-type crystals give a high efficiency, so they are very useful in detecting low intensity sources.

If we have a monoenergetic source with emission rate  $N_0$  and the photo peak area  $A_p$  in counts/sec. is observed for a particular source-to-crystal geometry, the absolute peak efficiency  $E_{Ap}$  will be given by:<sup>62.</sup>

$$N_0 = A_p / (f E_{Ap})$$

an alternative form is:

$$N_0 = A_p / (f E_{AT} P)$$

- where
- $f$  - is the fractional transmission of gammas by any absorber between the source and crystal.
  - $E_{AP}$  - is the absolute peak efficiency (the fraction of gammas emitted from the source which interact with the crystal such that the total source energy is transmitted to the crystal.)  $E_{AP}$  is calculated as the product of the absolute total efficiency,  $E_{AT}$  and the photofraction  $P$ .
  - $E_{AT}$  - is the fraction of gammas emitted from source that interact at least once with, and deposit some energy in the crystal.
  - $P$  - fraction of source gammas that are totally absorbed (photo fraction)

In the present work a 7F8 Harshaw well-type crystal was used. The absolute total efficiencies for such a crystal at a different height of

the specimen within the well have been calculated by B.J. Snyder and Geza L. Gyorey (1965)<sup>63</sup>. At zero height they give a figure of 0.5031 for 400 KeV radiation. Our work on the variation of the efficiency with the height will be explained later, in Chapter 4.

### 3.8 Advantages of NaI (Tl) detector

The main advantages of the detector are:<sup>64</sup>

1. The high density of the NaI (Tl) crystal which permits the detection of gamma-rays with a much higher efficiency than other techniques.
2. The fact that the light output of the detector is proportional to the gamma-ray energy absorbed provides a tool for the direct measurement of the energy of gamma-ray.
3. The detector has a relatively fast response to ionising radiation. The  $\frac{1}{\tau}$  decay time for the light is 0.25  $\mu$  sec. This makes it possible to use the detector in experiments with high counting rates or when fast coincidences are to be recorded.
4. The light emitted on the absorption of a gamma quantum is a band at  $4100\text{\AA}$  with a width of about  $800\text{\AA}$ . The refractive index of 1.77 is rather high, but when crystals are optically coupled to the photomultiplier window having a refractive index of about 1.5 much of the light is critically reflected into the crystal volume.

### 3.9 Disadvantages of NaI (Tl) detector

The NaI (Tl) detector has some inherent disadvantages which limit its use for thermal neutron capture gamma-ray studies.<sup>64</sup>

- 1 - Poor resolution, which is due to
  - the number of photons emitted per scintillation event in the crystal (due mainly to competition of quenching events with radiative transitions).

- the number of emitted photons that are incident on the photocathode.
- the number of photo electrons that are collected by first dynode.
- the secondary emission ratio at each succeeding diode.

The first two phenomena are due to the properties of the crystal and the optical coupling. While the remaining two arise from the properties of the photomultiplier.

2 - Temperature dependent effects, not only on the quantum efficiency of the detector but also on gain and channel drift which create problems in spectrum analysis.

3 - In capture gamma-ray analysis the spectra are complex and any spectrometer used for analysis of such spectra not only needs to have high efficiency but also must have high resolution so in cases of simple spectra NaI (Tl) detector is quite satisfactory but not in more complex cases.

### 3.10 Choice of the Detector

The right choice of suitable detectors which satisfy the conditions and the aims at a specific project is one of the important steps in the research. Different factors which influence the choice of gamma detector are:

1. The aim of the research, whether it is qualitative or quantitative.
2. The resolving power which determines the complexity of the spectrum that can conveniently be analysed.

3. The detection efficiency which dictates the source strength necessary for the measurement of the spectrum.
4. The simplicity of the arrangement and the ease of data accumulation.
5. Secondary factors such as the response linearity, the stability, the timing accuracy, etc.

According to the above factors, it seemed that the biggest drawback to the gas filled counters is their low sensitivity and the use limited to gamma-rays having ranges within the dimension of the chambers, which leads to limitations on the energy of the photon to be detected. Semi-conductor detectors have very good resolution but do not have such high efficiency as the NaI (Tl) detectors.

In the present work the activity to be observed is low enough to make the high efficiency and sensitivity factor very important. Also the gamma-ray spectrum was expected to be fairly simple which meant there was not requirement for good resolution. So a NaI (Tl) detector was quite satisfactory detector in this particular case.

### 3.11 Gamma-ray Spectrum

The pulse height spectrum produced in a detector by a gamma emitter will be a reflection of the relative importance of the various absorptive processes in the detector, as well as a characteristic of the emissions themselves. If we take what happens in the NaI (Tl) scintillator crystal, the light scintillations picked up by the photomultiplier tube can only come from ionizations and excitations produced by the electrons ejected when the photons are absorbed in the crystal.

In the photoelectric absorption all of the absorbed energy will go into kinetic energy of the ejected electron, except for that needed to supply the binding energy of the electron. An orbit vacancy resulting from a photon absorption will be promptly filled and characteristic x-rays will be emitted, but since they are very soft, they are often absorbed in the crystal. If all of these processes take place within the luminous life time of the phosphor the visible light produced by them will add to that produced by the original photo electron. Then the total light output for the event will be proportional to the energy of the primary photon. This gives the most prominent feature of the gamma-ray spectrum, the photo peak or total energy peak. When the soft x-rays not absorbed, it will be seen as a slight depression on the low-energy side of the photo peak.

Some of the primary photons will be absorbed by Compton instead of photo electric interactions. If the scattered photon is absorbed in the crystal the light output will correspond to the total energy of the photon, these serve merely to enhance the photo peak, but if the scattered photon escapes from the crystal, the light output will correspond only to the energy given up to the Compton electron. These electrons form a Compton continuum, from zero up to the maximum energy transferrable in the Compton event. The larger the crystal, the greater the probability that the scattered photon will be absorbed, so the ratio of the Compton continuum to the photo peak will vary with the size of the detector.

A small peak is usually seen near the low-energy end of the continuum, resulting from the absorption in the crystal of primary photons scattered with the shielding material, this is called the back scatter peak.<sup>65.</sup>

This explanation of gamma-ray spectra is valid when the gamma-ray energy is less than 1.02 MeV. Above this the pair production contributes the spectra. However, in this project, the gamma-rays involved were of too low an energy for this to be a significant effect. A typical spectrum for a monoenergetic emitted is shown in Figure 3.2.

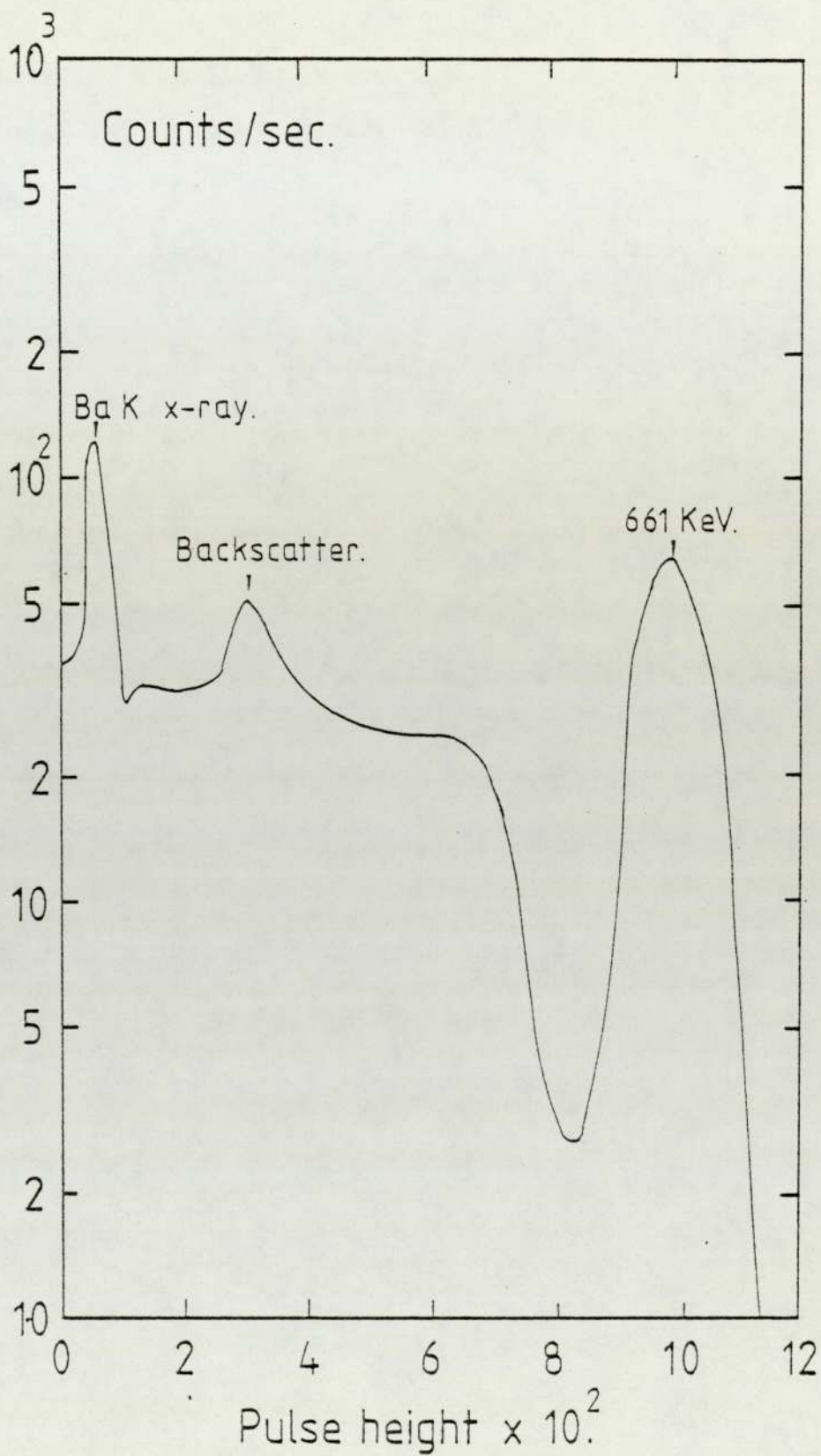


Figure 3.2 Response of a sodium iodide crystal to the 661 KeV gamma-ray of <sup>137</sup>Cs.

## CHAPTER 4

### EXPERIMENTAL AND RESULTS

#### 4.1 Preparation of Irradiation Materials

A - Blood samples: The group studied was made up of twelve hospital out-patients, suffering from rheumatoid arthritis, undergoing treatment by sodium aurothiomalate (Myocrisin) at the Fazakerley Hospital, Liverpool.

The blood was taken from an arm vein, then, typically, ten  $\mu\text{L}$  of each of whole blood, plasma, serum and washed packed cells, were separated and spotted on to 2.5 cm squares of cellulose acetate sheets. These sheets were allowed to dry at room temperature, then placed in polythene bags which were sealed ready for neutron activation. At the same time fractionation of the plasma proteins was carried out by applying an electrical potential difference across a strip of cellulose acetate bearing ten  $\mu\text{L}$  of plasma. This causes an ionization of the proteins and the charged particles move under the influence of the field. From this movement one can carry out separation of individual components of the sample which moves at different rates according to their charge and mass. This is called the electrophoresis method. In our work, Shandon equipment was used with the buffer Tris 1 EDTA acid 1 boric acid (60.5 g - 6.0 g - 4.6 g per litre), at a pH of 8.6. The ten  $\mu\text{L}$  of serum samples were applied to 78 x 150 mm strips of cellulose acetate and electrophoresis was carried out for ninety minutes across a gap of 120 mm at a constant current setting of  $0.04\text{mA mm}^{-1}$ . The strips were dried, immersed in Ponceau S stain (0.2% in 3% of trichloroacetic acid) for thirty minutes, then washed with 5% acetic acid. The strips were dried in air, at room temperature, then cut into fractions corresponding

to the pre-albumin, albumin,  $\alpha_1$ ,  $\alpha_2$ ,  $\beta$  and  $\gamma$  globulin regions. Some of these sections and a spot of whole blood are shown in Figure 4.1. Specimens of the cathode end and the anode end of the strips beyond the protein regions were also taken to check the percentage loss of the gold in the process. All sections were individually sealed in polythene bags as shown in Figure 4.2.

B - Standard: As gold is present in the human blood in a concentration of about 0.4 - 4.5 p.p.m., so the amount of the gold required in the standard is about  $10^{-8}$  g. Several methods of preparing the standard have been described. Using a piece of gold foil is possible but this is difficult in practice because the weight needed is very small, about  $10^{-8}$  g, and if a larger gold foil were used the need to dissolve and dilute after irradiation to get the quantity wanted would involve the risk and inconvenience of working with the high activity obtained from irradiating a large piece of gold foil.

The following method, which was used in our project, was found to be convenient in preparing the standard we needed. The standard was made by taking 0.1 ml from a standard gold chloride solution prepared commercially for use in atomic absorption spectroscopy of concentration 1 mg/ml. This was then diluted with distilled water until a concentration  $10^{-8}$  g/10  $\mu$ L was obtained. The standards were then made by dropping 10  $\mu$ L of this on to pieces of filter paper and sealing in polythene envelopes.

All the samples from each patient were marked and together with a standard, were put together in a cylindrical polythene container, after being wiped with acetone to remove much of the surface contamination of the polythene packets.

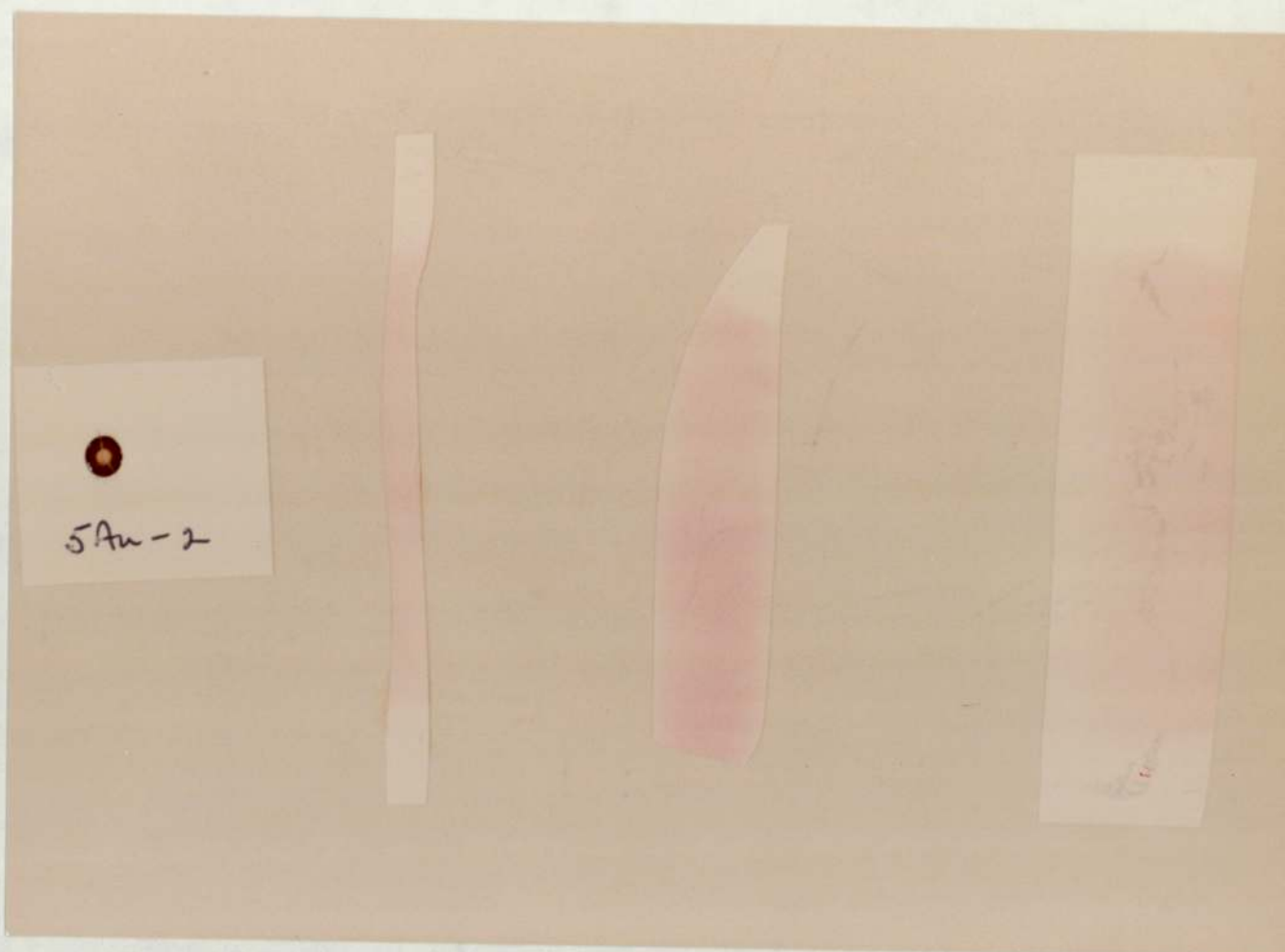


Figure 4.1 Some of the protein fractions and a spot of whole blood

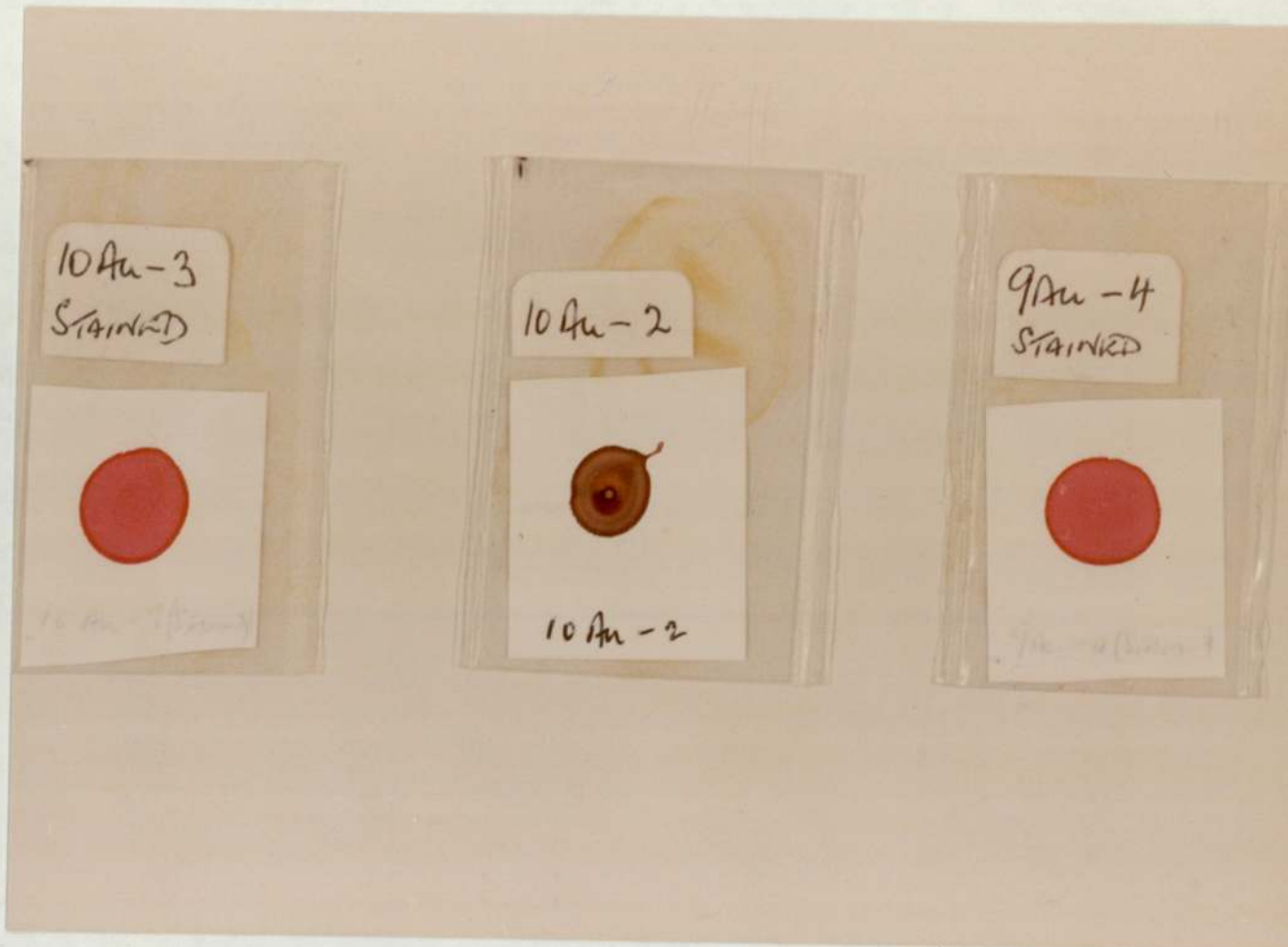


Figure 4.2 The samples sealed in polythene bags ready for irradiation.

#### 4.2 Irradiation Technique

As already described the blood specimens and the standard were sealed separately in small envelopes of thin polythene and were placed together in a clean polythene container, 2.5 cm in diameter and 7.5 cm long, sealed with a polythene plug. This kind of container is usually cleaned with a mixture of sulphuric and nitric acids (3:5) followed by rinsing with distilled water, or may just be washed with distilled water.

The irradiation process took place in either the London University Research Reactor, Ascot or, for the majority, the Universities Research Reactor, Risley. The reactors were run at a maximum thermal power of 100 kw. This power level was preferred because the temperature is less than  $100^{\circ}\text{C}$  which allowed us to use polythene rather than metal containers. Higher temperatures are reached at higher power levels and aluminium instead of polythene containers must be used which leads to very high activities of aluminium. This means a long period of time must elapse before it can be handled. The thermal neutron flux which is available in the vertical tube in the centre of the core is about  $2.3 \times 10^{12}$  n/cm<sup>2</sup>.sec. The polythene capsules were irradiated for seven hours. The irradiated samples were left to stand at the reactor site for five days until the activity was sufficiently low to make transport safe.

#### 4.3 Calibration of the Counting System

The counting system used included a NaI (Tl) Harshaw well-crystal type 7F8 of dimensions,  $1\frac{3}{4}$  in. high x 2 in. diameter, well  $1\frac{1}{2}$  in. deep x  $\frac{3}{4}$  in. diameter, attached to the photomultiplier tube as shown in

Figure 4.3. The signals were fed into a 252 multichannel analyser connected to a printer to print out the counts. The complete counting system is shown in Figure 4.4.

Before any measurement took place, calibration of the gamma-ray spectrometer was made by using three standard sources of,  $^{22}\text{Na}$ ,  $^{137}\text{CS}$ ,  $^{60}\text{CO}$  because the gold gamma-ray of energy 0.412 MeV lies close to the range of their gamma-rays energies. So from their pulse height spectrums, the gamma-rays energies could be plotted against the channel numbers corresponding to the photo peaks to show in which channel the gold gamma-ray of energy 0.412 MeV would be expected. Figures 4.5, 4.6 show typical calibration curves obtained at different times. As an example, the  $^{137}\text{CS}$  pulse height spectrum is shown in Figure 4.7. This was used to find the resolution of the counting system, it was calculated to be 12.5%. This resolution is not as good as with many NaI crystals, possibly because it was a well-crystal. However, in this project high sensitivity was more important than high resolution. Because the detector used is not efficient 100% and as the samples come on strips of cellulose acetate in 2.5 cm squares, the second step to consider was the variation of the efficiency with position within the crystal well. This efficiency calibration process was done by irradiating a small piece of gold foil with moderated neutrons from an Am-Be source. This gives the same  $^{198}\text{Au}$  activity as obtained in the reactor irradiation. Figure 4.8 shows the gold pulse height spectrum obtained.

Then the count rate of the photo peak was measured at different



Figure 4.3 The sodium iodide crystal and the photomultiplier tube.

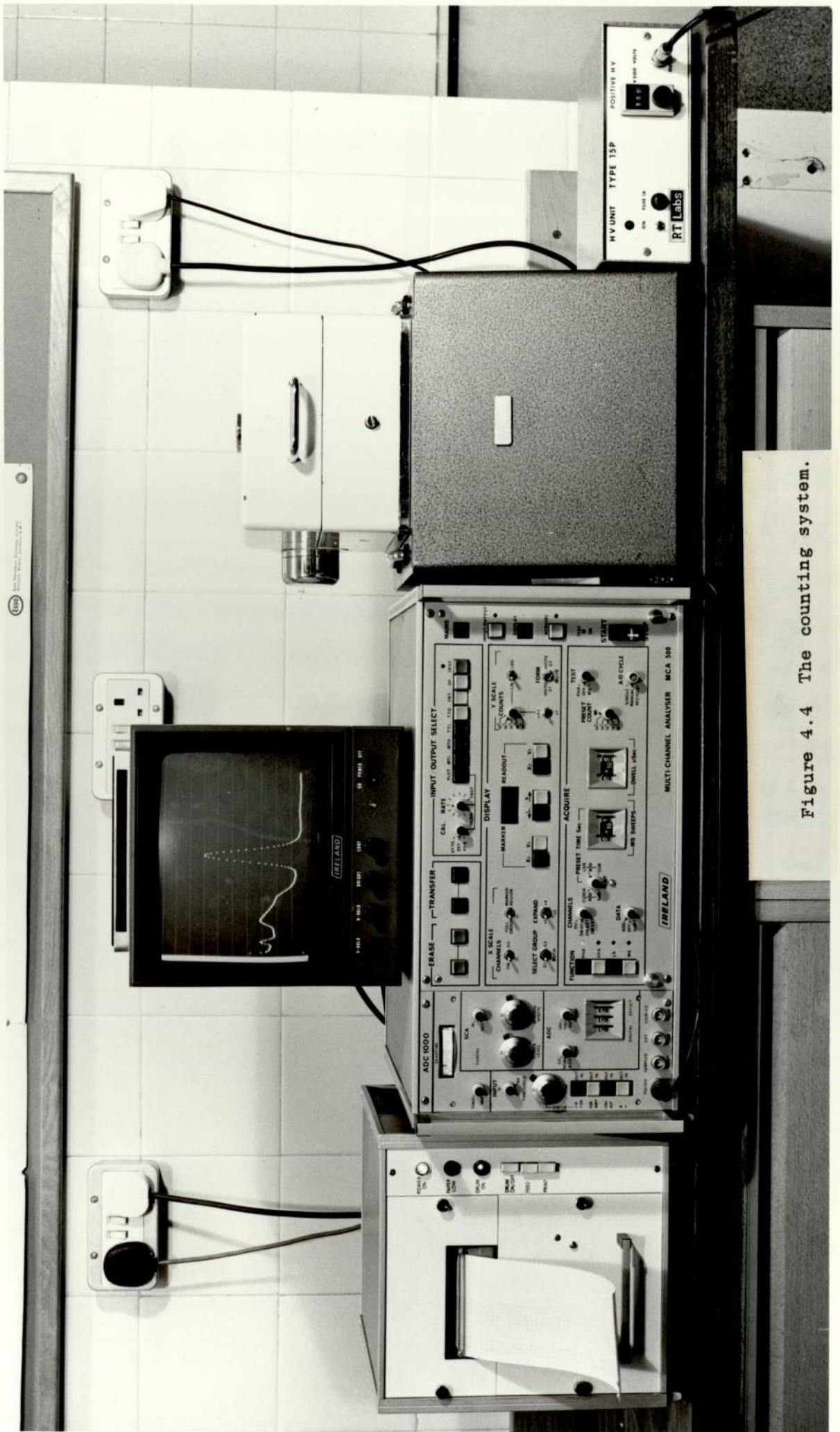


Figure 4.4 The counting system.

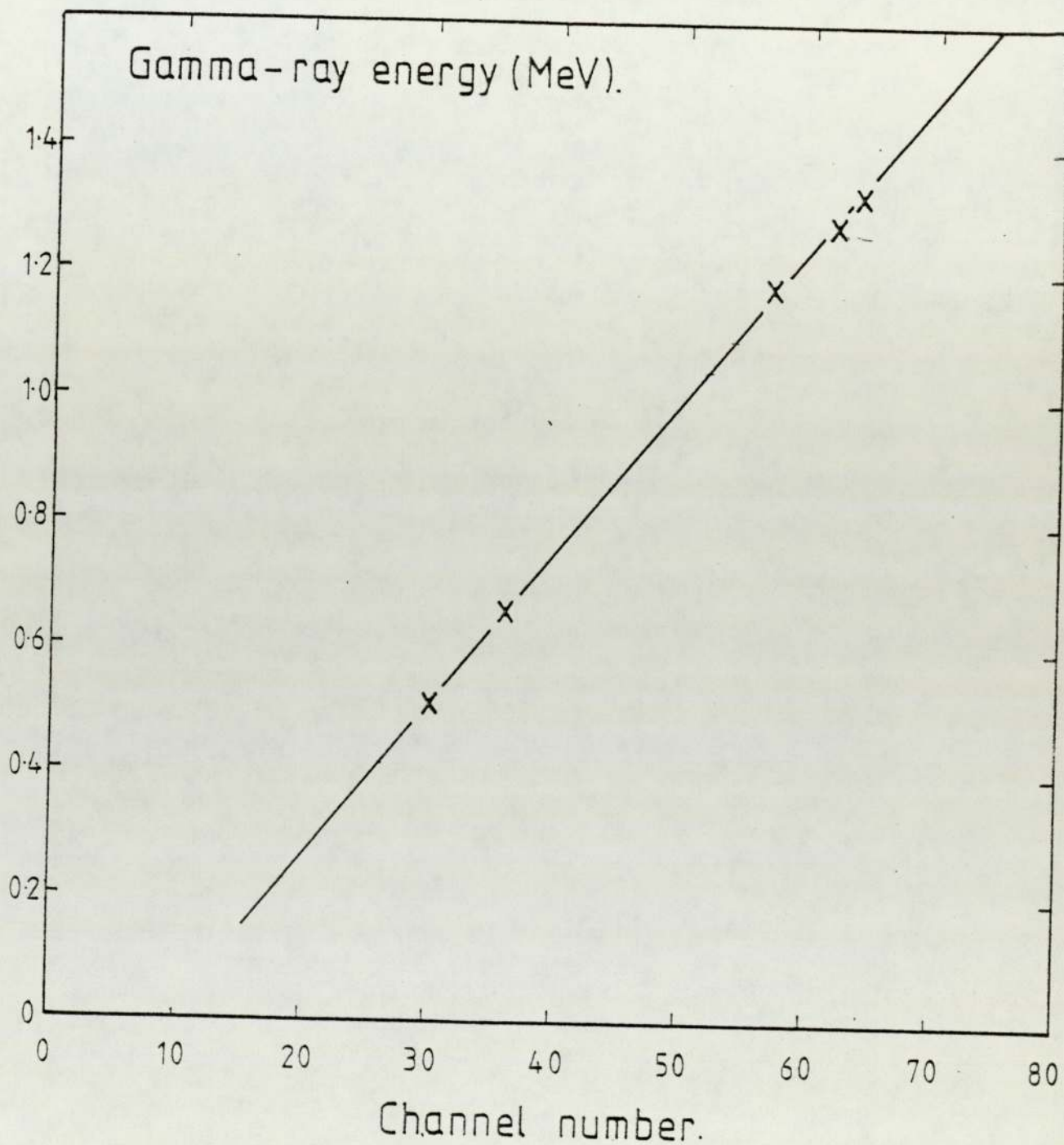


Figure 4.5 A calibration curve using  $^{22}\text{Na}$ ,  $^{137}\text{Cs}$ ,  $^{60}\text{Co}$  sources. The gold 0.412 MeV gamma-ray corresponds to channel number 26.

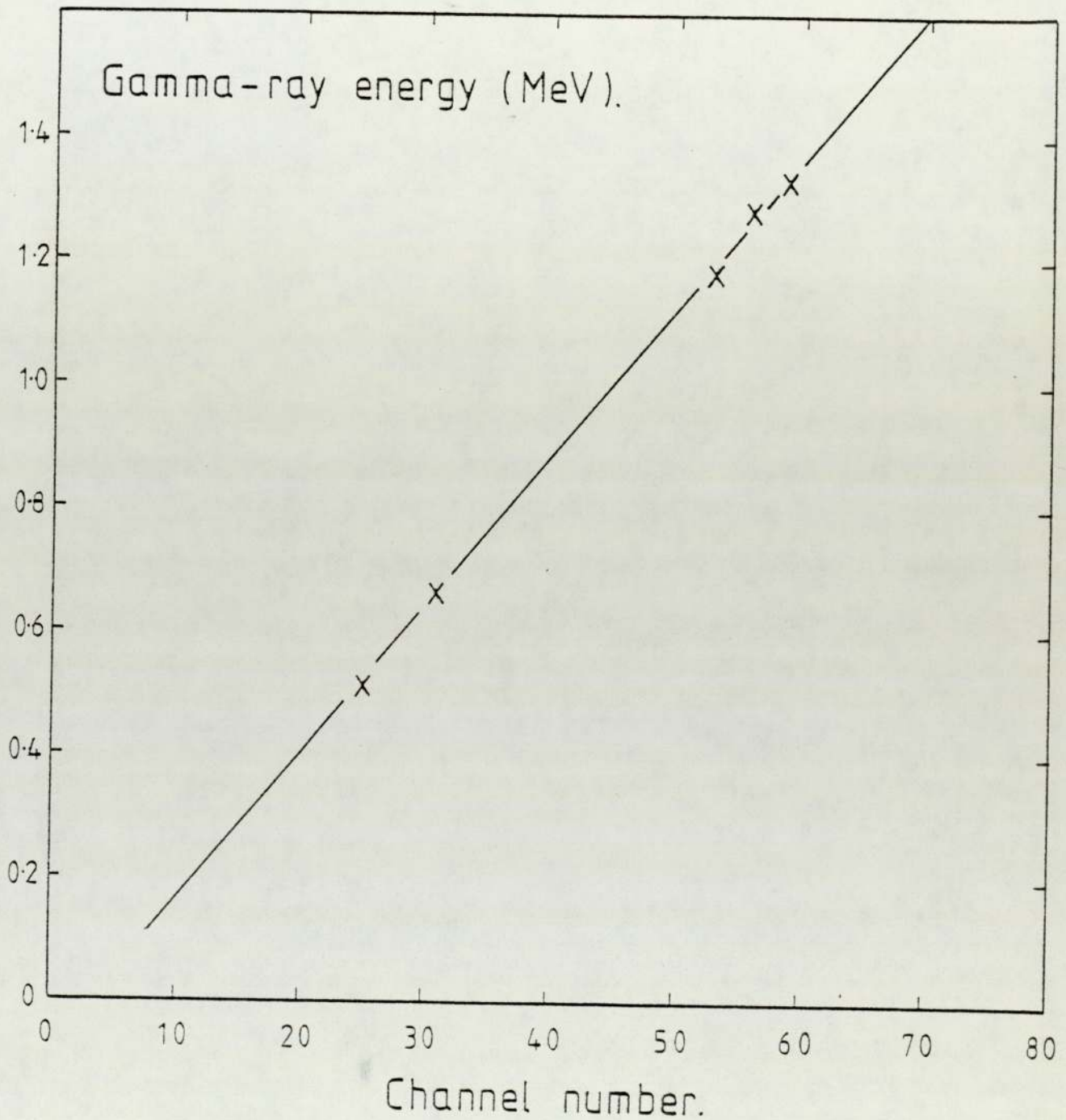


Figure 4.6 A calibration curve using  $^{22}\text{Na}$ ,  $^{137}\text{Cs}$ ,  $^{60}\text{Co}$  sources. The gold 0.412 MeV gamma-ray corresponds to channel number 21.

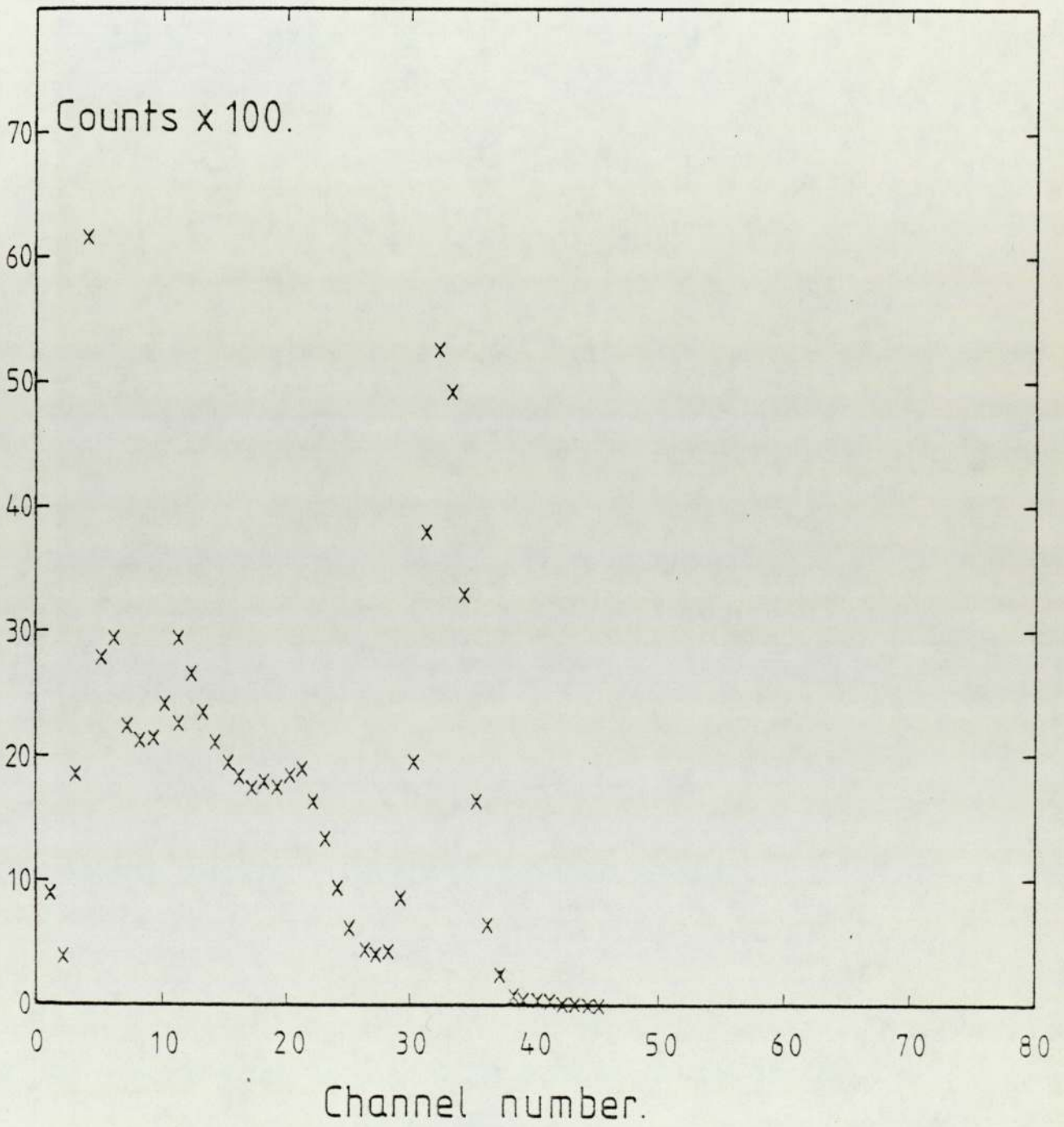


Figure 4.7 Pulse height spectrum of  $^{137}\text{Cs}$ .

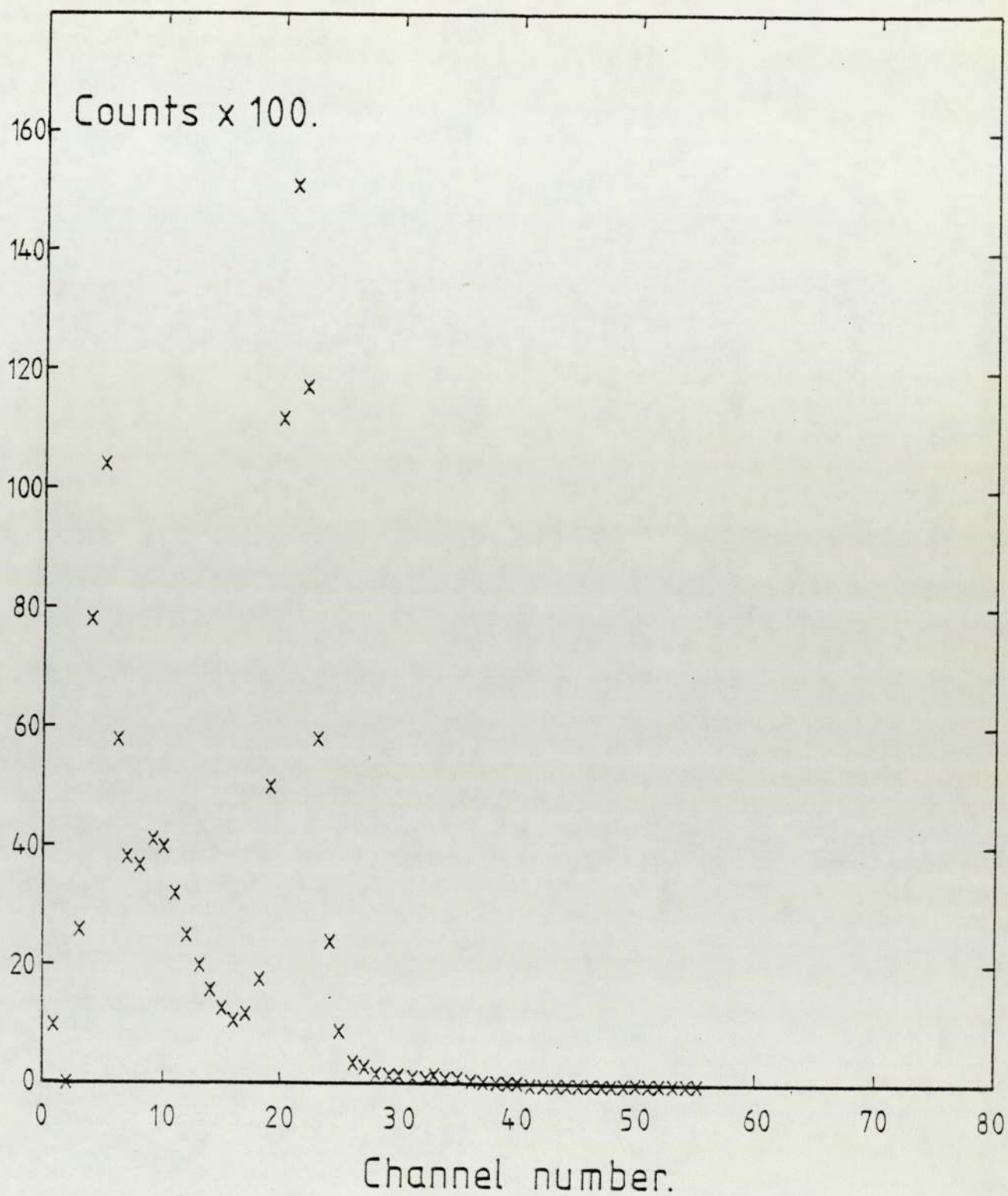


Figure 4.8 Pulse height spectrum of an irradiated gold foil.

specimen heights within the crystal well by placing the irradiated gold foil at various positions up to the top of the well. The ratio of the photo peak area at different heights, after correction for the background, to that at the zero position was plotted against the height to obtain the efficiency variation calibration curve, as shown in Figure 4.9. Also shown are points corresponding to calculations done by B. J. Snyder and Geza L. Gyorey (1965)<sup>63</sup>, which seem rather different from our results at some points, possibly because of the different assumptions and the conditions in their work. This efficiency calibration curve was used as a correction factor in our calculation. This was used to correct the area under the observed photo peak to estimate the real counts belonging to the activity.

#### 4.4 Methods of Determining Induced Activities

To determine the induced activities, the area under the photopeak of each spectrum has to be calculated. The method of choice for determination of the peak area depends on whether the gamma spectrum is complex, with many peaks, or the spectra contains no peaks other than from the activity of interest. In the first case of multicomponent gamma-ray spectra methods such as spectrum stripping and curve fitting are used.

In the second case another method of peak area determination was described by D. F. Covell (1959)<sup>67</sup>. He divided the area  $P$  by a line connecting the ordinate values of  $a_n$  and  $b_n$  as in Figure 4.10. Here the response of the channel containing the greatest number of counts is defined as  $a_0$ , and succeeding channel responses, progressing down the low amplitude side of the peak,

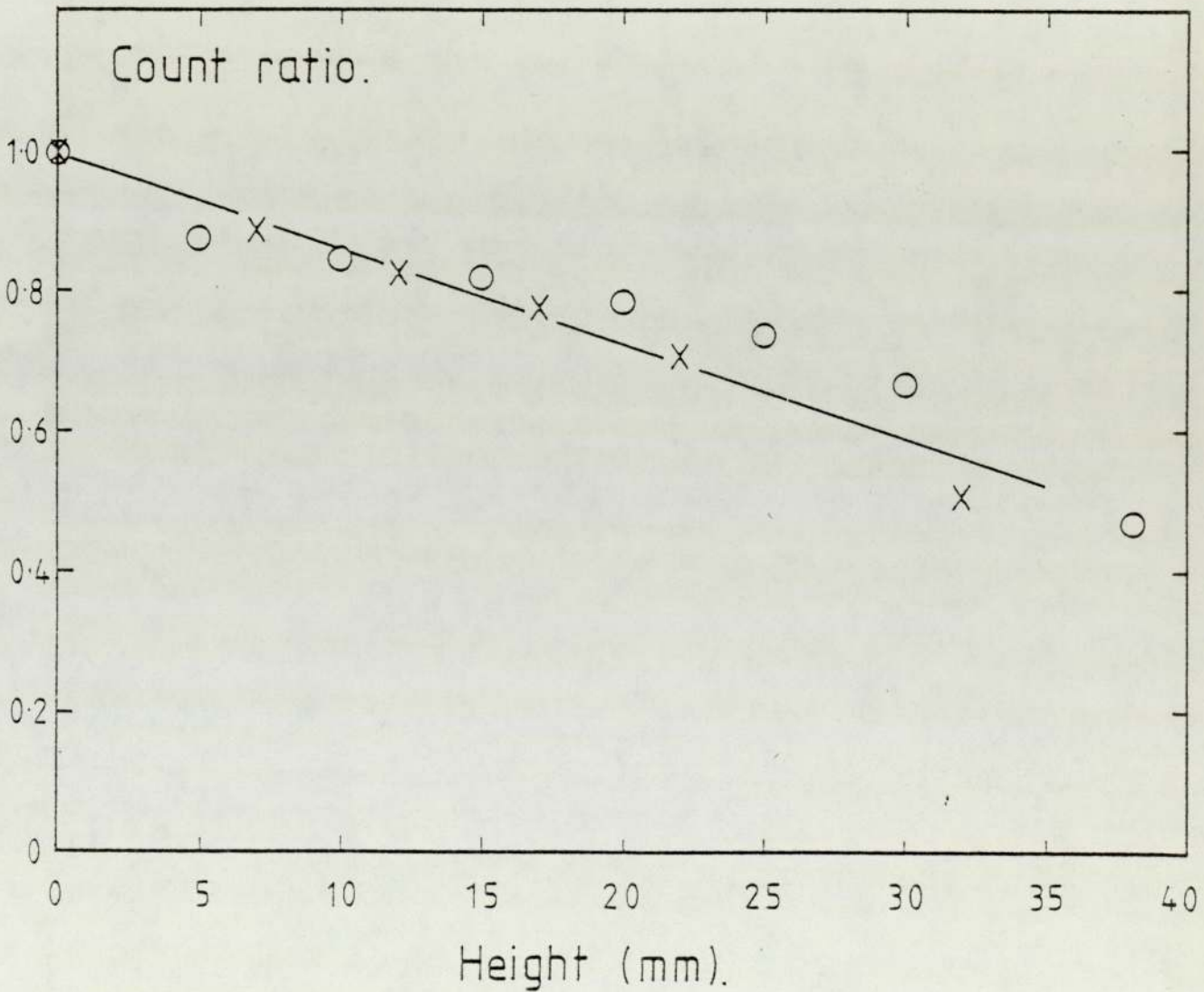


Figure 4.9 Efficiency calibration curve using an irradiated gold foil.  
 X - represent the results of the present work.  
 O - represent the results of reference 63.

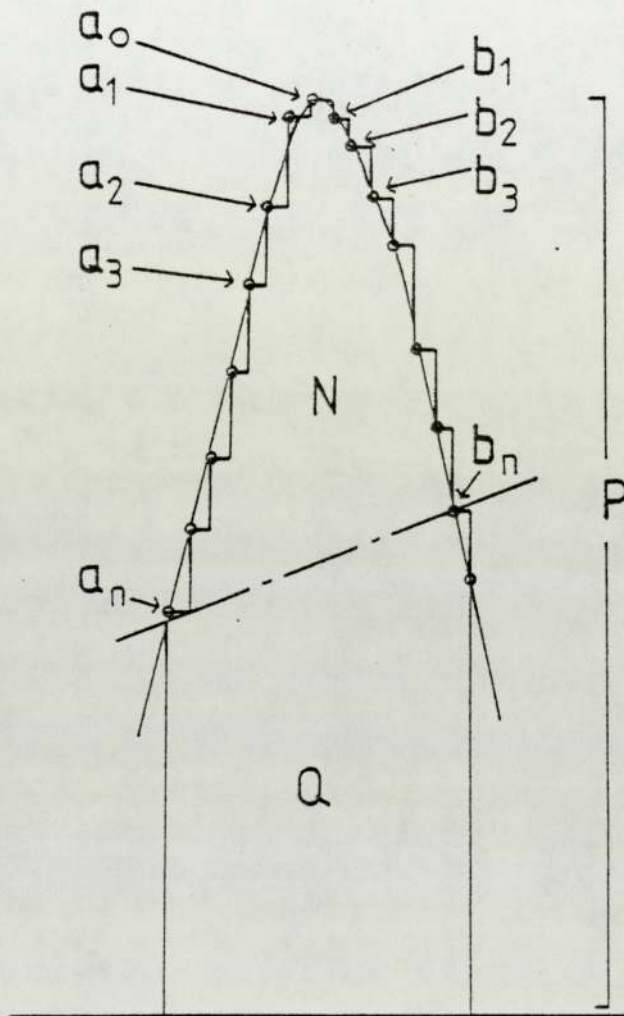


Figure 4.10 Method of Covell,  $N$  is the total counts contained in the peak channel,  $a_0$  and  $n$  channels on either side.

as  $a_1, a_2, a_3, \dots, a_n$ . Similarly, channel responses on the high amplitude side of the peak are defined as  $b_1, b_2, b_3, \dots, b_n$ . If the contributions from the  $a_0$  channel and the  $n$  channels on either side are added, the sum is a value representing the total counts contained in these channels; this value is graphically represented as the area  $P$  and is divided by a line connecting the ordinate values of  $a_n$  and  $b_n$ . The area above this line can be defined as

$$N = P - Q$$

From the graphical representation, expressions for  $P$  and  $Q$  can be written as follows:

$$P = a_0 + \sum_{i=1}^n a_i + \sum_{i=1}^n b_i$$

$$\text{and } Q = (n + \frac{1}{2}) (a_n + b_n)$$

$$\text{therefore } N = a_0 + \sum_{i=1}^n a_i + \sum_{i=1}^n b_i - (n + \frac{1}{2}) (a_n + b_n)$$

There are obvious limitations in the use of this method, particularly in determining the optimum selection of  $n$  and the interest area  $N$ , which comes from the total counts contained in peak channel,  $a_0$  and  $n$  channels on either side.

As this method seems more complicated than a simple base line subtraction method because of the need to be very careful in the choice of the  $n$  channels which lead to the estimate of  $N$  accurately, a simpler method was preferred. As we have simple gamma-ray spectrums with no indication that the background on

which the gold photopeak sits is not smooth, so the background under each photopeak could be estimated from the spectrum on either side of it. Then by subtracting the average of the counts in, say, three channels to both left and right of the peak from each channel of the peak, the background could be eliminated. The selection of the photopeak boundary channels, between which the channel counts were summed to obtain the area under the photopeak must be constant for a given gamma energy in all spectra which are compared. After background elimination, the counts in the channels belonging to the peak were added together and the following calculations were made:

1. The counts were corrected for decay corresponding to the time difference between counting each sample and counting the standard.
2. Corrections were made for the effect of different sample positions in the well of the crystal.
3. The observed count rates were converted to the masses of gold by comparison with the count rate of the standard.
4. The statistical errors were calculated.

All these calculations were computed by using the computer programme described in the appendix.

In general the accuracy of a measurement refers to the closeness of the measurement to the actual value or the real value of the physical quantity, and it becomes high as the errors become small. In the present work two sources of errors are possible, the statistical error which may be calculated from the numbers of counts observed and the errors which arise

from the cutting of the electrophoresis strip into its sections. This is less easy to assess, but it has been estimated that it may cause an error of about a few percent.

#### 4.5 Counting Procedure

After the calibration was done, the background was counted. The spectrum of the counts against channel number is given in Figure 4.11 which shows no obvious peaks appeared in it. The sources of the background are:

- i. External radiations, for example, cosmic rays, radioactivity in building materials etc.
- ii. Noise occurring in electronic devices, including the photomultipliers and amplifiers.
- iii. Natural activity in the materials used for the construction of the counter.

After the background had been counted, the irradiated standard and each sample were counted for 50 minutes. This was after they had been left to cool down for about five days at the reactor to allow interfering activities, particularly  $^{24}\text{Na}$ , usually present in the blood and also as a contaminant, to decay to a low level.

##### 4.5.1 Qualitative Analysis of the Gamma-ray Spectrum

Figure 4.12 shows a pulse height spectrum from one of standards. The large peak in channel number 26 corresponds to 0.412 MeV radiation. By following the decay of this activity the half-life was found to be approximately 2.7 days which together with the energy identified it as the gold activity. The very small peak at channel number 63 corresponds to an

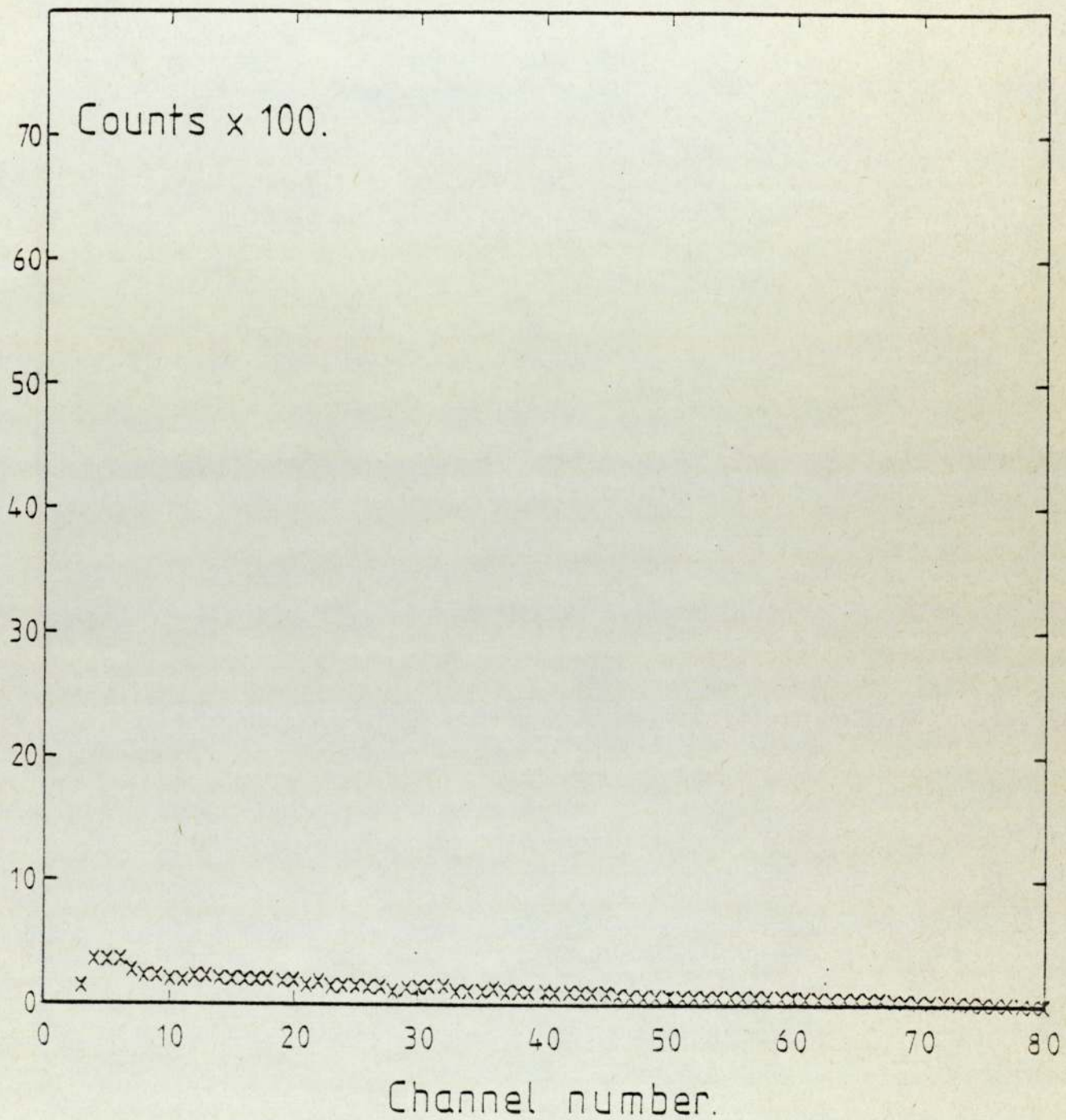


Figure 4.11 Pulse height spectrum of the background

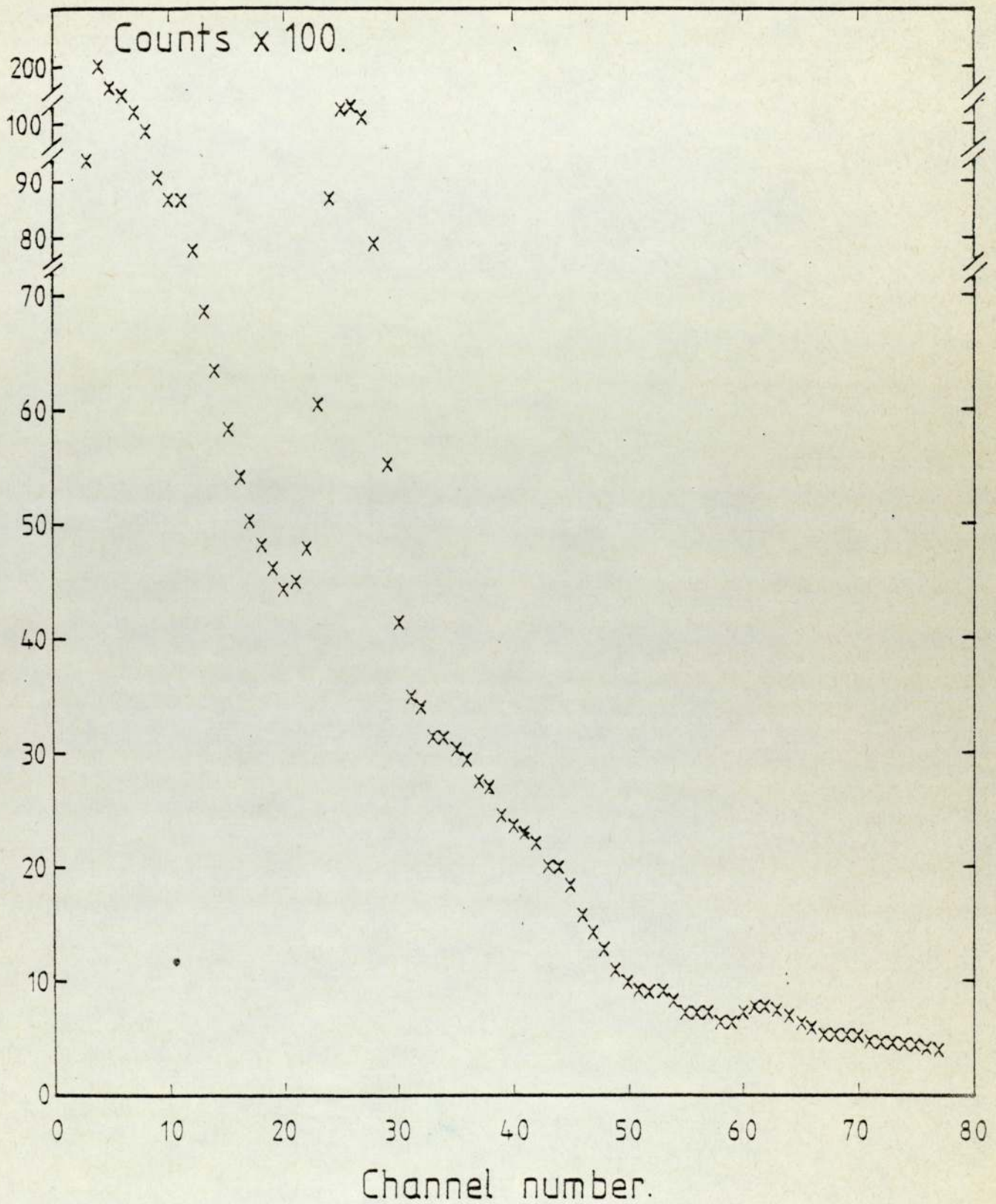


Figure 4.12 Pulse height spectrum of gold activity in a standard showing a very small residual sodium activity.

energy of 1.28 MeV which was identified to be due to  $^{24}\text{Na}$  which has a gamma-ray of energy 1.28 MeV and a half-life of 15 hours. This was assumed to come from a small residual contamination.

As an example the pulse height spectrum of each sample from patient number five obtained by plotting the counts against the channel numbers are shown in the Figures 4.13 - 4.22. All the Figures show a clear peak belonging to the gold activity, gamma-ray energy 0.412 MeV, at channel number 26. Also a very small peak corresponding to an energy 1.28 MeV belonging to the  $^{24}\text{Na}$  activity. Figures 4.14 and 4.15 show that the serum and plasma have nearly the same counts under the gold peak, while Figure 4.13 shows the pulse height spectrum of whole blood which seems to have a gold peak equal to about  $\frac{3}{4}$  of the plasma gold peak. Figures 4.16, 4.17, 4.18, 4.19, 4.20 and 4.21 which show the pulse height spectrums of the various protein fractions, show that the albumin fraction has the largest gold peak, and each of the others has a relatively small gold peak. Figure 4.22 shows the pulse height spectrum of the blood cells, which again shows a small gold peak. Figures 4.23 and 4.24 are the pulse height spectrums of the cathode and anode ends of the electrophoresis strip. They show a significant amount of gold. As a check on reproducibility measurements were duplicated on different plasma samples from one patient. The pulse height spectrums in Figures 4.25 and 4.26 show an example of how well they agree with each other.

#### 4.5.2 Contaminations in Some Samples

Figure 4.27 shows the pulse height spectrum of the prealbumin plus anode end from patient number 21. It shows a very clear, large peak at channel number 54 corresponding to an energy of 1.1 MeV. By studying the activity one week, two and three weeks later, no difference in the observed peak was found which means that this activity has a long half-life. Similar observations were found with patients number 20 and 22.

Figure 4.28 shows the pulse height spectrum of a blood sample from patient number 1. It shows two peaks at channel numbers 33 and 41 corresponding to gamma energies of 0.58 MeV and 0.77 MeV respectively. The decay of these peaks was followed for a few days and the half-life calculated to be about 36 hours. These unknown activities are discussed later in chapter 5.

#### 4.5.3 Quantitative Results

The results obtained for the gold bound to the blood samples taken from twelve patients, are all shown in Tables 4.1 and 4.2 and 4.3. For the first nine patients, Table 4.1 gives the ratio of gold content in each serum, whole blood, and blood cells specimen to that in the plasma, and also in the total protein fractions to that in serum. While Table 4.2 shows the gold content in the total protein fractions and the concentration ratio of the gold content in each protein fraction and in the anode and cathode ends to that in the total protein fractions.

The results for patient number 20, 21 and 22 are given in a separate table (Table 4.3) because the globulins came together in one section for each of them. The significance of the results is discussed in the next chapter.

Table 4.1

Gold content in the serum and the concentration ratios

Patient number	1	2	3	4	5
Serum in g/10 $\mu$ L	$(1.14 \pm .05)10^{-7}$	$(2.87 \pm .1)10^{-7}$	$(7.88 \pm .15)10^{-8}$	$(6.4 \pm .16)10^{-9}$	$(2.5 \pm .06)10^{-8}$
Plasma : serum	1.05 $\pm$ .11	1 $\pm$ .2	1.05 $\pm$ .3	.92 $\pm$ .3	.97 $\pm$ .11
Whole blood : plasma	.75 $\pm$ .08	.6 $\pm$ .11	.78 $\pm$ .25	.96 $\pm$ .32	.62 $\pm$ .07
Cells : plasma	.08 $\pm$ .006	.02 $\pm$ .002	.02 $\pm$ .002	.2 $\pm$ .03	.05 $\pm$ .005
Total Fractions: serum	.9 $\pm$ .08	.92 $\pm$ .06	.87 $\pm$ .03	.65 $\pm$ .06	.69 $\pm$ .1

Patient number	7	8	9	10
Serum in g/10 $\mu$ L	$(2.4 \pm .05)10^{-7}$	$(1.49 \pm .04)10^{-7}$	$(5.06 \pm .14)10^{-8}$	$(6.4 \pm .18)10^{-8}$
Plasma : serum	.93 $\pm$ .09	1.1 $\pm$ .09		
Whole blood : plasma	.99 $\pm$ .09	.92 $\pm$ .07	.76 $\pm$ .2	.88 $\pm$ .32
Cells : plasma	-	-	-	-
Total Fractions : serum	.72 $\pm$ .04	.85 $\pm$ .03	.82 $\pm$ .05	.79 $\pm$ .04

The errors quoted are the statistical errors



Table 4.2

Gold content in the total protein fractions and the concentration ratios of gold content of individual protein fractions as a proportion of the total protein-bound gold

Patient number	1	2	3	4	5
Total Fractions (T.F) in g/10 $\mu$ L	$(1.03 \pm .08)10^{-7}$	$(2.65 \pm .06)10^{-7}$	$(6.87 \pm .07)10^{-8}$	$(4.15 \pm .18)10^{-9}$	$(1.72 \pm .15)10^{-8}$
Prealbumin : T.F	.017 $\pm$ .001	.08 $\pm$ .004	.025 $\pm$ .003	.1 $\pm$ .03	.07 $\pm$ .01
Albumin : T.F	.75 $\pm$ .1	.73 $\pm$ .06	.82 $\pm$ .16	.31 $\pm$ .09	.69 $\pm$ .15
$\alpha_1$ -globulin : T.F	.014 $\pm$ .001	.075 $\pm$ .006	.04 $\pm$ .005	.09 $\pm$ .02	.035 $\pm$ .006
$\alpha_2$ -globulin : T.F	.09 $\pm$ .009	.03 $\pm$ .002	.04 $\pm$ .005	.1 $\pm$ .03	.03 $\pm$ .006
$\beta$ -globulin : T.F	.05 $\pm$ .005	.038 $\pm$ .002	.04 $\pm$ .006	.2 $\pm$ .07	.035 $\pm$ .007
$\gamma$ -globulin : T.F	.08 $\pm$ .009	.019 $\pm$ .001	.035 $\pm$ .005	.16 $\pm$ .06	.127 $\pm$ .026
Anode end : T.F					
Cathode end : T.F					

The errors quoted are the statistical errors

Table 4.2 (continued)

Patient number	7	8	9	10
Total Fractions (T.F) in g/10 $\mu$ L	$(1.72 \pm .03)10^{-7}$	$(9.83 \pm .04)10^{-8}$	$(4.15 \pm .08)10^{-8}$	$(5.05 \pm .07)10^{-8}$
Prealbumin : T.F	.003 $\pm$ .0001	zero	zero	.02 $\pm$ .002
Albumin : T.F	.85 $\pm$ .04	.96 $\pm$ .27	.93 $\pm$ .19	.9 $\pm$ .1
$\alpha_1$ -globulin : T.F	.02 $\pm$ .0006	.004 $\pm$ .0003	.001 $\pm$ .0001	.035 $\pm$ .004
$\alpha_2$ -globulin : T.F	.04 $\pm$ .001	.03 $\pm$ .003	.035 $\pm$ .004	.003 $\pm$ .0004
$\beta$ -globulin : T.F	.03 $\pm$ .001	zero	.02 $\pm$ .002	.02 $\pm$ .002
$\gamma$ -globulin :T.F	.048 $\pm$ .001	.005 $\pm$ .0004	.01 $\pm$ .001	.02 $\pm$ .003
Anode end : T.F	.058 $\pm$ .002	.046 $\pm$ .005	zero	.17 $\pm$ .027
Cathode end : T.F	.038 $\pm$ .001	.04 $\pm$ .005	.117 $\pm$ .02	.1 $\pm$ .015

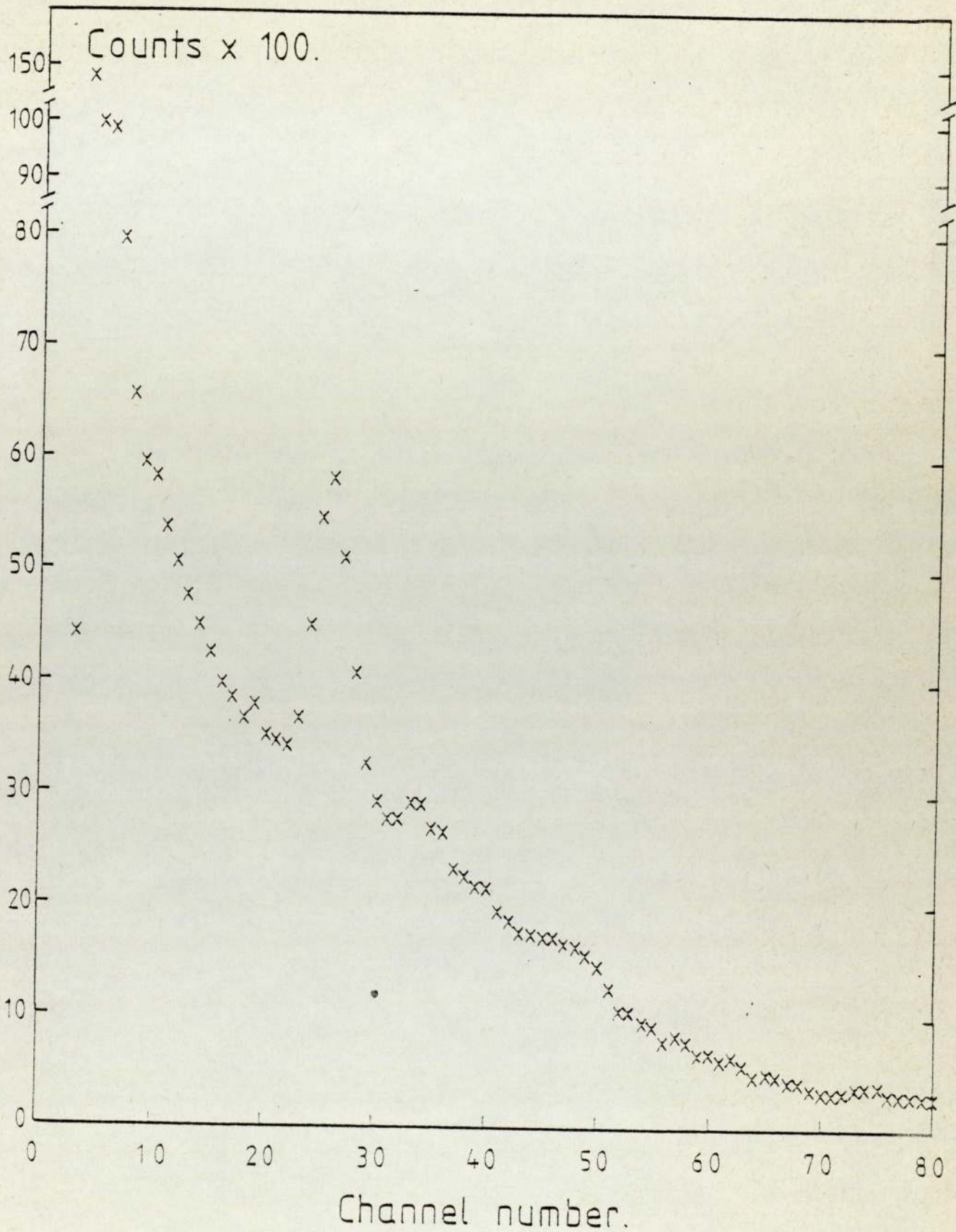
The errors quoted are the statistical errors

Table 4.3

Gold content in the total protein fractions and the concentration ratios of gold content of individual protein fractions as a proportion of the total protein-bound gold

Patient number	20	21	22
Total Fractions (T.F) in g/10 $\mu$ L	$(4.55 \pm .04)10^{-8}$	$(.79 \pm .08)10^{-8}$	$(2.68 \pm .07)10^{-8}$
Prealbumin plus anode end : T.F	zero	zero	zero
Albumin : T.F	$.87 \pm .07$	1	$.82 \pm .12$
Globulins plus cathode end : T.F	$.12 \pm .01$	zero	$.17 \pm .02$
Concentration ratios			
Whole blood : plasma	$.77 \pm .32$	$.73 \pm .09$	$.54 \pm .17$
Cells : plasma	$.31 \pm .11$	$.76 \pm .11$	$.007 \pm .001$
T.F : plasma	$.51 \pm .13$	$.46 \pm .05$	$.41 \pm .1$

The errors quoted are the statistical errors



4.13 Pulse height spectrum of the whole blood specimen from patient number five showing the gold activity in channel number 26.

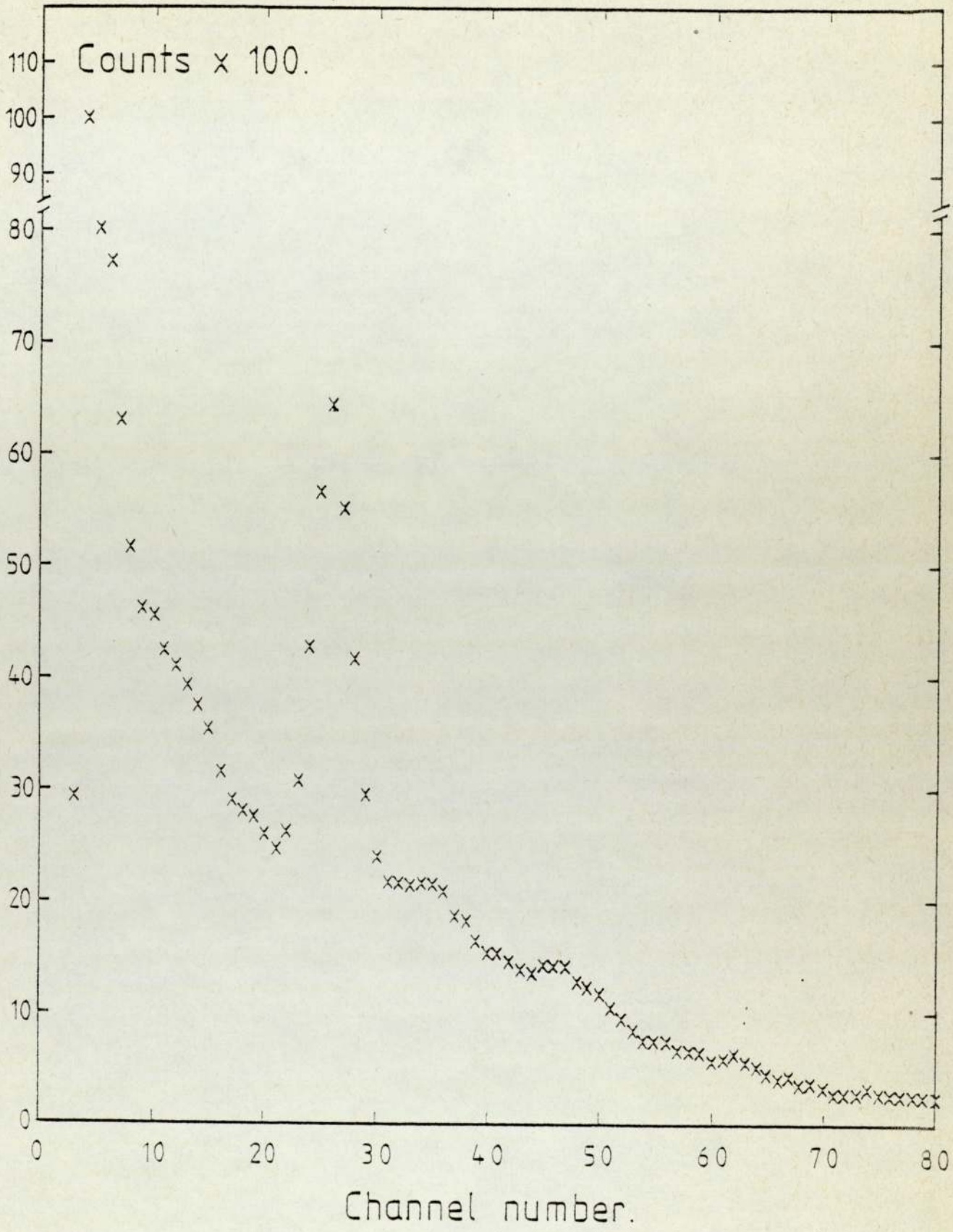


Figure 4.14 Pulse height spectrum of the serum specimen from patient number five showing the gold activity in channel number 26.

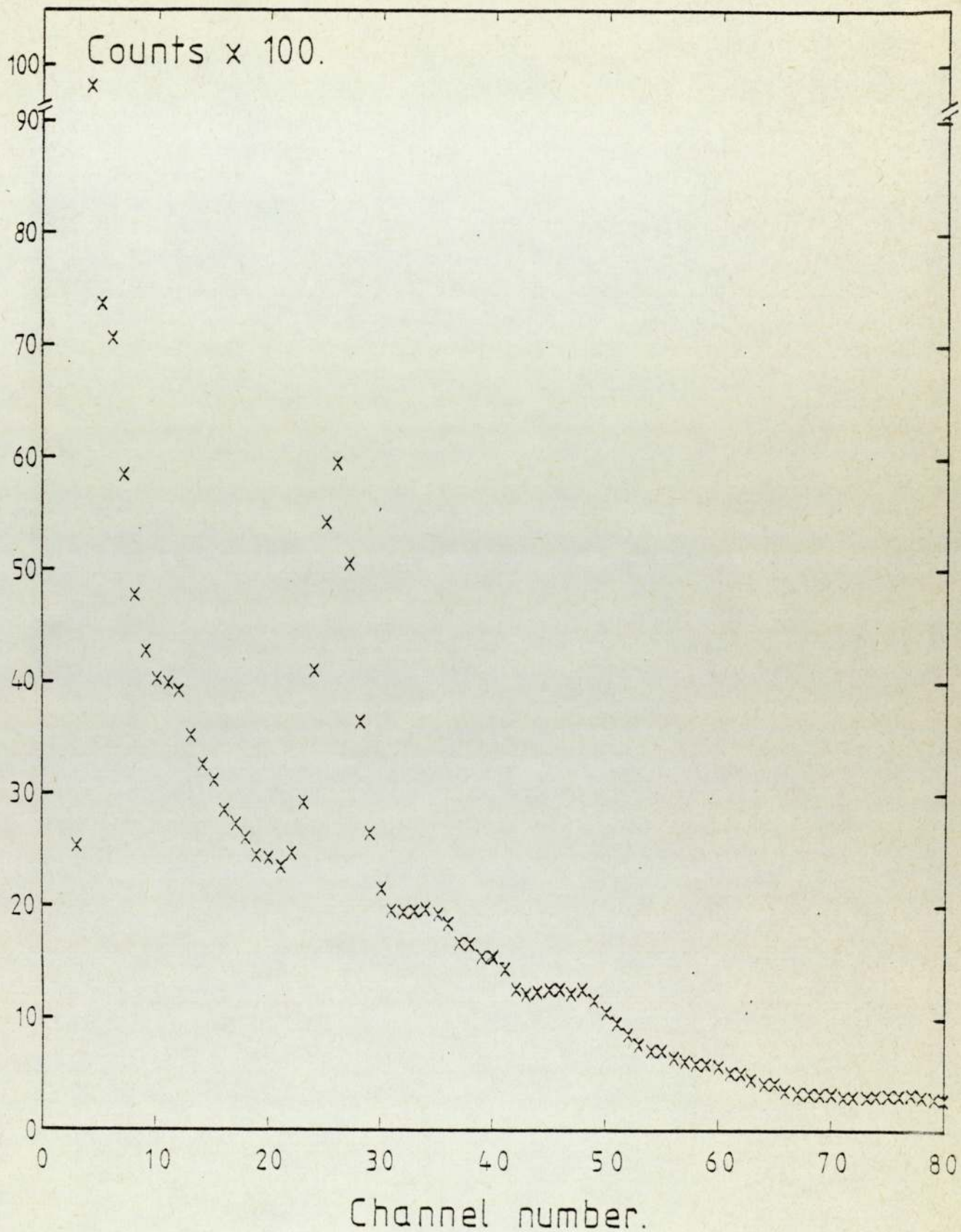


Figure 4.15 Pulse height spectrum of the plasma specimen from patient number five showing the gold activity in channel number 26.

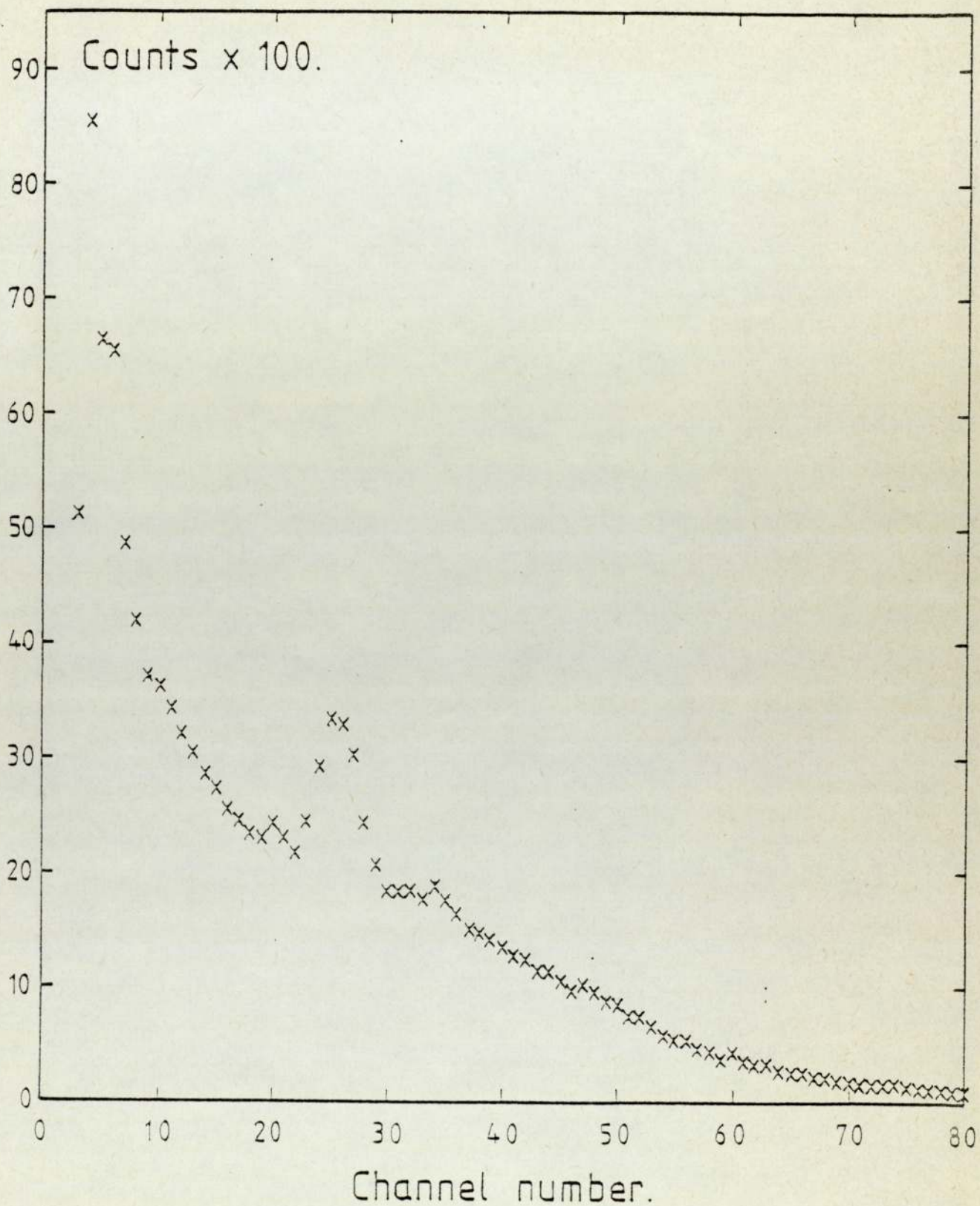


Figure 4.16 Pulse height spectrum of the albumin region from patient number five showing the gold activity in channel number 26.

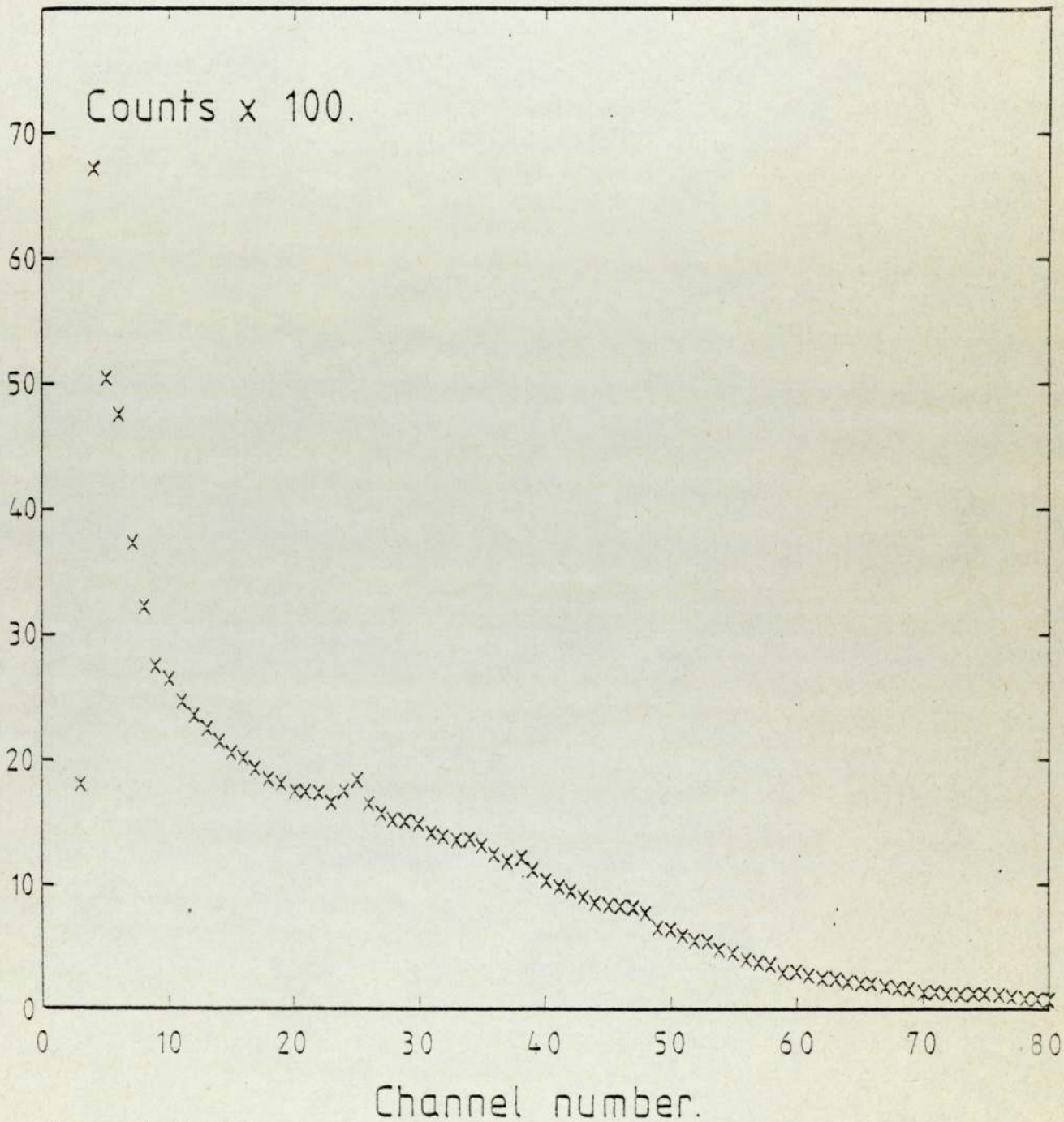


Figure 4.17 Pulse height spectrum of the prealbumin region from patient number five showing the gold activity in channel number 26.

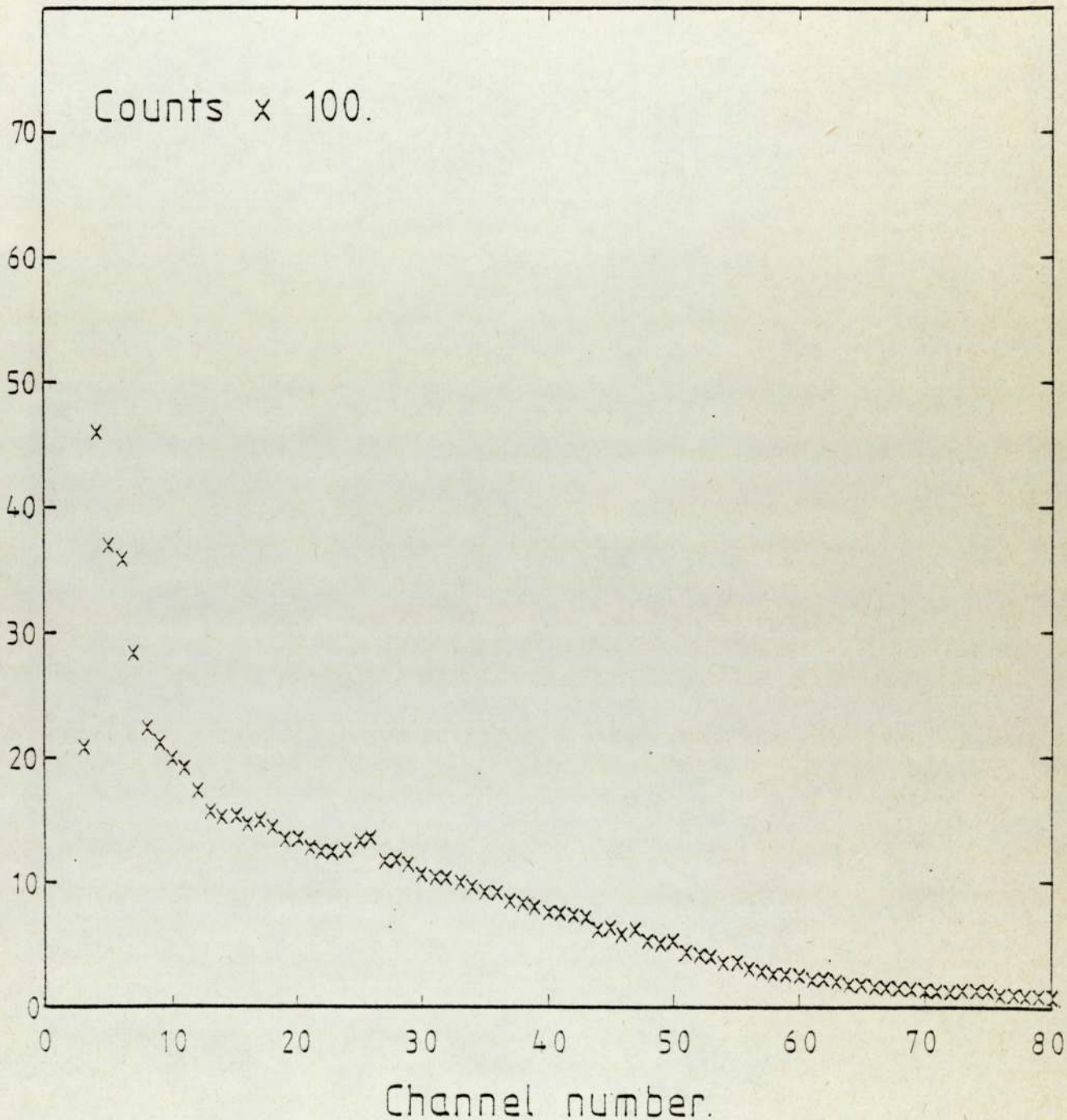


Figure 4.18 Pulse height spectrum of the  $\alpha_1$ -globulin region from patient number five showing the gold activity in channel number 26.

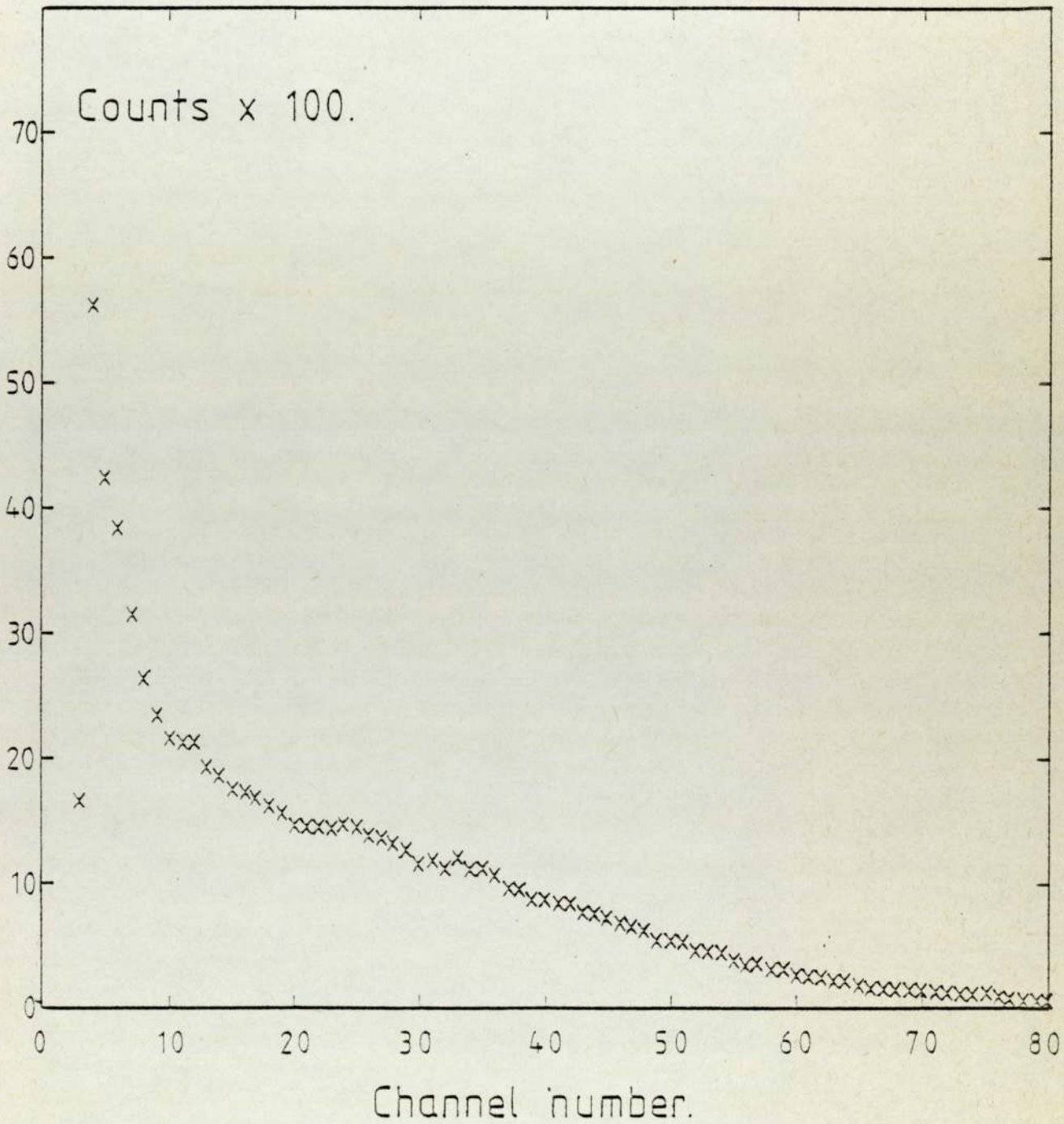


Figure 4.19 Pulse height spectrum of the  $\alpha_2$ -globulin region from patient number five showing the gold activity in channel number 26.

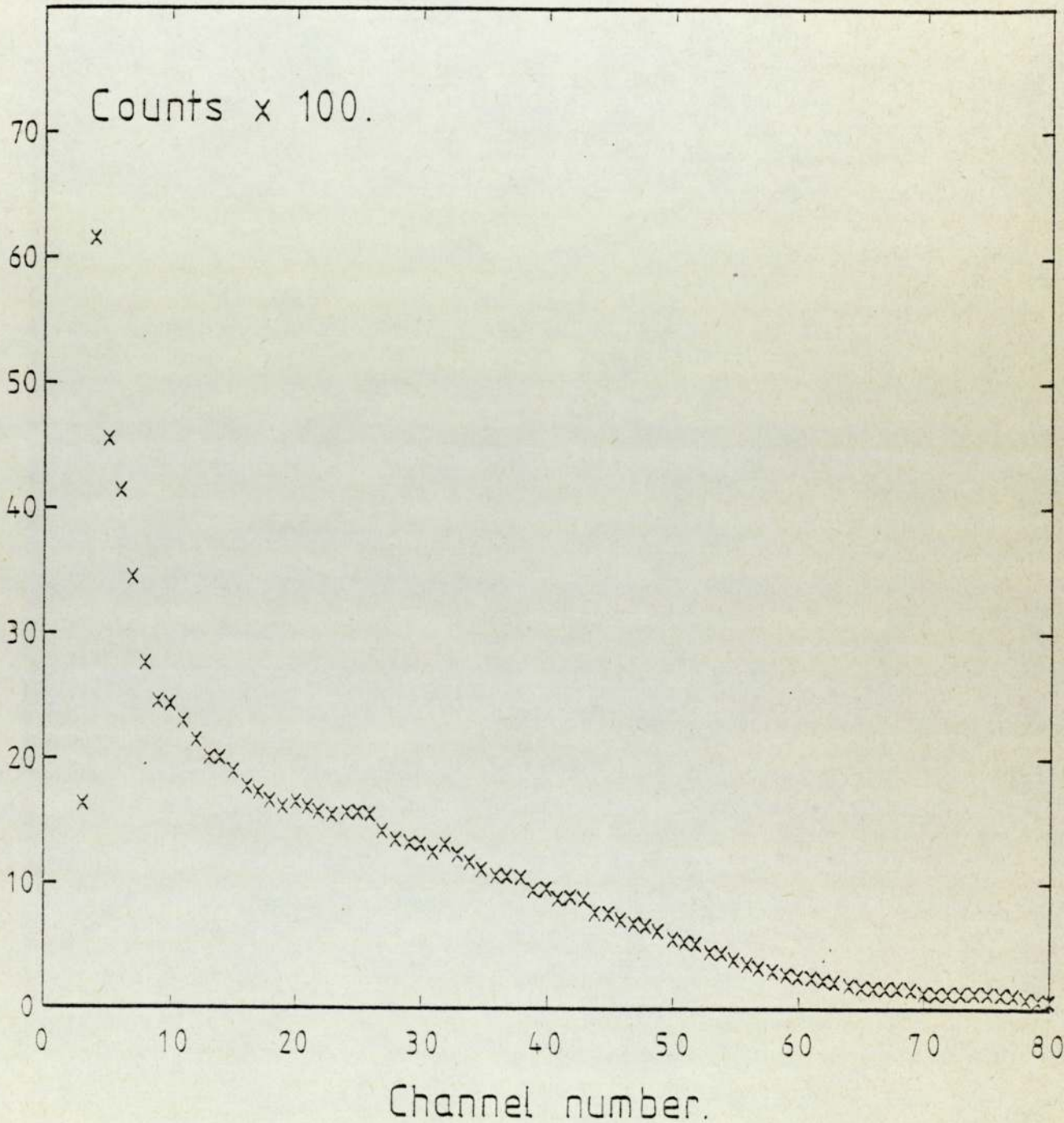


Figure 4.20 Pulse height spectrum of the 3-globulin region from patient number five showing the gold activity in channel number 26.

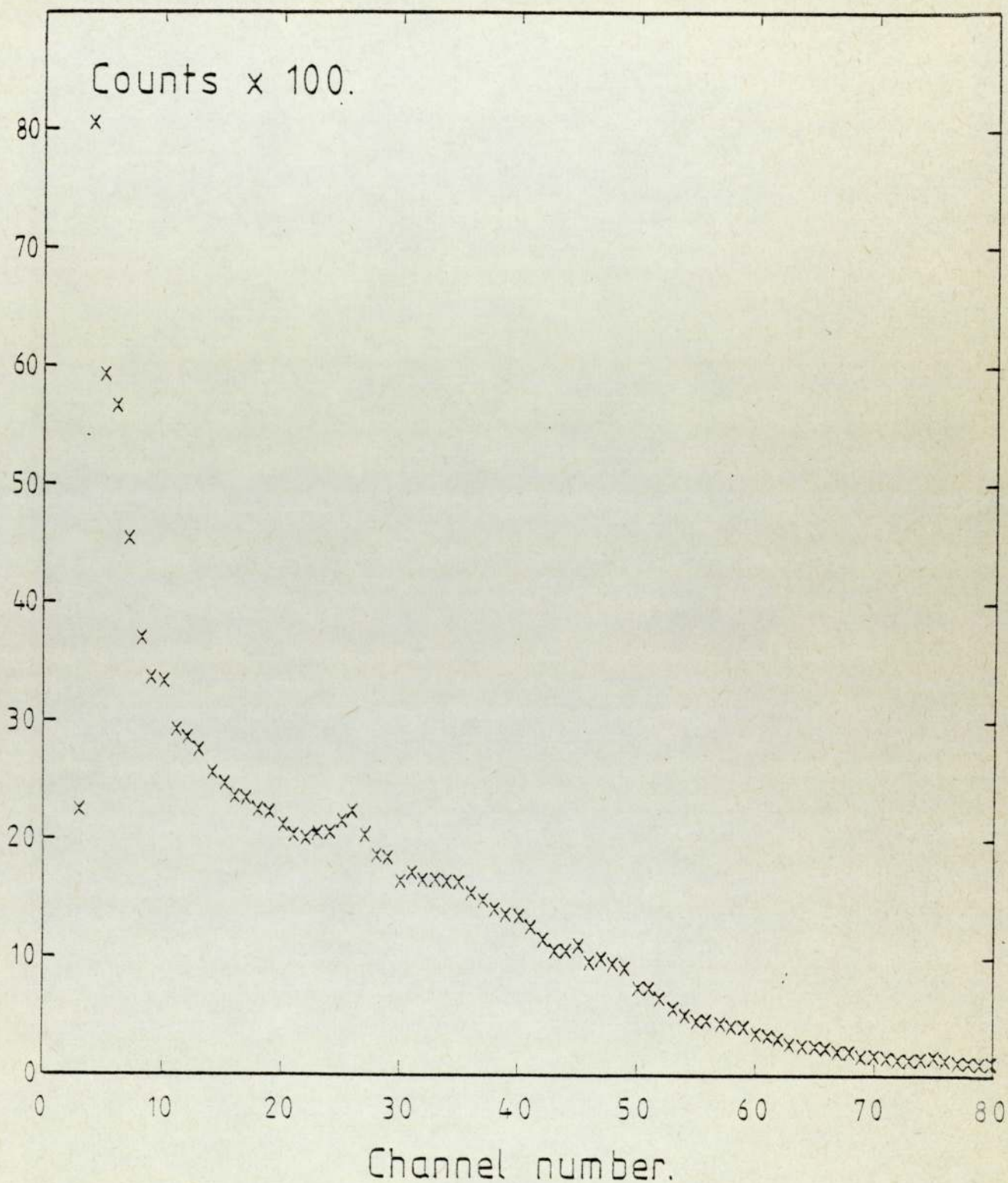


Figure 4.21 Pulse height spectrum of the  $\gamma$ -globulin region from patient number five showing the gold activity in channel number 26.

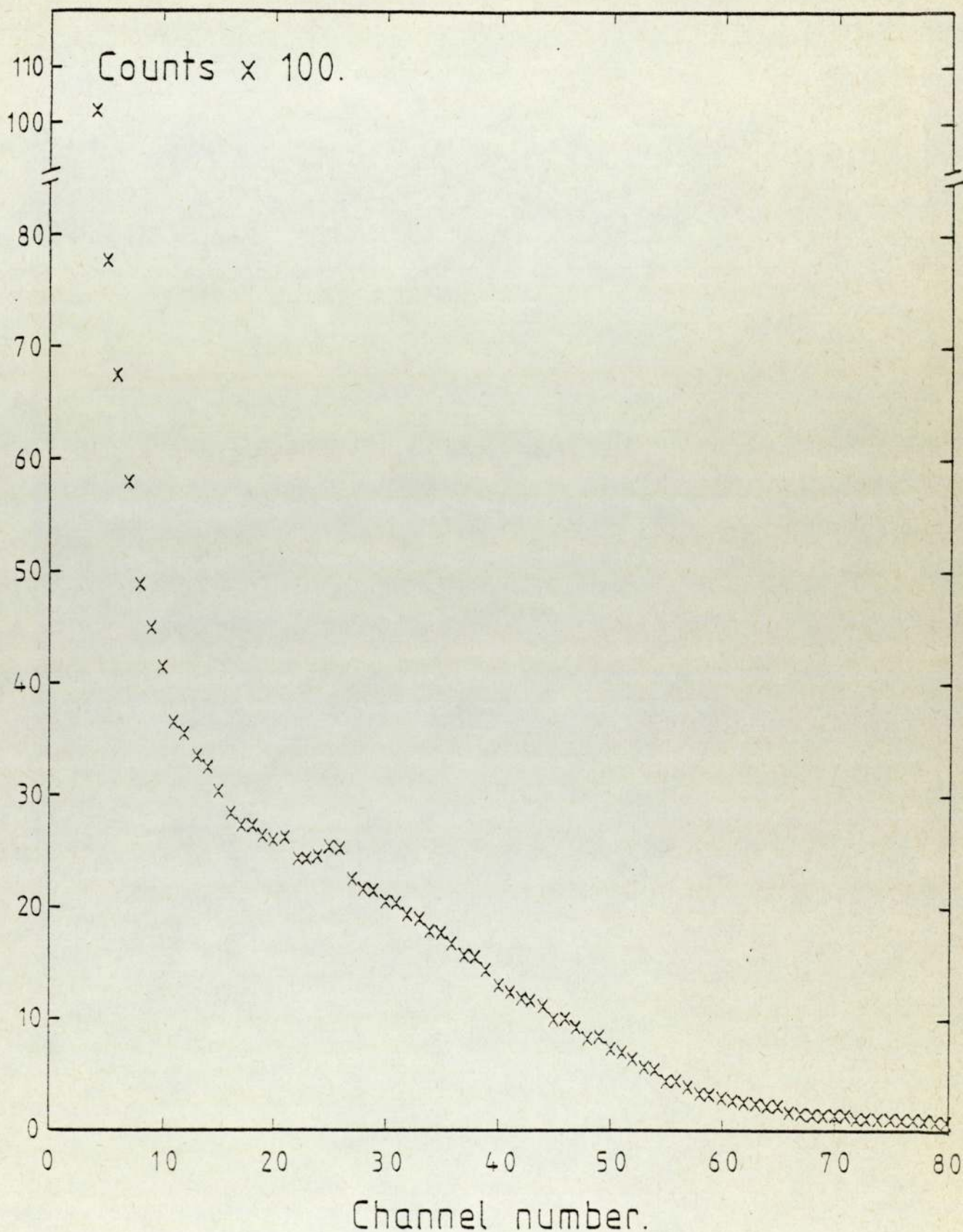


Figure 4.22 Pulse height spectrum of the blood cells from patient number five showing the gold activity in channel number 26.

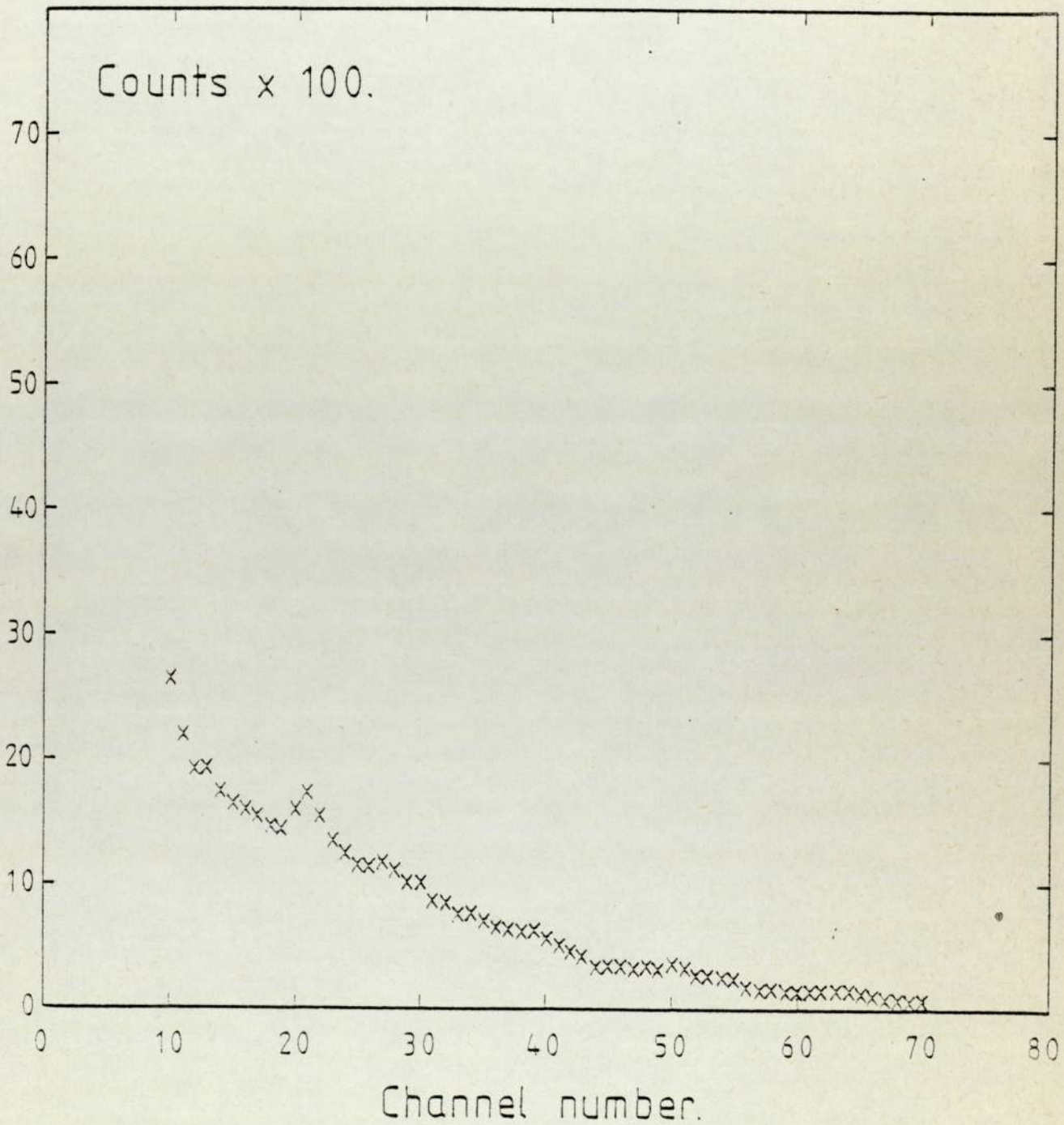


Figure 4.23 Pulse height spectrum of a cathode-end specimen.

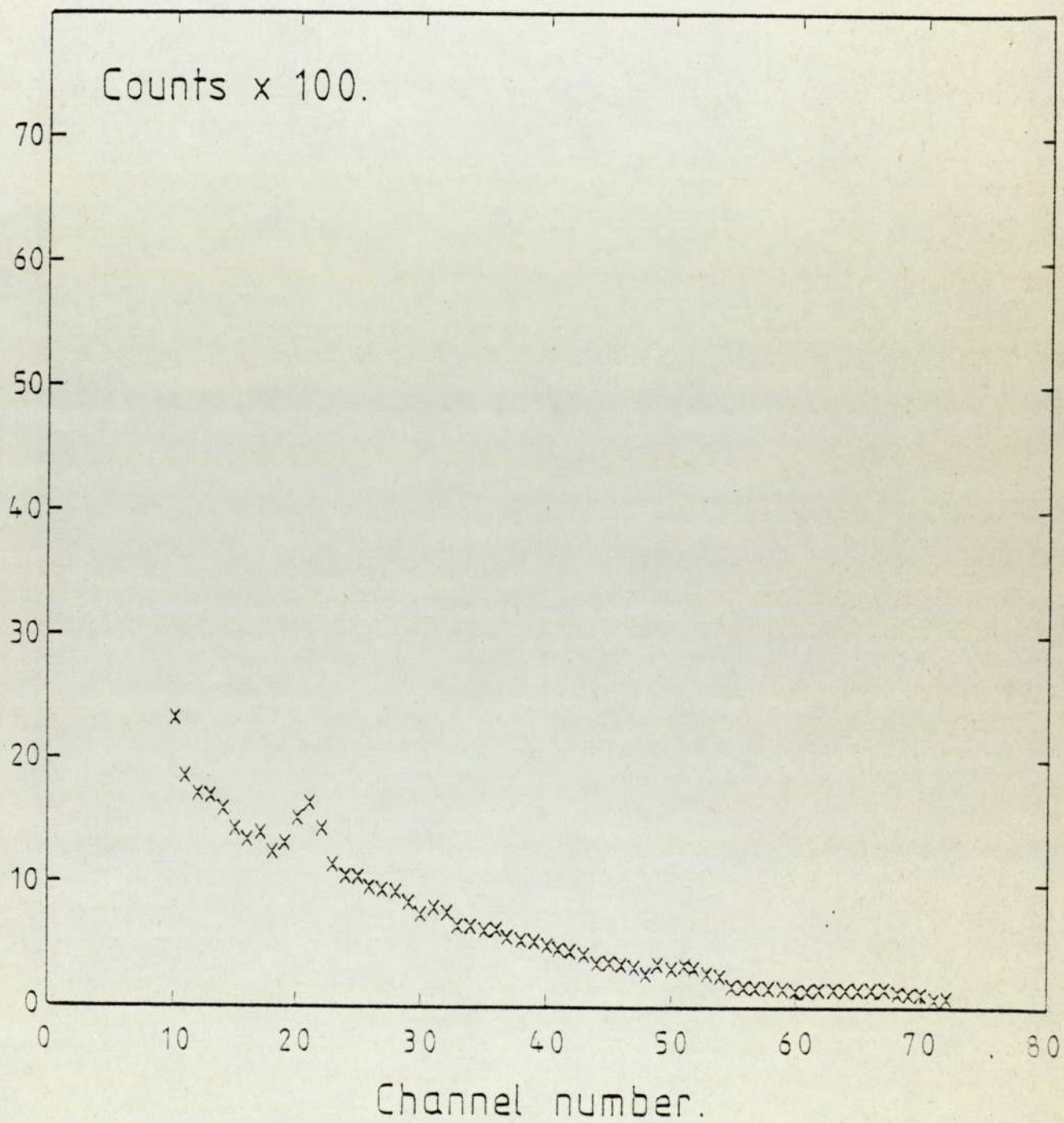


Figure 4.24 Pulse height spectrum of an anode-end specimen.

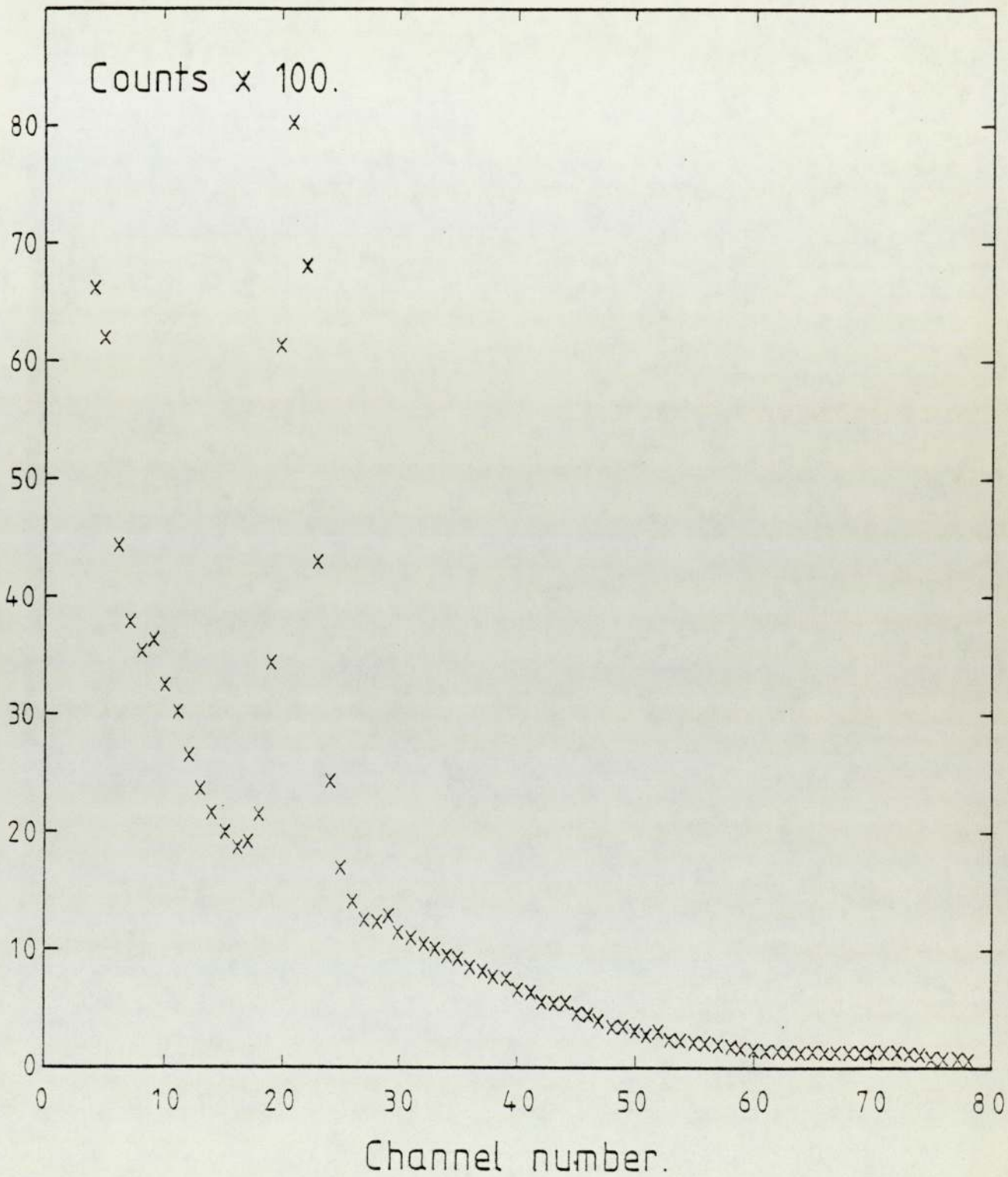


Figure 4.25 Pulse height spectrum of the gold activity in a plasma specimen from patient number 21.

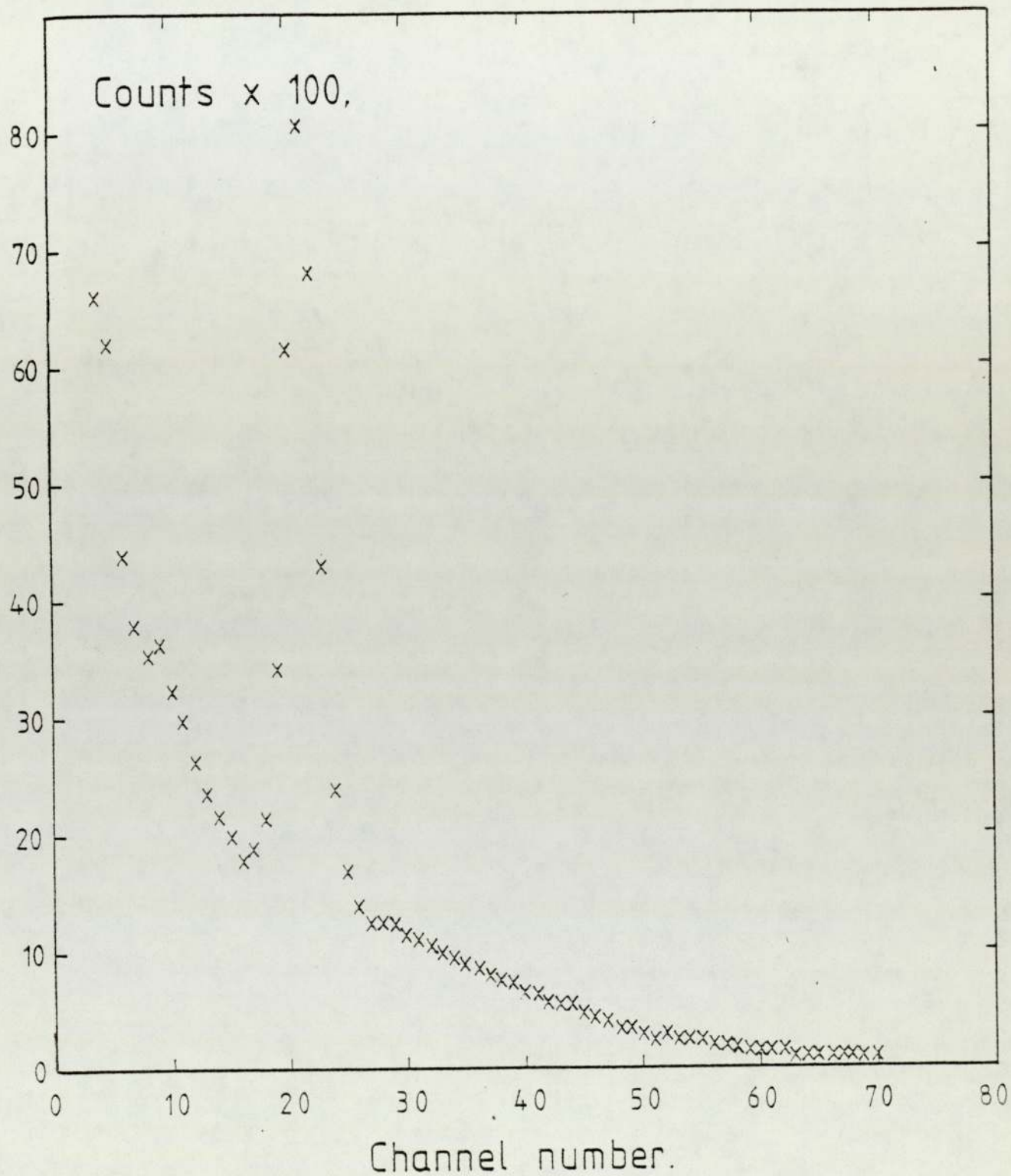


Figure 4.26 Pulse height spectrum of the gold activity in a second plasma specimen from patient number 21.

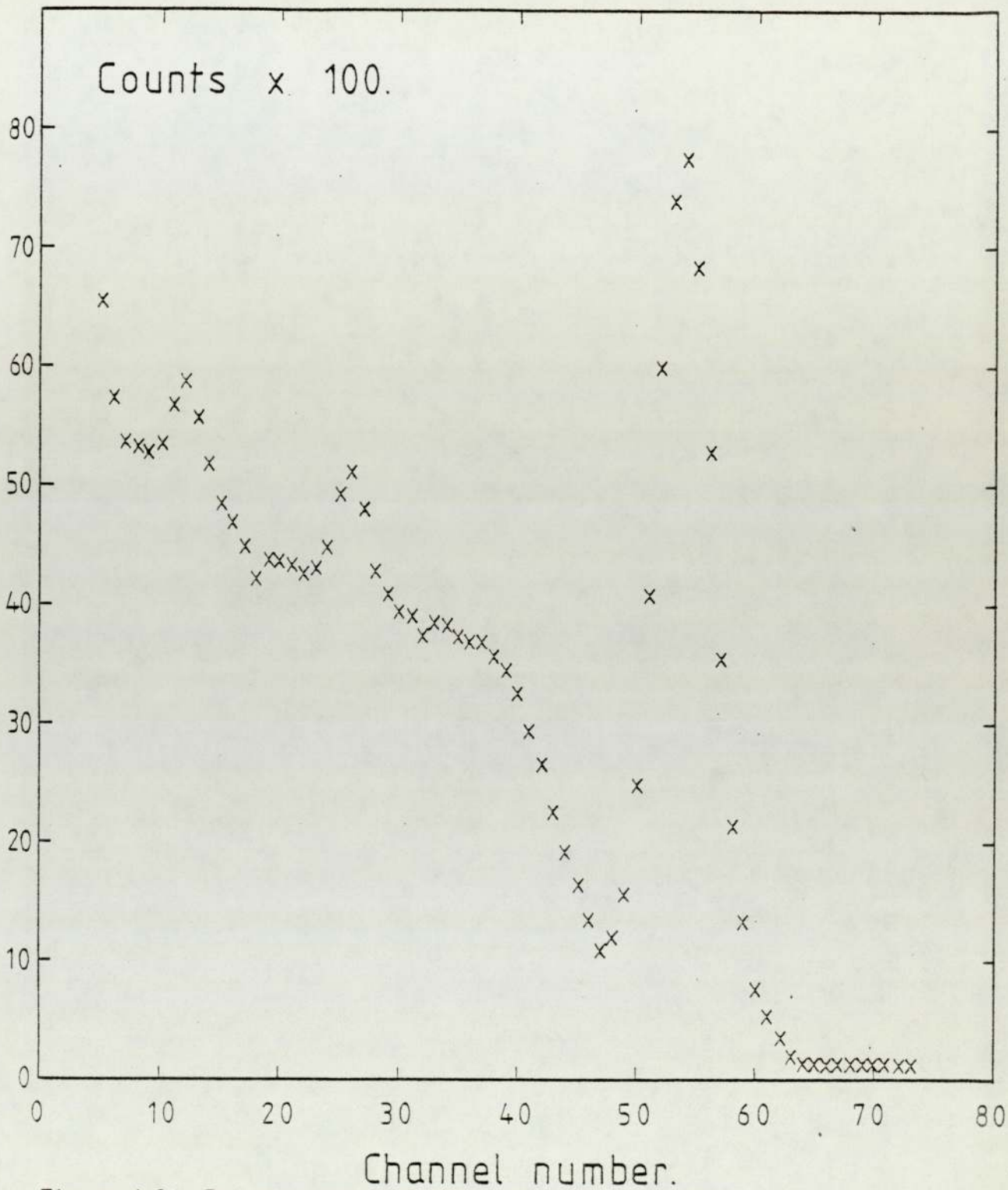


Figure 4.27 Pulse height spectrum of the gold activity in the prealbumin plus the cathode-end showing a high activity at channel number 54 corresponding to 1.1 MeV.

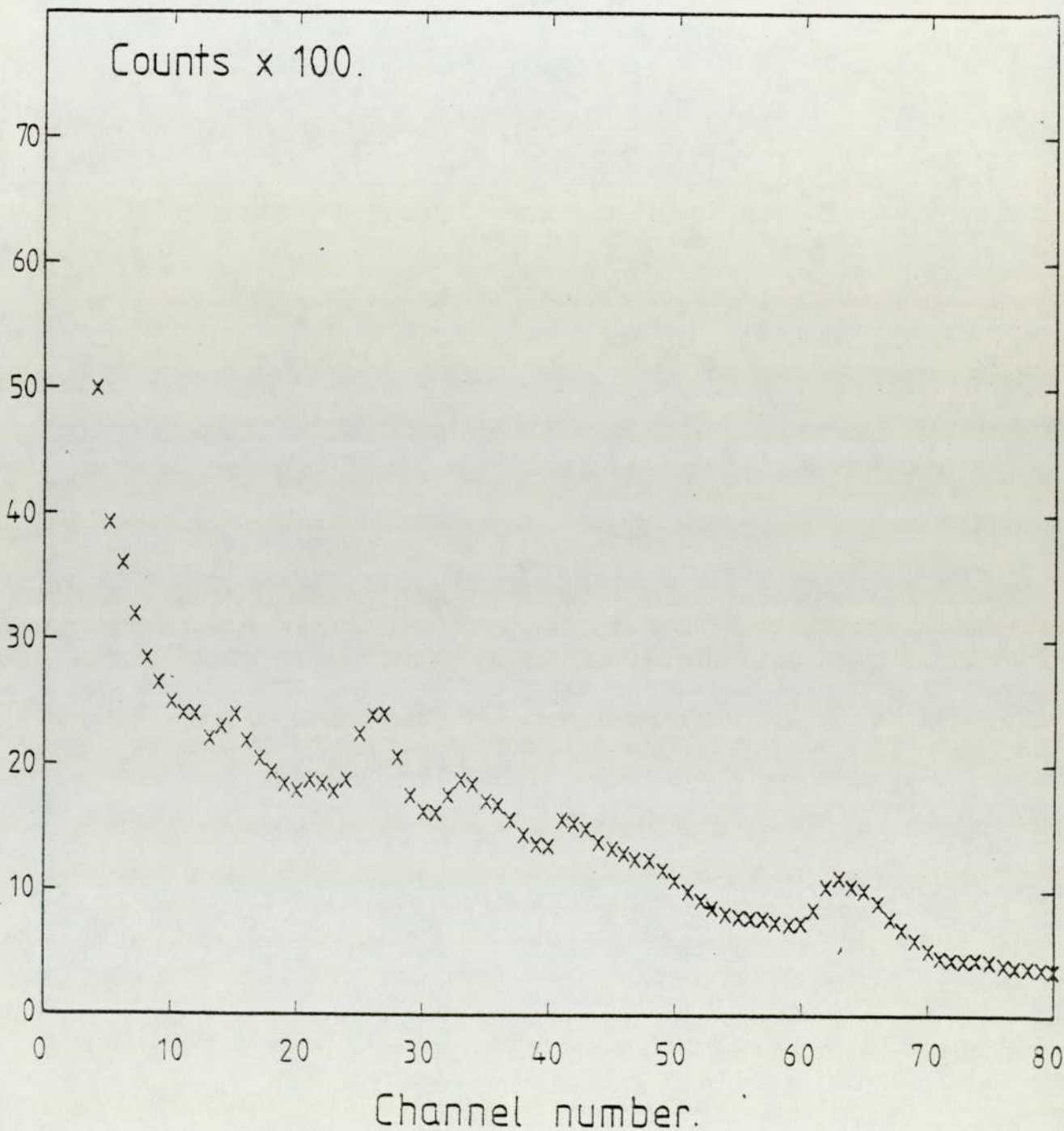


Figure 4.28 Pulse height spectrum of the gold activity in a specimen from patient number one showing another activity corresponding to 0.58 MeV and 0.77 MeV at channels number 33 and 41 respectively.

CHAPTER 5

DISCUSSION AND CONCLUSION

Neutron activation analysis has been successfully applied to measurements on twelve patients with rheumatoid arthritis, undergoing treatment with the gold salt sodium aurothiomalate (Myocrisin), to study the gold distribution in the blood. The results obtained are summarised in Tables 4.1, 4.2 and 4.3.

5.1 Gold Content of Fibrinogen

In Table 4.1 the ratio of the plasma gold content to the serum gold content lies between 0.92 to 1.1 with a mean of 1.002 and standard deviation  $\pm 0.07$ . This result shows that the gold level in serum is about the same as in the plasma which means that there is little, if any, binding to the fibrinogen, because the difference between the serum and the plasma is the fibrinogen as the serum is plasma without it. This agrees with the majority of other workers like E. G. McQueen and P. W. Dybes (1969)<sup>9</sup>, Nicholas D. H. Balazs et. al. (1972)<sup>10</sup>, Manfred Harth (1973)<sup>11</sup>, A Oohara et. al. (1974)<sup>12</sup>, but disagrees with J. S. Lawrence (1961)<sup>8</sup>.

There does not now seem to be much doubt that fibrinogen does not bind gold to any significant extent. For this reason, the measurements on plasma/serum ratios were not continued on the later patients.

5.2 Gold Content of the Cellular Fraction

The results given in Table 4.1 and 4.3 on this point show that there is a gold content in the cellular fraction. In the five patients, 1 to 5, it seems, as would be expected,

that the ratio of gold content in blood cells to that in plasma increases as the ratio of the whole blood gold level to that of plasma increases.

The cells/plasma ratio lies in the range 0.7% to 8% with an average of nearly 4%, except for patients number 4, 20 and 21 who show high gold levels in the blood cells of 20%, 31% and 76% respectively. Cell samples were not available for patients number 7, 8, 9 and 10, but the high whole blood to plasma levels in some of these patients implies a high cell level of gold.

Our average value of 4% agrees with the findings of H. Kamel et. al. (1976)<sup>14</sup>, and with J. S. Lawrence (1961)<sup>8</sup>, as his results lie in the range .8% to 4%. Also the high gold level found in some patients from the group we studied agrees with the high gold content found by Patricia M. Smith et. al. (1973)<sup>13</sup> which range from 1% to 38%. We disagree with those who detected no gold in the blood cells. These include H. Coke (1963)<sup>15</sup>, and R. H. Freyberg (1966)<sup>15</sup> who used chemical methods which are not very sensitive for detecting the small amount of the gold present in the blood cells. Also Nicholas D. H. Balazs et. al. (1972)<sup>10</sup> used the atomic absorption spectroscopy method which even if it is used successfully for this kind of analysis, it may be that in the cases studied by them the amount of the gold associated with the blood cells was too small to be detected.

Thus it seems that while many patients have cells/plasma

ratios of a few percent, some do have higher values. The reason for this is not clear.

### 5.3 Gold Content of the Albumin Fraction

Our results in Tables 4.2 and 4.3 agree with the majority of other workers in finding the greater part of the protein bound gold to be associated with the albumin. We found that with the exceptions of patients number 4 and 21, the gold bound to albumin is in the range between 69% and 96% of the total protein fractions level with an average of 83%. This range agrees reasonably with the albumin gold levels obtained by H. Kamel et.al. (1977)<sup>31</sup> whose values lie in range 45% to 76%, and the higher gold levels in our range agree with the range from 87.7% to 93.4% obtained by Roberta J. Ward et.al. (1977)<sup>32</sup>. Also the higher figures in our results seem to agree with that found by Micha Abeles et.al. (1977)<sup>27</sup> which shows 95% of the gold associated with the albumin fraction. The average obtained in the present work nearly agrees with that found by A. E. Finkelstein et.al (1976)<sup>30</sup> which was 81.8%. We disagree with N. Simon (1954)<sup>33</sup> in that he found no gold bound to the albumin.

The results on patient number 21 show that 100% of the gold was bound to the albumin fraction and no gold was bound to the other protein fractions which seems unreasonable because we believe that there is gold associated with the other protein fractions as the result of the other eleven of the twelve patients used for this study show. A possible reason is that the pulse height spectrum of the other fractions

should show a small gold peak but the high contamination background masks this peak. The low level obtained from patient number four is unusual. A possible reason is discussed in section 5.5.

#### 5.4 Gold Content of $\alpha_1$ , $\alpha_2$ , $\beta$ , $\gamma$ globulins

Our figures appear to vary in a range from 2% to 9% but still prove that there is a significant amount of gold in these protein fractions which agrees generally with most other workers who differ somewhat in the range from one to another. But this disagrees with Dr. M. Schattenkirchner and Z. Grobanski (1977)<sup>34</sup> who reported that no gold was bound to these other protein fractions except for a little gold associated with  $\alpha_1$ -globulin. Again our work taken with that of other workers shows beyond much doubt that there is a small but significant of gold associated with the globulins.

#### 5.5 The Correlation Between Serum Gold Level and the Clinical Response

Unfortunately our results do not provide much evidence on this question because all the patients available during the period of the investigation showed good response to gold therapy and the clinicians were unable to class any of them as non-responders.

However, two patients numbers 4 and 8 had toxic reactions, notably patient number 4, who had marked nephrotic symptoms. This may well be associated with some of the unusual findings, for example, the low albumin content, found in this patient.

It is surprising that the toxic reactions in patient number 4 are associated with a low gold level, because other workers found toxic reactions are associated with higher levels.

#### 5.6 Zinc in the Prealbumin Fraction from Patients Number 20, 21 & 22

Figure 4.27 is an example of one of the prealbumin pulse height spectrums which show a very clear large peak at channel number 54 corresponding to an energy of 1.1 MeV. By studying the activity decay at one week, two, and three weeks later, no difference was found in the observed peak which means that this activity has a long half-life. As the sample was prealbumin plus the anode end, the only source of contamination expected is from the electrophoresis method and the materials used for it. The electrode is usually made from material containing zinc so it is suggested that this activity belongs to the  $^{65}\text{Zn}$  of half-life 245 days formed by the reaction  $^{64}\text{Zn}(n, \gamma)^{65}\text{Zn}$ . This kind of contamination appeared only in the prealbumin from the group of patients numbers 20, 21 and 22, and because we received the blood samples of patients as batches at different times, it may be that at the time of preparing the protein fraction from this particular group of patients, some chemical reaction happened between the buffer and the electrode which caused this contamination.

The radioactive  $^{65}\text{Zn}$  decay includes positron emission but our spectra do not show peaks corresponding to the 0.511 MeV annihilation radiation as the electron capture process dominates ( $\beta^+$  1.7% EC 98.3%). The 1.1 MeV gamma-ray arises in 49% of decays.

### 5.7 Bromine in Patient Number One

Figure 4.28 shows the pulse height spectrum of the whole blood sample from patient number one, two peaks appeared, one at channel number 33 corresponding to an energy of 0.58 MeV, and the other at channel number 41 belonging to an energy of 0.77 MeV. Those peaks were seen in all the spectrums of the blood specimens from this particular patient. By following its decay for a few days these were identified to be due to  $^{82}\text{Br}$  with a half-life of 36 hours, formed by the reaction  $^{81}\text{Br}(n, \gamma) ^{82}\text{Br}$ . This possibly came from bromine containing drugs that had been taken by this patient.

Radioactive  $^{82}\text{Br}$  decays by beta emission to a number of different excited states giving principle gamma-rays 0.77 MeV, 0.55 MeV and 0.62 MeV peaks appeared in Figure 4.2.6. The larger peak corresponds to an energy of 0.58 MeV and is the result of mixing two peaks, one of 0.62 MeV and the other of 0.55 MeV. This is caused by the poor resolution of the well type crystal of the sodium iodide detector used.

### 5.8 Gold in the Cathode and Anode Ends

There was a percentage loss of gold in the cathode and anode ends beyond the protein region. It was found to range from 4% to 10% in the cathode end and from 3% to 10% in the anode end. This partly explains why the concentration ratio of the gold content of the total fractions to that in the serum was less than one in all the patients as shown in Tables 4.1 and 4.3. The percentage loss may mean that there is unbound gold freely diffusible in the blood, or that the electrophoresis process itself dissociates some of the bound gold.

## 5.9 Conclusion

As is well known, a major problem in the activation analysis method is contamination, which may arise through the process of sampling, the fractionation of the plasma protein and how far the containers of the samples have perfectly clean surfaces. From this point of view much care is needed to avoid such things causing an error in the quantitative calculations.

There are four suggestions I would like to make for future work:

1. I think it is much better if a project like this is carried out at the hospital itself to allow the investigator to be more in touch with the work of preparing the blood samples, the situation of the patients, and to obtain all the information needed from the hospital.

2. It seems to me that it is necessary to study three groups of the patients: the responders, non-responders and those who develop toxic reactions to cover all the needs of section 5.5.

3. I think it is worthwhile to complete this work by studying the relation of the gold level in the blood with that excreted through the urine and how much this is associated with the clinical improvement of the patients.

4. Also, I suggest to carry on this work in the future by using other methods of analysis besides the method followed here for comparison purposes. It would also be useful to

consider other methods of fractionation of the proteins in order to investigate further the question of unbound gold.

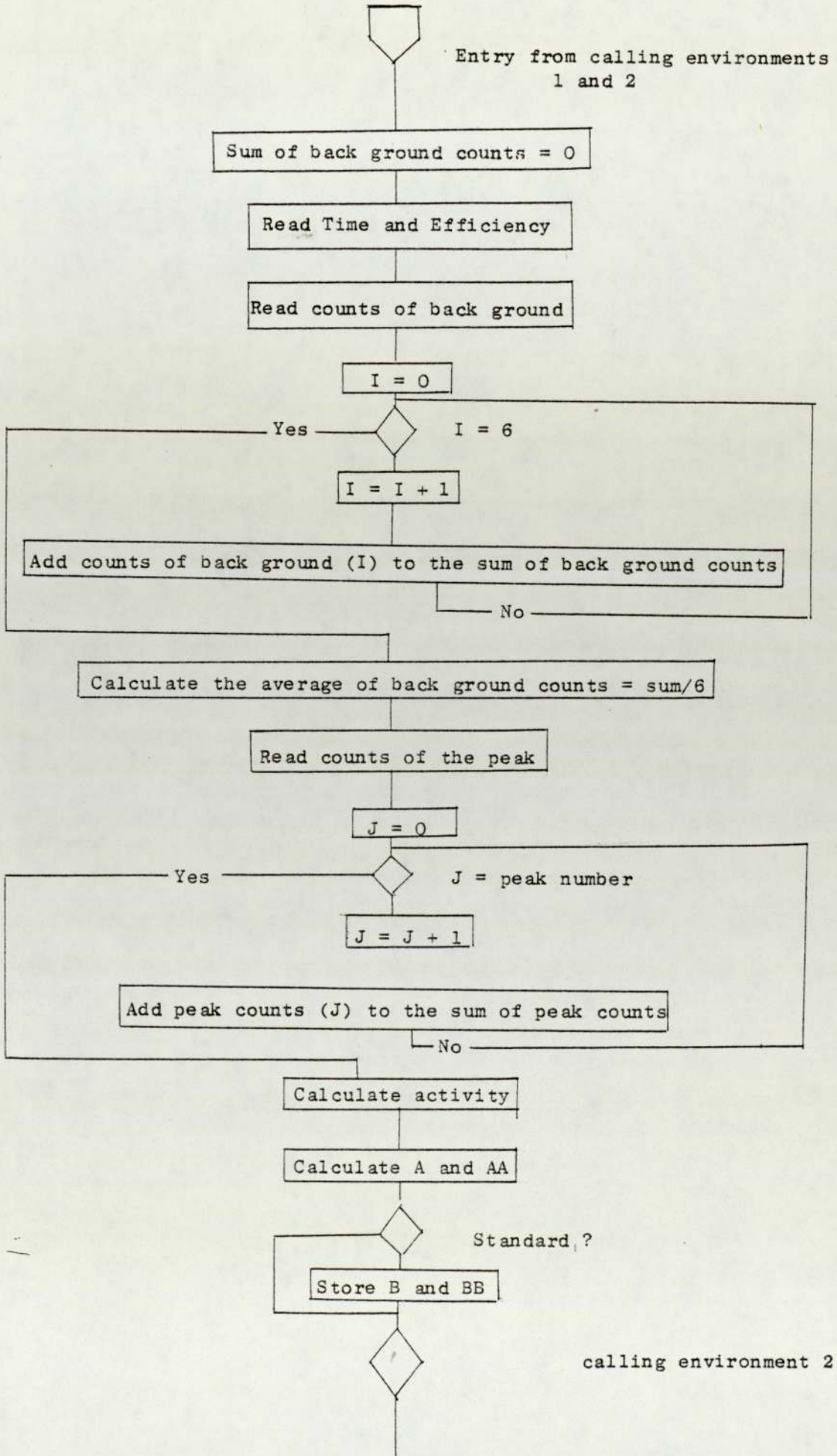
APPENDIX

### Appendix

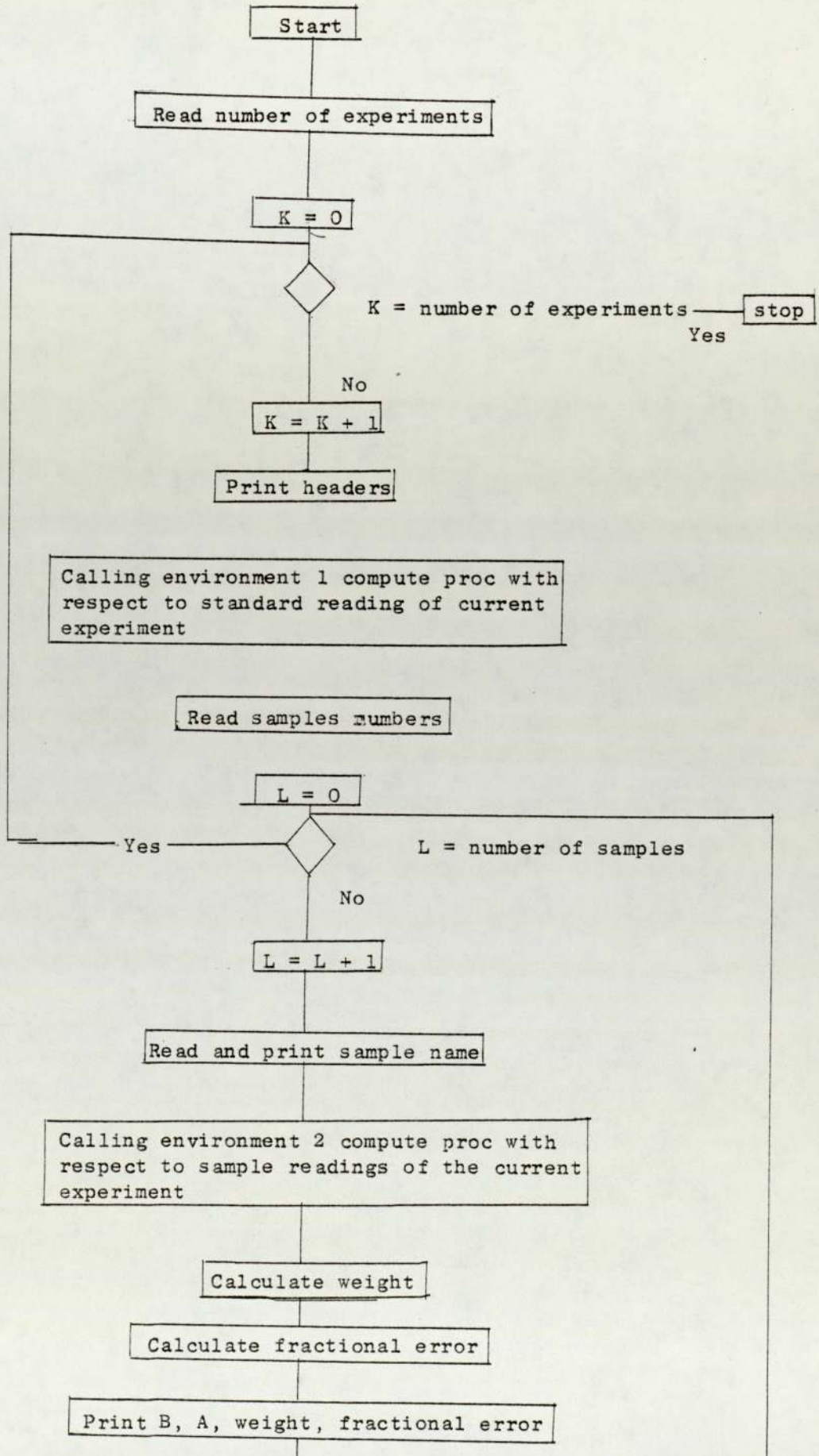
An Algol 68 computer program was used to estimate the gold level in the blood and the protein fractions. The program includes all the calculation steps which were mentioned in section 4.4. The identifiers used in the program and the flow chart are described as follows.

Identifiers	Description
Activity	Sum of peak counts - average of background x peak number.
A	Activity after correction for time and efficiency = $(\text{Activity} \times \text{Exp}(\text{Landa} \times \text{Time})) / \text{Eff}$ .
Time	Time between first counting (standard) and the second (sample).
Eff	The ratio of the area under the peak at a certain position to that at zero position, see Figure 4.9.
AA	Activity error after correction to time and efficiency = Error of $(\text{activity} \times \text{Exp}(\text{Landa} \times \text{Time})) / \text{Eff}$ where Error = (Sum of peak counts + sum of background counts).
A = B	For the standard.
AA = BB	For the standard.
Weight	$= A/B \times 10^8$ .
Fractional error	$= (AA/A + BB/B)10^8$ .

Compute procedure



Flow chart of the program





### LIST OF REFERENCES

1. G. D. Kersley, The Rheumatic Diseases, addition, London Heinemann, 4th ed., (1962).
2. J. A. Boyle and W. W. Buchanan, Clinical Rheumatology, Blackwell Scientific Publication, Oxford and Edinburgh (1969).
3. W. S. C. Copeman, Text Book of Rheumatic Diseases, 4th edition, E. and S. Livingstone Ltd., Edinburgh and London (1971).
4. D. C. Dumonde and M. K. Jasani, The Recognition of Anti-Rheumatic Drugs, published by MTP Press Ltd., Lancaster, (1978).
5. J. Forestier, Bull. Soc. Med. Hop. Paris, 53, 323 (1929).
6. J. L. Hollander, Arthritis and Allied Conditions, Henry Kimpton, 7th ed., (1966).
7. T. N. Fraser, Ann. Rheum. Dis., 4, 71 (1945).
8. J. S. Lawrence, Ann. Rheum. Dis., 20, 341 (1961).
9. E. G. McQueen and D. W. Dybes, Ann. Rheum. Dis., 28, 437 (1969).
10. Nicholas D. H. Balazs et.al., Clinica. Chimica. Acta, 40, 213 (1972).
11. Manfred Harth, Clinical Pharmacology and Therapeutics, 354 (1973).
12. A. Oohara et.al., Excerpta. Med. Int. Congr. Ser., 78, 299 (1974).
13. Patricia M. Smith et.al., J. Lab. Clin. Med., 82, 930 (1973).
14. H. Kamel et.al., Analyst, 101, 790 (1976).
15. H. Coke, AIR 6, 39 (1963).
16. R. H. Freyberg, Arthritis and Allied Conditions, 7th edition, J. L. Hollander, 302 (1966).

17. F. E. Krusius et.al., Ann. Rheum. Dis., 29, 232 (1970).
18. A. Lorber et.al., Ann. Rheum. Dis., 32, 133 (1973).
19. J. D. Jessop et.al., Ann. Rheum. Dis., 32, 228 (1973).
20. Paul Young et.al., Arthritis and Rheumatism, 17, 1059 (1974).
21. I. Bahous and W. Muller, Verh. Dtsch. Ges. Rheumatol., 4, 395, (1976).
22. R. H. Freyberg et.al., J. Clin. Inves., 20, 401 (1941).
23. S. S. S. Ørensen, Nordisk. Medicin, 84, 1508 (1970).
24. R. C. Gerber et.al., Ann. Rheum. Dis., 31, 308 (1972).
25. Norman L. Gottlie et.al., Arthritis and Rheumatism, 17, No. 2, 171 (1974).
26. D. Schorn et.al., S. A. Medical Journal, 1505 (1975).
27. Micha Abeles et.al., Southern Medical Journal, 70, 604 (1977).
28. R. Eberl and H. Altmann, Chemical Abstract, 27, 215 (1970).
29. A. Lorber et.al., Nature. New Biology, 236, 250 (1972).
30. A. E. Finkelstein et.al., Ann. Rheum. Dis., 35, 251 (1976).
31. H. Kamel et.al., Analyst, 102, 645 (1977).
32. Roberta J. Ward et.al., Clinica. Chemica. Acta, 81, 87 (1977).
33. N. Simon, Science, 119, 95 (1954).
34. M. Schattenskischer and Z. Grobanski, Atomic Absorption Newsletter, 16, 84 (1977).
35. A. Lorber et.al., Arthritis and Rheumatism, XI, 170 (1968).
36. Walter G. Berl, Physical Methods in Chemical Analysis, Academic Press Inc., Publishers, New York, 3, 219 (1956).
37. N. A. Dyson, X-rays In Atomic and Nuclear Physics, Longman (1973).

38. L. O. Plantin, International Conf. Modern Trends In Activation Analysis, College Station Texas, 141 (1961).
39. R. F. Coleman, The Analyst, 92, 1090 (1967).
40. Paul Kryger, Principles of Activation Analysis, A division of John Wiley and Sons Inc. (1971).
41. R. G. Jaeger et. al., Engineering Compendium on Radiation Shielding, Springer-Verlag Berlin Heidelberg New York, 1, (1968).
42. B. T. Price et. al., Radiation Shielding, Pergamon Press (1957).
43. L. F. Curtiss, Introduction to Neutron Physics, D. Van Nostrand Company Inc. (1964).
44. William S. Lyon, Guide to Activation Analysis, D. Van Nostrand Company Inc. (1964).
45. H. J. M. Bowen and D. Gibbons, Radioactivation Analysis, Oxford at the Clarendon Press (1963).
46. G. Hevesey and H. Levi, Vidensk. Selsk. Math. Fys. Medd. XIV, 5, (1936).
47. G. T. Seaborg and J. J. Livingood, J. Amer. Chem. Soc., 60, 1784 (1938).
48. A. M. Bruce and O. H. Robertson, (ANL 4108), 104 (1947).
49. C. A. Tobie and R. W. Dunn, Science, Feb 4, 109, 109 (1949).
50. J. M. A. Lenihan and S. J. Thomson, Advances in Activation Analysis, Academic Press, London and New York, 1, (1969).
51. W. Wayne Meinke, Science, Feb., 121, 177 (1955).
52. P. Yule, Ann. Chem., 37, 129 (1965).
53. J. M. A. Lenihan and S. J. Thomson, Activation Analysis Principle and Applications, Academic Press Inc. (1965).
54. H. J. M. Bowen, Isotope Research Division (A.E.R.E.), Feb. (1963).

55. C. Kellershohn et. al., J. Lab. and Clin. Med., 66, No. 1, July, 168 (1965).
56. J. B. Birks, The Theory and Practice of Scintillation Counting, Pergamon Press, Oxford (1964).
57. W. Heitler, The Quantum Theory of Radiation, Oxford University Press, 2nd ed. (1944).
58. O. Klein and Y. Z. Nishina, Physik., 52, 853 (1929).
59. H. A. Bethe and J. Ashkin, Experimental Nuclear Physics, Serge, John Wiley and Sons Inc., New York, 1, 337 (1953).
60. William J. Price, Nuclear Radiation Detection, McGraw-Hill Book Company, 2nd ed. (1958).
61. F. Adams and R. Dams, Applied Gamma-Ray Spectrometry, Pergamon Press, 2nd ed. 40 (1970).
62. B. J. Snyder, Nuclear Instruments and Methods, 53, 313 (1965).
63. B. J. Snyder and Geza L. Gyorey, Nucleonics, Feb., 80 (1965).
64. R. B. Murray, edited by Arthur H. Snell, Nuclear Instruments and Their Uses, John Wiley and Sons Inc., New York, 1, (1962).
65. Ralph E. Lapp and Howard L. Andrews, Nuclear Radiation Physics, Prentice-Hall Inc., 4th ed. (1972).
66. P. Quittner, Ph.D., C.Sc., Gamma-Ray Spectroscopy, Adam Hilger Ltd., London, (1972).
67. D. F. Covell, Analytical Chemistry, 31, No. 11, November, 1785 (1959).